# A Study of 3D Graphene-based Scaffolds for Advanced Neural Engineering

by

**Negar Mansouri**

B. Eng. (Electronic, Honours)
Multimedia University (MMU), Malaysia, 2014

M. Eng. (Biomedical Engineering)
The University of Malaya (UM), Malaysia, 2016

Thesis submitted for the degree of

**Doctor of Philosophy**

in

School of Electrical & Electronic Engineering
Faculty of Engineering, Computer & Mathematical Sciences
The University of Adelaide, Australia

December 2020

# Contents

# Abstract

The field of tissue engineering aims to create functional tissues/organs using scaffold biomaterials and cell sources to treat a multitude of diseases. To guide the regeneration process, the development of biomaterials with desirable characteristics, described as scaffold, is required. It is believed that 3D scaffolds can effectively reflect the realistic characteristic of living tissues, in contrast to 2D culture systems. Graphene, a 2D carbon allotrope, brings several advantages in neural tissue engineering owing to its unique properties including high surface area, suitable biocompatibility, mechanical properties and excellent electrical conductivity. In this study, 3D graphene-based composite scaffolds, consisting of Graphene Oxide (GO) and Sodium Alginate (Na-ALG), were fabricated as functional neural scaffolds. The fabrication method, physical and chemical characterizations of synthesized scaffolds are extensively studied and analysed to match neural tissue engineering requirements. Besides, electrically conductive scaffolds are developed based on the *in-situ* bioreduction of GO/Na-ALG aerogels which makes scaffolds more favourable for engineering of electroactive tissues. GO/Na-ALG scaffolds showed great improvement in hydrophilicity, electrochemical properties and mechanical integrity. Furtheremore, *in vitro* biodegradation study reveals that the proposed composite scaffolds have a controlled biodegradation rate. The prepared scaffold with interconnected porous structure and suitable mechanical properties is an appropriate platform for 3D stem cell culture.

As a result, human dental pulp stem cells (hDPSCs) are combined with the fabricated graphene-based scaffolds to support cellular responses. The biological effects of prepared graphene-based 3D scaffolds on dental pulp stem cells (DPSCs) in terms of proliferation, cell viability, and cytotoxicity were investigated. The Alamar Blue (AB) assay shows that DPSCs viability cultured onto Na-ALG and GO/Na-ALG scaffolds was higher than that of 2D controls confirming the desirable initial cell adhesion to the scaffolds' surface followed by cell spreading through pores. Besides, the LDH release measurements show that DPSCs toxicity on the GO/Na-ALG and RGO/Na-ALG scaffolds was comparable to that obtained on the 2D surface in the absence of the biomaterial. The cellular viability and activity are improved on scaffolds coated with PLL, being superior to combined PLL+LAM coating. The incorporation of graphene into the composite scaffold supported higher DPSCs viability and function, suggesting that the selected biomaterials are biocompatible with DPSCs which is ascribed to unique surface chemistry, good mechanical properties, high surface area, and excellent physicochemical properties of graphene-based nanomaterials. The cytotoxicity of GO/Na-ALG and RGO/Na-ALG scaffolds indicates that DPSCs can be seeded in serum-free media without cytotoxic effects. This is critical for human translation as cellular transplants are typically serum-free. The findings from the current study suggest that proposed composite 3D graphene-based scaffolds had a favourable effect on the biological responses of DPSCs. The knowledge and contributions made in the current work can be exploited for further studies on electrical stimulation and *in vivo* investigation of the engineered scaffolds for neural regeneration.

# Statement of Originality

I certify that this work contains no material which has been accepted for the award of any other degree or diploma in my name, in any university or other tertiary institution and, to the best of my knowledge and belief, contains no material previously published or written by another person, except where due reference has been made in the text. In addition, I certify that no part of this work will, in the future, be used in a submission in my name, for any other degree or diploma in any university or other tertiary institution without the prior approval of the University of Adelaide and where applicable, any partner institution responsible for the joint-award of this degree.

I acknowledge that copyright of published works contained within this thesis resides with the copyright holder(s) of those works.

I also give permission for the digital version of my thesis to be made available on the web, via the University's digital research repository, the Library Search and also through web search engines, unless permission has been granted by the University to restrict access for a period of time.

I acknowledge the support I have received for my research through the provision of an Adelaide Scholarship International (ASI).

# Acknowledgements

Now that the multidisciplinary journey of this research has come to an end, I truly understand the power of collaboration. Throughout this period, I have received a great deal of support and assistance. I would like to express my sincere gratitude and acknowledgement to all the people who played a role in my personal and academic life.

First and foremost, I would like to thank my principal supervisor, Dr Said Al-Sarawi from the School of Electrical and Electronic Engineering at The University of Adelaide, for valuable guidance, insightful comments, and considerable encouragement to complete this thesis. Without his unwavering support and belief in me, the goal of this project would not have been realized.

I am deeply grateful to my co-supervisors, Prof. Dusan Losic from the School of Chemical Engineering and Advanced Materials at The University of Adelaide, for his guidance and assistance at every stage of the research project. Without his support and funding, this project could not have reached its goal. I want to thank you for all of the opportunities I was given to conduct my research. I also had great pleasure of working within Losic Research group. In addition, I would like to extend my gratitude to my other co-supervisor, Prof. Jagan Mazumdar, for his continuous support and insightful advice throughout my studies.

This research work would not have been possible without the help and support of Dr Ryan O'Hare Doig from Neil Sachse Centre for Spinal Cord Research at the South Australian Health and Medical Research Institute (SAHMRI). His scientific advice, knowledge and many insightful discussions and suggestions enriched the content of this thesis for which I will forever be thankful. My sincere appreciation also goes to Prof. Jillian Clark and Prof. Stan Gronthos who provided me precious support and great advice throughout the biological aspects of this study.

I would also like to offer my special thanks to The University of Adelaide for the funding and support of this research to make it a success. This project would have not been accomplished without financial assistance via the Adelaide Scholarship International (ASI). Constant support and help of the academic and professional staff at the School of Electrical and Electronic Engineering at The University of Adelaide, undeniably, deserves a special thanks. I also gratefully acknowledge the support from the Australian Research Council Research Hub for Graphene Enabled Industry Transformation (project no. IH 150100003). In addition, I would like to extend my sincere thanks to AOSpine Asia Pacific Research Grant 2019 (AOSAUNZ(R)2019-05).

Last but not the least, I would like to thank my parents, without whom none of my success would be possible, for their continuous and unparalleled love, help and support. I owe a special thanks to my aunt, Arezoo, for always being there for me.

Negar Mansouri

# Publications

## Journal Publications

- **Mansouri, N.**, Al-Sarawi, S. F., Mazumdar, J., & Losic, D. (2019). Advancing fabrication and properties of three-dimensional graphene–alginate scaffolds for application in neural tissue engineering. RSC Advances, 9, 36838–36848.
- **Mansouri, N.**, Al-Sarawi, S. F., Losic, D., Mazumdar, J., Clark, J., Gronthos, S., Doig, R. O. H., (2021). Biodegradable and Biocompatible Graphene-based Scaffolds for Functional Neural Tissue Engineering: A Strategy Approach Using Dental Pulp Stem Cells and Biomaterials, Biotechnology and bioengineering, DOI: 10.1002/bit.27891.

## Conferences

- **Mansouri, N.**, Al-Sarawi, S. F., Mazumdar, J., Gronthos, S., Losic, D., Doig, R. O. H., "Functional Tissue Engineering for Spinal Cord Injury: A strategy approach using stem cells and bio-engineering" presented at the Graphene Research Hub Workshop, Melbourne, Australia, 2020.
- **Mansouri, N.**, Al-Sarawi, S. F., Mazumdar, J., Gronthos, S., Losic, D., Doig, R. O. H., "Functional Tissue Engineering for Spinal Cord Injury: A Strategy using Teeth and Bio-engineering" in Adelaide Spinal Research Symposium, Adelaide, South Australia, 2019.
- **Mansouri, N.**, Al-Sarawi, S. F., Mazumdar, J., Losic, D., "Fabrication and Characterization of 3D Graphene-alginate Scaffolds for Tissue Engineering Applications" in First Australian-Europe Graphene Workshop, Adelaide, South Australia, 2018
- **Mansouri, N.**, Al-Sarawi, S. F., Mazumdar, J., Losic, D., "Feasibility Study of 3D Graphene-alginate Scaffold for Tissue Engineering Applications" presented at the Australian Biomedical Engineering Conference (ABEC), Sydney, Australia, 2018

# Abbreviations

| Notation | Description |
|---|---|
| 3D | Three-dimensional |
| 2D | Two-dimensional |
| AB | Alamar Blue |
| ADSCs | Adipose-derived stem cells |
| BMSCs | Bone marrow-derived mesenchymal stem cells |
| CNS | Central nervous system |
| CNT | Carbon nanotubes |
| CV | Cyclic Voltammetry |
| CVD | Chemical vapor deposition |
| DMA | Dynamic Mechanical Analysis |
| DOC | Sodium deoxycholate |
| DPBS | Dulbecco's phosphate-buffered saline |
| DPSCs | Dental pulp stem cells |
| ECM | Extracellular matrix |
| EDAX | Energy-dispersive X-ray spectroscopy |
| EIS | Electrochemical Impedance Spectroscopy |
| ESCs | Embryonic stem cells |
| FBS | Fetal Bovine Serum |
| FDA | Food and drug administration |
| FTIR | Fourier-transform infrared spectroscopy |
| GO | Graphene oxide |
| GONPs | Graphene oxide nanoplatelets |
| GONRs | Graphene oxide nanoribbons |
| HCl | Hydrochloric acid |
| LAM | Laminin |
| LDH | Lactate dehydrogenase |
| MSCs | Mesenchymal stem cells |
| Na-ALG | Sodium Alginate |
| NSCs | Neural stem cells |
| NTE | Neural tissue engineering |
| PAA | Polyacrylic acid |
| PADM | Porcine acellular dermal matrix |
| PBS | Phosphate-buffered saline |
| PCL | Polycaprolactone |
| PDMS | Polydimethylsiloxane |
| PEG | Polyethylene glycol |
| PGA | Polyglycolic acid |
| PLGA | Poly (lactic-co-glycolic acid) |
| PLL | Poly-L-lysine |
| PLLA | Polylactic acid |
| PNS | Peripheral nervous system |
| PVA | Polyvinyl alcohol |
| rGO | Reduced graphene oxide |
| rGOs | Reduced graphene oxide sheets |
| rGONRs | Reduced graphene oxide nanoribbons |

| | |
|---|---|
| ROS | Reactive oxygen species |
| SCI | Spinal cord injury |
| SEM | Scanning Electron Microscopy |
| SWCNT | Single-walled carbon nanotube |
| TE | Tissue engineering |
| TGA | Thermogravimetric Analysis |
| UV | Ultraviolet |
| XRD | X-ray diffraction |

# List of Figures

# List of Tables

# CHAPTER 1: INTRODUCTION AND MOTIVATION

## 1.1 Abstract

In neurobiology, a useful treatment method to reconstruct the brain damage has been questioned to research during the last decades due to its limited regeneration capacity and lack of appropriate guidance cues. The central nervous system (CNS) traumatic injuries have left the patients with profound and permanent neurologic deficits. The focus of current researchers is on developing methods to promote neuronal and axonal regrowth as well as building up synapses. Neural tissue engineering (NTE) field is considered as a potential therapeutic strategy to compensate neurons loss for a wide range of neurological diseases. For the success of clinical applications, a three-dimensional (3D) scaffold is required in order to mimic the natural environment of neural tissues and provide synergistic cell guidance cues to assist tissue recovery. Target cells are loaded in the 3D scaffold and implanted at spinal cord contusion to create a neural network at the site of injury. This chapter starts with an introduction to the CNS disease focusing on spinal cord injury (SCI) and discusses common treatment options for the injury. NTE as the main focus of this thesis is then expanded. Finally, a summary of the thesis and original contributions are outlined.

## 1.2 Central Nervous System (CNS)

Nervous system contains basic functional elements defined as neurons. Neurons consist of three main components including cell body, axons and dendrites. The main function of neurons is transmitting electrochemical signals throughout their axons and lead to the release of neurotransmitters at synapses. In addition to neurons, the nervous system contains other supporting cells called glia (such as astrocytes, oligodendrocytes, Schwann cells) and facilitate the metabolic and structural support [1]. Figure 1.1 depicts different types of nerve cells in the nervous system. As the figure shows, there are three types of nerve cells including multipolar interneurons, a motor neuron, and a sensory neuron.

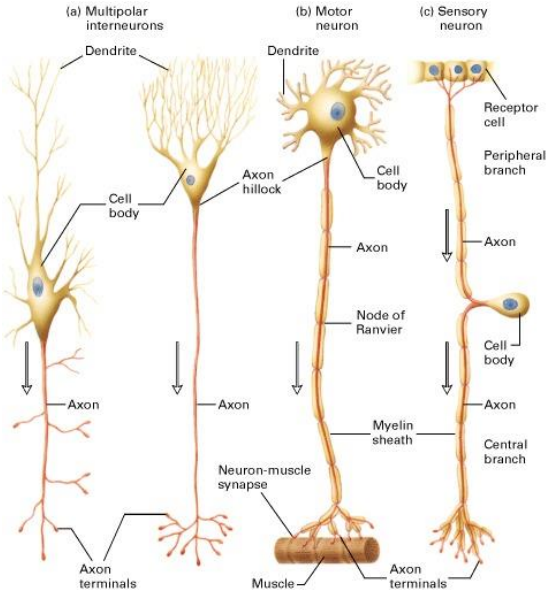


*Figure 1.1. Different type of nerve cells in the nervous system: (a) Multipolar interneurons, (b) A motor neuron, (c) A sensory neuron (arrows indicate the direction of conduction of action potentials in axons)[2].*

The nervous system, the most complex and delicate structure that controls all functions of the body, is divided into the central nervous system (CNS) and peripheral nervous system (PNS). The CNS consists of the brain and spinal cord in which the brain is the command centre of the nervous system with billions of nerve cells and the spinal cord is the communication means between the body and the brain. One of the most significant differences between the CNS and PNS is the limited nerve and axon regeneration capacity of CNS which is ascribed to its native inhibitory environment. This could be due to glial scar, inflammation, accumulation of inhibitory factors, and absence of myelinating oligodendrocytes.

Following the primary injury to the CNS, the fee radicals flow via the blood-brain barrier causes nerve cells damage, which eventually results in secondary injury causing prevention of nerve regeneration [3]. Severe disruption of CNS can be caused by stroke, traffic accidents, falls, brain trauma, sports injuries, gunshots or other degenerative neurologic diseases which severely affect patient's quality of life and economic costs. In addition to common causes of traumatic SCI including automobile accidents, violence and falls, there are some cases on spinal cord birth defects which occur in fetal development and are known as neural tube defects. Affected infants suffer from loss of sensation and motor functions, bowel and bladder control problems, and intellectual disabilities as a result of incomplete enclosure of spine nerves [4].

The complex physiology of the nervous system brings about numerous challenges to address neural damages. The conventional methods to repair neural defects including autografts or allogenic grafts have some limitations due to the mismatch of nerve size, lack of donors, and immune rejections. In addition, the administration of post-injury drug therapy has no effect on lost functions and only focuses on further progression of the damage. Regarding traumatic injuries and particularly SCI, no effective treatment strategy has been found to restore or enhance the lost tissue function. The devastating conditions of patients suffering from CNS diseases inspired NTE researchers to focus on developing an effective treatment method. However, providing therapeutic regimens to engineer tissue constructs for CNS are challenging due to its complex architectural and functional nature. Several strategies have been employed to re-establish a functional neural network and tissue contiguity including cell therapy, delivery of growth factors and tissue engineering (TE) products; each with varying degree of success [5]. Among all reported therapeutic methods for devastating conditions of neuronal loss, tissue engineering technology which combines cell sources, benefits of scaffold matrix, and growth factors can be considered as the most promising method to maximize the repair effect. The consequences of neurotrauma involve a kind of tissue disruption at the injury site and nerve tracts discontinuity resulting in neural network demolition in CNS [6-9]. Therefore, bridging the lesion site with the help of tissue engineering strategies can help biological and architectural tissue integration at the cavitary site.

## 1.3 Spinal Cord Injury

The spinal cord, a long tubular bundle of nervous tissue (with the length of ~45cm in male and ~43cm in female), is a part of CNS that extends from the brain and primarily acts as a link between the brain and the PNS and transmits neural signals. There are two cross-sectional regions in the spinal cord, as indicated in Figure 1.2, known as white matter, containing myelinated axons, and grey matter, butterfly-shaped, containing unmyelinated axons, neuroglia cells and motoneurons. The important functions of the spinal cord involve motor and sensory functions as well as coordinating reflexes [1].

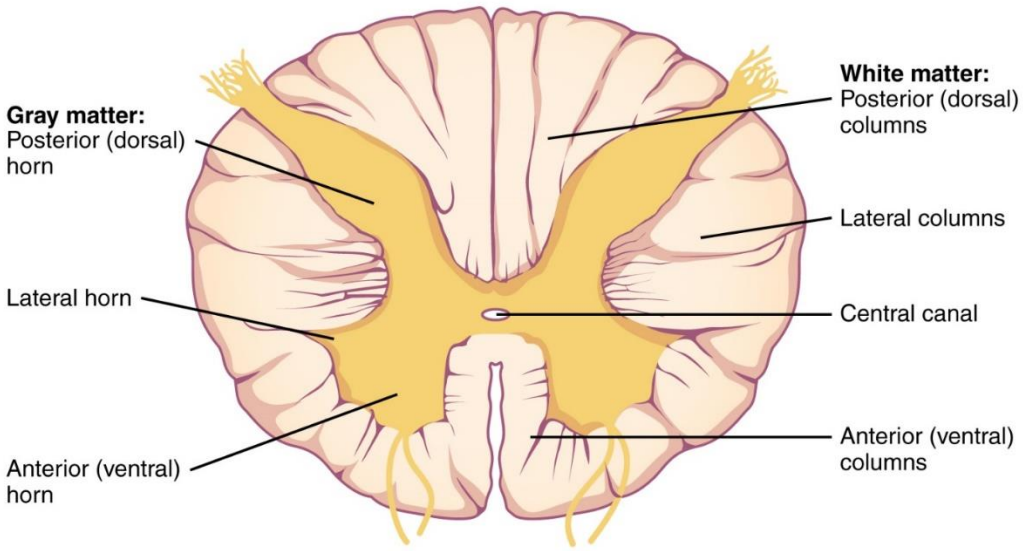


*Figure 1.2. Cross-sectional view of spinal cord [10].*

SCI is defined as the devastating damage to nerves at the spinal canal that is impacting 250-500,000 people all over the world annually and often results in long-term disability. It is estimated that 20-30% of patients experience significant signs of depression, which in turn has negative impacts on economic participation, physical and psychological wellbeing, and results in individual and societal costs (based on WHO statistics, 2013).

In Australia, 15,000 people are living with SCIs and near 350 new cases reported annually. Other than personal devastating impacts of SCI, the economic cost and care of patients living in Australia are estimated to be more than $3 billion annually (based on the statistics provided by Australian Institute of Health and Welfare (AIHW). This condition results in paraplegia or quadriplegia with no feasible treatment approach to date. Patients undergo various loss of functions of limbs, bowel, bladder and struggle with sexual function. Failure of regeneration following the injury affected the physical, psychological, and social well-being of people sustaining a SCI. The pathological changes after an injury can be divided into primary injury following by secondary injury. The irreversible process of primary injury involves the spinal cord tissue damage, neural death, hemorrhagic necrosis and edema. Secondary injury causes spinal cord hypoxia, the formation of cavity, inflammation and glial scar which could be managed by medical intervention. The glial scar is formed as a result of inflammation of surrounding spinal cord sections which have led to hyperplasia and hypertrophy of astrocytes. The resultant glial and stromal scarring at the site of injury hinder axon regrowth followed by an increase in inhibitors upon myelin debris and proteoglycan deposition in the environment. This hostile environment causes a decrease in neuronal regrowth following SCI [11, 12]. Therefore, finding plausible strategies to maintain and improve the functional stability of SCI patients has become one of the most challenging topics in the neuroscience field. Researchers have agreed that designing substrates to provide guidance for axonal and nerve growth after spinal cord transection can enhance the regenerative capacity of neurons in animal models with spinal cord defect [13-16]. Besides, other studies examined the implantation of various stem cell sources into spinal cord lesions to stimulate neural regrowth [17-19].

## 1.4 Neural Tissue Engineering

One of the common surgical techniques to repair nerve gaps is autologous nerve grafting in which a nerve segment from less important body parts such as sural nerve is used to replace the damaged part of another nerve [20]. However, due to inherent limitations of this technique such as lack of donors and comorbidity, the clinical recovery rate is only 80% for the treatment of nerve injuries with autologous grafts [21]. An alternative treatment approach for segmental nerve damages is nerve allograft transplantation using cadavers. However, the application of cadaver-based nerve allografts is limited due to histocompatibility, long-term use of immunosuppression, and immune response issues [22].

In regards to pursuing a replacement to organ transplants, tissue engineering has been found to offer the most effective approach for modelling and repairing the function of damaged/diseased tissues. Particularly, NTE is aimed at functional recovery of nervous system tissues for *in vivo* transplantation for a variety of neurological medical conditions. This strategy involves regulating and improving the cell behaviour and tissue regeneration through the design of biomaterials which can support the three-dimensional neuronal cell regrowth. It has been extensively demonstrated that neural growth three-dimensionally facilitating cell-cell and cell-scaffold interactions in all directions can promote neural outgrowth and replicate a highly similar physiological environment of living tissue [23].

The neuron loss, cavity formation, damaged tissue, and paralysed functions as a result of the injured spinal cord could be repaired through NTE approaches combining three-dimensional scaffold and cell sources. The appropriate physical, chemical, mechanical and biological characteristics of scaffold biomaterials can give rise to developed nerve regeneration and functional recovery at the site of lesioned spinal cord tissue. Biomaterials could establish a suitable environment for vascularization, structural support and regeneration of axons and neuron cells. It has been reported that nerve regeneration can be significantly impacted by length, diameter, rigidity, permeability, degradability, morphology, and composition of the designed neural conduit [24]. The potential of designed/fabricated biomaterials should be evaluated thoroughly and carefully in terms of efficient integration with the host tissue. Tissue-engineered scaffolds with matched properties to the nerve tissue, as represented in Figure 1.3, combined with cell transplantation can act as a bridge to reconstruct the damaged nerve pathways with the ultimate goal of enhanced motor and sensory functions. In view of this, NTE research has gained a great deal of attention for effective medical management of brain diseases. Therefore, the application of biomaterial scaffolds in NTE has raised great hope for prospective treatment regimens of SCI [25]. In addition, the recent application of stem cell technology has revolutionized the great progress in compensating cell loss caused by traumatic injuries [26].

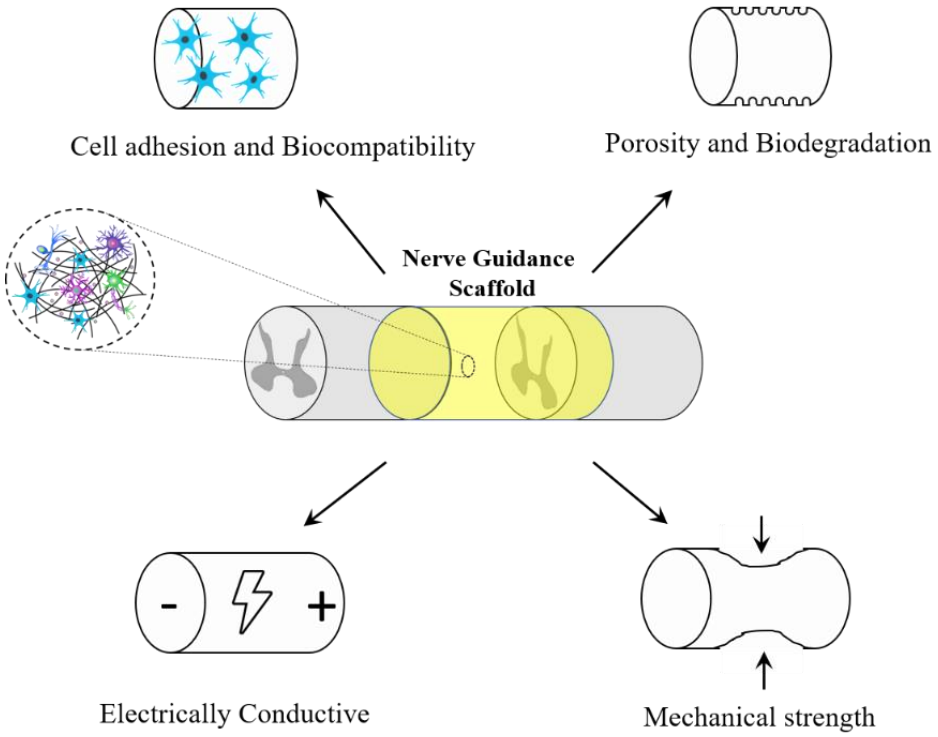


*Figure 1.3. Key design elements in the construction of nerve guidance channels (adapted from [27]).*

A suitable tissue-engineered nerve graft for CNS should ultimately play a significant role in providing structural support, delivering cells and growth factors, regulating the expression of particular genes and inducing tissue regeneration [27]. As in the case of TE-based therapies aimed at SCI, an appropriate scaffold biomaterial should have a similar Young's modulus to the spinal cord, mimicking the natural milieu and induce neuroregeneration to allow space filling, axonal ingrowth and inhibiting scar formation of damaged spinal structures [28]. A desirable scaffold for SCI should not only support neuronal regeneration but also be adjustable to fit a defect in complicated physiological geometry. Since the introduction of TE strategies to SCI models, several tissue-engineered platforms have been investigated in terms of preclinical effectiveness. For instance, Espinosa-Jeffrey et al. developed a biocompatible 3D hydrogel framework to induce neuroregeneration of SCI using a combination of neural TE system and stem cell technology. It is shown that scaffold could not only control inflammation and scar formation but also facilitate differentiation and repair of the injured spinal cord of cats by restoring locomotor functions [29].

Scaffolds can successfully act as a permissive delivery vehicle to support the regeneration of spinal nerve fibres. It can be observed from previous studies that scaffolds could significantly enhance the survival of stem cells and functional recovery after implantation. Despite the apparent benefits of stem cell-based therapy in some animal models, there is still a need for a deeper understanding of stem cell manipulation to provide efficient and safe cellular therapy. Although the combined application of scaffolds and stem cell technology in the treatment of SCI is encouraging, current methods present some limitations and the challenge is to develop biomaterial scaffolds that can fulfil multiple requirements including mimicking *in vivo* microenvironment, modulating cellular behaviour and functions, supporting regenerative growth and functional recovery of damaged neural tissues, and providing axonal regeneration and network connection [30, 31]. Therefore, the transition from 2D cell cultures to 3D scaffolds

could open remarkable grounds in therapeutic strategies of the spinal cord. In this context, graphene with advanced multidimensional characteristics holds strong promise in mediating reconstruction of damaged neural tissue. Also, excellent conductivity of graphene-based materials could assist in increased cell proliferation, differentiation and protein absorption. Besides, the development of composites with controllable microstructure has remarkable potential for guiding suitable reparative responses in NTE applications. [32-34]. Thus, the aim of this current work is to engineer graphene-based composite scaffolds that interact with neural cells and induce nerve regeneration in the spinal cord. Furthermore, it introduces a new 3D graphene-based scaffold loaded with dental pulp stem cells (DPSCs) in order to promote stem cell fate.

## 1.5 Chapter Summary

Researchers have focused on a combination of stem cell technology and tissue engineering fields to respond to the expectations of treatment of nervous system disorders. It is believed that for the success of stem cells clinical applications, a 3D scaffold is required in order to mimic the natural environment of neural tissues and provide synergistic cell guidance cues to assist tissue recovery. The important design elements in the fabrication of nerve conduits are identified. The combination of a scaffold with cells has been developed with a tendency for achieving greater survival and integration of cells with the host tissue. The stem cell-encapsulated scaffolds are expected to optimize the nerve regeneration process as well as axonal regeneration and specific neuronal differentiation. The ultimate goal of this research is to enhance the functional recovery of patients suffering from SCI after transplantation of neural TE product.

## 1.6 Thesis Structure and Original Contributions

The current PhD thesis aims at researching the potential of graphene-based composite scaffolds in neural tissue engineering applications. The current state of knowledge in the field consists of limitations in existing therapeutic approaches of CNS injuries for clinical translations. Therefore, significant work has been directed towards the development of advanced tissue engineering strategies for functional nerve regeneration. In contrast to the existing studies, this study considers multiple roles of suitable biomaterial scaffolds as neural tissue substitutes including high porosity, bioactivity, tuneable properties, electrical conductivity and appropriate mechanical strength. This study aims at contributing to the literature in the field of advanced neural engineering by incorporating 3D graphene-based nanocomposite scaffolds to enhance stem cell functions. It also investigates the impacts of synthetic conditions on physical, chemical, biological and mechanical characteristics of the prepared scaffolds. The primary objective of this thesis is to test the hypothesis that graphene-based composite scaffolds will promote increased cell viability, proliferation and neural induction of seeded DPSCs compared to control scaffolds. Also, this study argues why it is important to find out a suitable biocompatibility assay in accordance with scaffold biomaterials to estimate an accurate representation of scaffold cytotoxicity level.

The key research findings and contributions of this thesis are compiled into separate chapters at each significant stage of the research as illustrated in Figure 1.4, which also provides an overview of the thesis structure and describes each chapter's content.

- The general background of the study along with current limitations associated with the conventional therapeutic methods of SCIs and neuronal loss in nervous system disorders have presented in Chapter 1.

- Chapter 2 elaborated the justification of the study by identifying the most relevant and significant research in this field. It also provides an overview of tissue engineering requirements, scaffold biomaterials and scaffold fabrication techniques.

- Fabrication and characterization of 3D graphene-based scaffolds are proposed in Chapter 3. The proposed scaffold aims to provide cell guidance cues which can induce neuronal regeneration. Besides, the physical, chemical, mechanical and electrical properties of the fabricated scaffolds are investigated in order to match the specific properties of neural tissue engineering. The optimization of synthetic conditions of this composite fibrous scaffold is also described which are specifically selected to comply with CNS tissue.

- In Chapter 4, cytotoxic effects of the fabricated scaffolds are assessed to understand the scaffold-cell interactions. Methods and procedures involving culture of DPSCs in a 3D cell culture system using the fabricated scaffolds are discussed. In addition, biological responses of DPSCs upon exposure to graphene are reported with the aim to highlight the potential capacity of graphene-based nanomaterials for the future tissue engineering and regenerative therapy. With the ultimate goal of successful clinical treatment, this chapter highlights cell viability and toxicity of various graphene contents to prove the concept of the graphene-based scaffold as a vehicle to deliver stem cells.

- In the final chapter, a summary of the research carried out in this thesis is provided followed by suggesting the future works. Moreover, the significance of this work to the field as well as challenges in conducting the research are elaborated.

The knowledge and contributions made in the current work, in addition to the design, development, and experimental results provide a foundation for future studies on nerve tissue alternatives as a permissive environment in disorders of the nervous system.

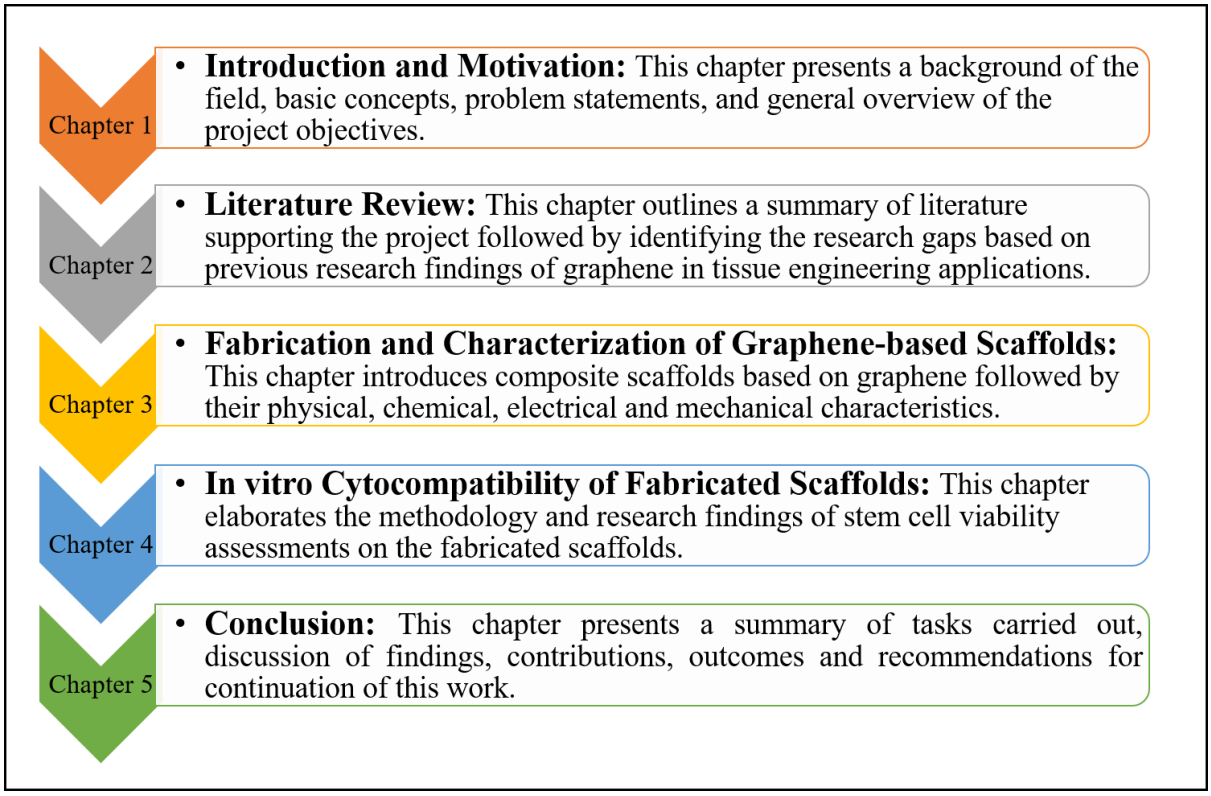


*Figure 1.4. Overview of thesis structure.*

# CHAPTER 2: LITERATURE REVIEW

## 2.1 Abstract

Tissue engineering is a multidisciplinary field that combines the principles and methods of biology, clinical medicine, materials science, and engineering and aims to regenerate functions of damaged tissues/organs by making use of cells and scaffolds. However, scaffold development is challenging due to the difficulties in arranging cells in a desirable three-dimensional (3D) environment which provides molecular signals to stimulate cell regrowth in the desired tissue structures. Hence, there is a need to develop 3D bioscaffolds loaded with cells whose microenvironment is matched with the host tissue and pores can facilitate cell growth and migration. After the introduction provided in Chapter 1, it is fundamental to recognize the requirements of scaffolds and scaffolding approaches from a tissue engineering perspective. In the development of an ideal scaffold, the choice of material(s), structures and fabrication technology of a scaffold highly affects the ultimate tissue regeneration outcome. In this chapter, an overview of various scaffold materials, and fabrication methods are presented. Among current scaffold materials, graphene has attracted considerable scientific attention as nanocomposite carriers or scaffold materials for a various range of connective tissue such as cartilage and scaffold in bone, nerve, skin, heart and muscle tissue engineering, owing to its porous morphology, great surface area, excellent mechanical strength, and good electrical conductivity. Furthermore, the potential of graphene-based nanomaterials in tissue engineering as a promising scaffold material is also discussed. Graphene-based scaffold in tissue engineering applications as the main focus of this research is then expanded to provide a review of previously developed scaffold materials and their outcomes. Iterating the advantages and shortcomings of tissue engineering scaffolds, the research gap is emphasized.

## 2.2 Introduction

The ‘tissue engineering’ term corresponds to the development of biological replacements to improve or restore the function of diseased/malfunction tissues by the means of engineering and life science approaches. This field mainly relies on incorporating scaffolds, cells, and biochemical factors to address problems associated with organ transplantation and surgical reconstruction. Previous studies demonstrated that cells cultured in 3D scaffolds, in comparison with 2D culture system, improved the proliferation and differentiation for constructing tissues in heart, liver, kidney, spinal cord and brain [35]. The use of 3D scaffolds as supportive matrices offers an appropriate microenvironment for tissue regeneration. Thereby, these structures are eventually cultured with cells or exposed to biophysical stimulations in order to engineer viable and functional tissues similar to native tissues. The scaffold-based methods are advantageous compared with conventional 2D cell cultures owing to their ability to competently recreate *in vivo* physiological conditions. Scaffold should present the needed support for cell proliferation and eventually tissue regeneration. Recently, the development of appropriate scaffold biomaterials that are conducive to cell growth is a trivial question among researchers [36, 37].

Furthermore, researchers are currently focusing on combinatorial approaches using scaffold materials and stem cell sources to effectively stimulate nerve regeneration. Some selected studies using the combination of scaffolds and stem cells as potential treatment methods are

outlined in Table 2.1. For example, Shoichet et al. prepared a hydrogel loaded with neural stem cells for a mice model of SCI. According to their results, the combination of stem cell source, fabricated scaffold and growth factor could significantly reduce the lesion size and improve differentiation and locomotor functions [38]. In another study, PLGA scaffolds were loaded with human NSCs in order to investigate its capability in bridging the gap of the hemisected canine spinal cord. It was indicated that the proposed scaffold could deliver therapeutic cells and genes at the site of injury [39]. Another similar study investigated the capability of gellan gum hydrogel for the repair of SCI models. This FDA approved hydrogel is well-known for the identical mechanical and electrical properties to the spinal cord. According to this study, it was shown that the biofunctionalized hydrogel improved cell attachment, proliferation and the activity of adipose-derived stem cells and olfactory ensheathing cells resulted in a substantial enhancement in motor and histological functions of animals suffering from SCI [40]. In addition to the great efforts to combine TE-based strategies with stem cell technology for SCI, some other studies discussed transplantation of Wharton's jelly mesenchymal stem cells (WJ-MSCs) which resulted in the restoration of neurological functions and improvement of axonal regeneration [41, 42].

Results from various researches demonstrated the great hope for the reconstruction of neural and axonal networks for appreciable improvements in SCI. More specifically, as shown in Table 2.1, these studies provided experimental evidence that the utilization of scaffold biomaterials and stem cells significantly improve cell survival, the formation of synapses, reduction of cavitation, neuronal and axon regeneration and functional recovery of animals with the injured spinal cord.

*Table 2.1. Benchmarking of studies on the repair of injured spinal cord using biomaterial scaffolds and stem cells.*

| Injury | Animal model | Scaffold composition | Stem cell type | Outcome | Ref |
|---|---|---|---|---|---|
| Acute clip impact-compression injury at T2 | Rat | Hyaluronan and methyl cellulose (HAMC) | Adult brain-derived neural stem/progenitor cells (NSPCs) | • Improved behavioural recovery<br>• Significantly reduced cavitation<br>• Improved graft survival<br>• Increased oligodendrocytes' differentiation | [38] |
| Acute T11 hemisection | Canine | PLGA | Human NSC | • Grafted NSC survived implantation procedure<br>• Showed migratory behaviour to residual spinal cord tissue | [39] |
| T10 Transection | Rat | Matrigel | Primary NSC | • Improved behavioural recovery and neuronal and reactive astrocyte | [43] |
| T3 Complete transection | Rat | PEG-GelMa | Spinal cord derived neural progenitor cells | • Enhanced axon regeneration,<br>• Aligned host astrocytes with the growth axis of the host axonal fascicles | [44] |
| C7 lateral hemisection | Rhesus monkeys | Fibrin Matrix | Human spinal cord derived neural progenitor cells | • Improved axon regeneration and formation of synapses | [45] |
| Acute contusive SCI | Rat | PLGA or chitosan | BMSCs | • Improved cell engraftment and functional recovery | [46] |
| Acute hemisected SCI | Rat | Collagen | BMSCs | • Reduced the expressions of inflammatory cytokines,<br>• Enhanced axonal regeneration, and motor functional recovery | [47] |
| Acute hemisected SCI | Rat | Acellular spinal cord (ASC) | BMSCs | • Decreased macrophages and lymphocytes around the injury site,<br>• Reduced neural cells apoptosis,<br>• Enhanced locomotor functions | [48] |

A wide range of scaffolds manufactured using various fabrication techniques has been investigated to design tissue engineering constructs towards the goal of tissue reconstruction and repair. Scaffolds are considered as structural support for cell delivery and tissue regeneration to create a 3D microenvironment for cell cultures. Utilization of bioscaffolds and 3D cell culture methods have received attention owing to the great possibility of remodelling biological environment [49-51]. Scaffolds with tuneable properties have also been given growing attention and proved to have significant effects on cellular responses. However, scaffold materials suffer from poor bioactivity and increased risk of rejection, later can be reduced by coating of the scaffold with ECM proteins to improve cell adhesion and growth [52]. Mainly, fabrication techniques and material compositions of scaffolds play important roles in their potential properties for tissue engineering products. In the following subsections, these requirements and materials commonly used will be discussed and how graphene can play a significant role on both of these fronts.

## 2.3 Scaffold Requirements

There are some essential requirements, regardless of the tissue type, for designing scaffolds in tissue engineering and biomedical applications. The very first key consideration in determining the appropriateness of a scaffold is its suitable biocompatibility. This feature is important for both *in vitro* and *in vivo* conditions in a way that the scaffold material must not elicit toxicity to cultured cells and also prevent inflammatory response and rejection of the host tissue upon its implantation. This is the reason why naturally obtained polymers have received a great amount of attention for the design and fabrication of tissue engineering scaffolds [36]. It is generally believed that unsatisfactory biocompatibility could provoke poor cell attachment and growth. Thus, some post-fabrication processes are required to modify the bulk properties of scaffold materials to develop their biocompatibility [53].

Moreover, scaffold's architecture is another main criterion that is characterized by porosity and interconnectivity of pores as well as surface area. High porosity and interconnected porous structure are critical for cellular migration, penetration and vascularization as well as the exchange of nutrients and waste products out of the scaffold [37]. Cellular performance and interactions can be considerably influenced by the mean pore size of the scaffold with pore sizes large enough to allow cell penetration into the construct and small enough to allow effective culture of a critical number of cells on the scaffold. Thus, a scaffold is strictly required to be fabricated with specific pore sizes depending on the optimum porosity based on the tissue being engineered [54, 55]. For axonal growth, for instance, it was reported that scaffold with pore sizes ranging from 20 to 50 μm is efficient for cell migration and transport. However, in brain tissue regeneration, pore sizes between 80 to 100 μm are recommended for the development of tissue formation [56]. In addition to the porosity, scaffold geometry greatly affects the cell intrusion, cellular network formation and tissue ingrowth. Mostly, cells have a tendency to align along the scaffold geometry depending on the pore shapes throughout the 3D structure. Improved tissue regeneration process in response to the geometrical design of scaffolds has been evaluated recently. A number of studies have consistently explored that surface curvatures and topography could stimulate tissue growth process [57, 58]. Accordingly, it was shown that concave surfaces are more favourable for tissue growth in comparison with convex and flat surfaces. Moreover, variations in the geometrical design of scaffolds found to be effective in cell attachment, migration and morphology [59].

Biodegradability is considered as another important criterion of scaffold biomaterial which enables the substitution of the implanted scaffold with a controlled interconnected cellular infusion. This also eliminates the need for a second surgery to remove the implanted scaffold in clinical practice. The by-products of biodegradation must not be toxic or cause an inflammatory response to other organs or tissues [60, 61]. It is observed that the biodegradability of scaffold materials positively affects cellular migration and proliferation [62]. The by-products of biodegradation must not be toxic or cause inflammatory response to other organs and tissues [60, 61]. Moreover, the rate of biodegradation should supportively follow the regeneration rate of nerve tissue at the injury site. Reconstructing neuronal cells requires a low degradable scaffold with swelling properties to resist nerve compression and implantation collapse [63].

Another key factor in designing tissue engineering constructs is the mechanical properties of the scaffold. The mechanical integrity should be maintained at a sufficient level to handle surgical implantation while withstanding forces generated from surrounding tissues after the injury such as wound contraction forces. For each specific tissue in the body, there exists a range of mechanical strength which should be taken into account when designing and preparing scaffold to allow proper regeneration process and load-bearing. Moreover, it has been reported that there should be a balance between scaffold stiffness and porosity of any scaffold to give rise to the desired capacity for vascularization and cell infiltration [37, 64].

In terms of the commercial viability of scaffolds in the clinical perspective, the scaffold materials and fabrication process should be cost-effective and scalable in a research laboratory. Furthermore, reproducible and controlled fabrication process with minor batch-to-batch variations can ensure the effective translation of tissue engineering approaches to clinical applications [65, 66].

## 2.4 Scaffold Fabrication Techniques

There are many fabrication techniques for designing scaffolds with different characteristics. A summary of these techniques is discussed below.

### 2.4.1 Solvent Casting/Salt Leaching Technique

Solvent casting is one of the straightforward and cost-effective preparation methods of scaffolds. This method is based on the evaporation of some polymeric solvent solution to create scaffolds out of the mould. Pores are created by leaching out the salt crystals after the scaffolds are soaked in a water bath as shown in Figure 2.1. The dissolution of salt and evaporation of the solvent creates a porous structure which is favourable in biomedical applications [67]. Salt leaching was employed in a study by Kumar et al. to fabricate 3D scaffolds based on graphene and PCL to examine the biological behaviour of osteoblasts. It was found that osteoblasts could differentiate and proliferate in the fabricated porous composite foams [68]. However, one of the main problems of this technique is the toxicity of solvent residues remained in the scaffold. Therefore, an extra step of full vacuum drying process is required to take away the toxic solvent which makes the process time-consuming [69, 70]. In a work by Cha et al., graphene-based hydrogels were fabricated using a solvent casting technique. The structure contains a mixture of methacrylated graphene oxide and gelatin methacrylate. The prepared hydrogels showed improved mechanical properties and biocompatibility with fibroblast cells [71].

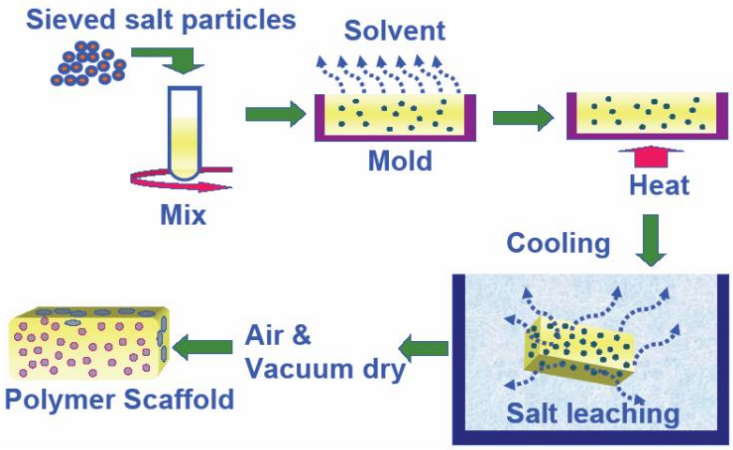


*Figure 2.1. Schematic Diagram of Solvent Casting/Salt Leaching technique [72]*

### 2.4.2 Self-assembly Technique

The self-assembly technique has been used to fabricate different nanofibers with the potential of constructing tissue engineering scaffolds. This method can be defined as non-intervention organization of molecules into structures/patterns [73]. This strategy has been extensively utilized in the fabrication of graphene-based scaffolds for tissue engineering applications. For instance, a recent study evaluated the therapeutic efficacy of scaffold fabricated by self-assembly technique [74]. The composite scaffold based on hydroxyapatite and reduced graphene oxide could promote bone regeneration and can be effectively used for the treatment of tumours. In other work, Nie et al. constructed a porous bioscaffold via self-assembly for *in vivo* evaluation of bone defects healing [75]. The 3D biocompatible scaffold composed of reduced graphene oxide and hydroxyapatite was studied in terms of bone mineralization and cellular behaviour. It was reported that the self-assembled rGO-based composite promoted cell proliferation and reconstruction of the defect site upon scaffold implantation. In addition, Girão et al. took advantage of the self-assembly method for the production of 3D graphene oxide/collagen scaffolds. It was indicated that the resulted porous network with desirable structural integrity could be beneficial in cellular activity and microenvironments [76].

### 2.4.3 Freeze-drying Technique

Freeze-drying is also a common fabrication route, based on the sublimation principle, to engineer scaffolds. The synthesized mixed solution is frozen and the solvent, which is normally water, forms ice crystals and is removed under high vacuum. The resulted freeze-dried scaffolds have high porosity, and a homogenous pore structure with interconnected pores [67, 77-79]. However, the pore size is controllable via the freezing temperature, freezing profile and stirring rate. Although this technique does not require a high temperature or leaching step, it suffers from a long processing time and limited pore size [80]. This method has been applied for the fabrication of graphene-based scaffolds to investigate their potential in tissue engineering and stem cell fields. For instance, graphene/PLLA and GO/gelatin-hydroxyapatite sponge-like scaffolds were used in bone tissue engineering [81, 82]. In addition, chitosan-graphene oxide scaffolds were prepared via the freeze-drying method by Valencia et al. The *in vivo* results presented scaffolds' ability to reconstruct bone tissues and excellent biocompatibility [83]. In another study, a 3D porous scaffold based on hydroxyapatite,

collagen, PLGA and graphene oxide was fabricated in a freeze dryer with various concentrations of GO. The freeze-dried composite scaffold with suitable biocompatibility was reported as a potential structure with well-established pores for bone tissue regeneration [84]. In a study by researchers in India, it was found out that PVA/CMC bioscaffolds containing different amounts of reduced graphene oxide prepared using the freeze-drying technique significantly improved *in vitro* proliferation of endothelial cells as well as *in vivo* angiogenesis and arteriogenesis [85]. Mohandes et. al, successfully synthesized a graphene-based composite scaffold containing chitosan and hydroxyapatite by the means of the freeze-drying method. The excellent bioactivity, proper morphological properties and high elasticity of the produced scaffold are also applied in bone tissue engineering applications [86].

### 2.4.4 Electrospinning Method

Electrospinning is a fabrication technique that uses the electrostatic force to produce polymeric ultrafine nanofibrous to microfibrous scaffolds as indicated in Figure 2.2. In this technique, the polymer solution is ejected as a result of a high-intensity electric field (10–40 kV) to deposit the nanofibers on the collector. Owing to high surface area and similar structure of produced fiber matrices to the natural ECM, these matrices demonstrated promising potential in the production of biomedical scaffolds. In addition, this method has been widely utilized for the fabrication of graphene-based tissue engineering scaffolds. For example, He et al. fabricated GO/alginate fibers by wet-spinning and studied the effect of GO concentration on mechanical strength and biocompatibility of cartilage cells [87].

In other work on coaxial spinning, composite biofibers containing graphene oxide and chitosan were prepared by Mirabedini et al. After injection of the composite solution into an ethanolic sodium hydroxide bath and creating the fiber on a stretching collector, the authors investigated the mechanical strength and biocompatibility with L-929 and PC-12 cells. In order to prepare electroactive fibers, L-ascorbic acid was utilized for the mild reduction of graphene oxide which can be subsequently useful in electrical stimulation purposes [88]. Furthermore, electrospun conductive scaffolds based on silk fibroin and graphene were examined for bone tissue engineering applications by Yang et al. This study claimed that the developed fibrous scaffolds with enhanced electrical and mechanical properties could make improvements to mesenchymal stem cells proliferation and tissue regeneration [89]. Another study on graphene-based scaffolds fabricated using the electrospinning method investigated the ability of the scaffolds in rat bone repairs. The scaffold which is composed of poly(3- hydroxybutyrate-co-4-hydroxybutyrate) and graphene oxide showed an enhanced porosity, mechanical strength, cellular behaviour, and fast bone regeneration capability [90].

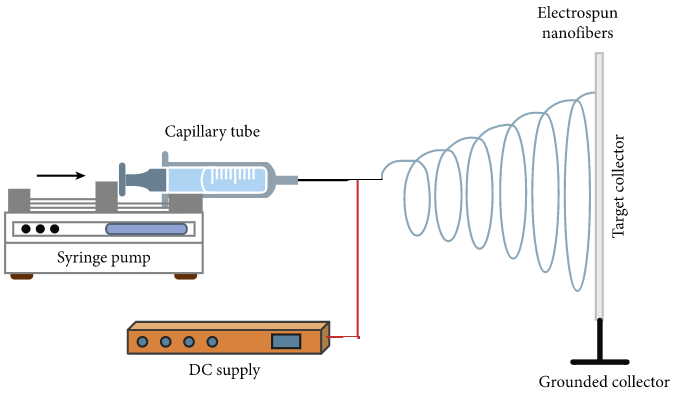


*Figure 2.2. Electrospinning Device [91]*

### 2.4.5 3D printing

3D printing is another controlled fabrication method for designing customized and precise structures for biomedical applications. This method, which is based on the rapid prototyping (RP) technology, can address drawbacks of the conventional methods in terms of their poor ability to strictly mimicking the biomechanical properties of tissues. Recently, 3D printed structures have attracted researchers' attention due to their ability to print various biomaterials with high precision and creating cell-laden scaffolds [69]. Particularly, graphene-based inks are being developed to be used for 3D fabrication of biomedical structures owing to graphene's suitable biocompatibility, electrical conductivity and hydrophilicity [92]. For instance, one study focused on the utilization of the poly(ε-caprolactone)/graphene scaffold in stem cell technology and bone tissue engineering. This scaffold was developed using an extrusion 3D printer and showed good biocompatibility with human adipose-derived stem cells [93]. In another similar work by Wang et al., a 3D-printed scaffold containing PCL and pristine graphene was investigated in terms of human stem cell viability, morphology and proliferation. It was found that scaffolds with good dispersion of pristine graphene resulted in competent biological performance for bone tissue engineering [94].

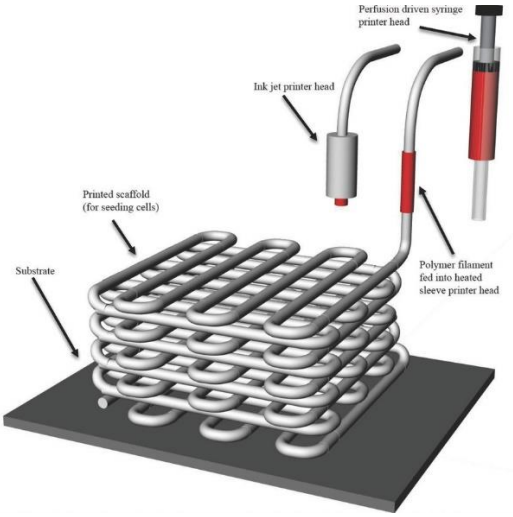


*Figure 2.3. Three-dimensional Printing Method [95]*

## 2.5 Scaffold Materials

There are a number of important factors which highly contribute to the success or failure of tissue engineering product development. Above all, tissue regeneration success critically depends on the scaffold biomaterial and its properties. Furthermore, scaffold biomaterials play a significant role in structural support and integrity, cell binding and tissue reconstruction rate [96]. It is important that the developed biomaterials efficiently mimic the native tissue microenvironment and encourage tissue formation [97, 98]. The biomaterials employed in the fabrication of tissue scaffolds are classified as naturally derived or synthetic based on their source [96]. In the provision of designing an appropriate carrier scaffold for production of clinically feasible tissue substitute, various natural and synthetic materials have been developed to regulate cellular behaviour and regenerate new cell types. Each of these biomaterials has advantages and disadvantages and thus utilization of biocomposites for the fabrication of tissue engineering scaffolds is becoming increasingly common [36].

### 2.5.1 Natural Materials

Numerous natural biological materials have been used in tissue engineering scaffolds owing to their excellent biocompatibility and structural resemblance to ECM. Additionally, natural biomaterials including collagen, cellulose, chitosan, alginate, hyaluronic acid, and gelatin are biologically active, promote excellent cell growth, and have non-toxic biodegradability [99]. A brief description of these is provided below.

Alginate: In the literature, it has been confirmed that alginate-based scaffolds have remarkable properties in tissue engineering and regenerative medicine including ease of manufacturing process, rapid gelation, low cost, biodegradability, high water uptake capability and biocompatibility [100]. Wang et al. have prepared 3D alginate scaffold with interconnected porous structure and investigated the cellular behaviour upon chondrocyte culture. It was reported that the fabricated scaffold is effective in terms of cell viability and proliferation for cartilage tissue repair [101].

Cellulose: The fabrication of low-cost 3D structures with a favourable microenvironment was discovered by the utilization of cellulose in tissue engineering biomaterials due to its suitable biocompatibility, bioactivity and customizability of mechanical and chemical properties [102-105]. For instance, a recent work by Laromaine et al. reported the successful fabrication and biological characterizations of 3D cellulose-based bioscaffold with controllable size and geometries seeded with mouse stem cells [106]. In another work by Sundberg et al, porous nanocellulose scaffolds showed enhanced proliferation and differentiation for bone repair [107].

Chitosan: Many studies have been undertaken to examine the potential use of chitosan-based scaffolds in several forms (sponges, fibers, and hydrogels) for the regeneration of various tissues such as skin, bone, cartilage, nerve, liver and muscle. The similar chemical structure of this natural polymer to ECM induced an appropriate platform for biological interactions with the host tissue [108]. In an *in vivo* study on dogs with injured phrenic nerve, it was found that implanted chitosan tube improved the nerve regeneration [109].

Gelatin: Another commonly used natural polymer as scaffold material is gelatin with promising applications in skin, bone, cartilage, nerve and kidney tissue engineering. The biodegradability,

biocompatibility, non-toxic by-products, and multiple available functional groups of gelatin have made this versatile biopolymer a suitable platform for cell adherence and growth [110]. A gelatin-based scaffold was prepared recently by Martin et al, [111] using a freeze-drying approach and tested with neural-lineage cells. Results showed that the fabricated 3D scaffold is highly biocompatible and is capable of promoting stem cell proliferation and differentiation.

Despite their various advantages, natural biopolymers have a weak mechanical strength, rapid degradation rate, poor structural integrity and batch-to-batch variations [112]. Hence, synthetic polymers received increasing attention during the last decades to overcome problems related to naturally-derived polymers.

### 2.5.2 Synthetic Materials

In the provision of designing an appropriate carrier scaffold for production of clinically feasible tissue substitute, various synthetic materials have been developed to regulate cellular behaviour and regenerate new cell types. There have been great efforts to produce scaffolds based on synthetic polymers including polystyrene, poly-l-lactic acid (PLLA), polyglycolic acid (PGA) and poly-dl-lactic-co-glycolic acid (PLGA). These scaffolds can be produced with tuneable architecture and characteristics depending on the composition of each polymer. Several synthetic polymers are demonstrated to be biocompatible based on FDA approval and have promising applications in tissue engineering products [113]. For example, PLA porous scaffolds showed good biocompatibility with Schwann cell proliferation and differentiation. Moreover, it is concluded that the prepared PLA foams could be used in rat injured spinal cord to promote axonal regeneration and myelination [114]. Another study reported the utilization of polyethylene glycol hydrogels for 3D neural precursor cell culture. The results of the study demonstrated that PEG hydrogel encourages cellular network formation, proliferation and differentiation to neurons and glia cells [115]. However, the low bioactivity and hydrophobicity of synthetic materials are one of the main concerns in the case of biological interactions.

*Table 2.2. Biomaterials in manufacturing of tissue engineering scaffolds*

| Source | Scaffold Material | Remarks | Ref |
|---|---|---|---|
| Natural | Alginate | • Biocompatible<br>• Easily functionalized<br>• Good cell recognition<br>• Simple gelation methods | [116, 117] |
| | Cellulose | • Good biocompatibility<br>• Good cellular interaction<br>• Poor mechanical strength | |
| | Chitosan | • Biologically renewable<br>• Biodegradable<br>• Non-toxic<br>• Poor mechanical properties | |
| | Gelatin | • Biodegradable<br>• Biocompatible<br>• Poor mechanical properties | |
| Synthetic | PLLA, PLGA, PGA | • Biocompatible | [118] |

| | | | |
|---|---|---|---|
| | | • Tuneable mechanical degradation properties<br>• Good biodegradation rate<br>• Poor cell adhesion<br>• Acidic degradation by-products | |
| | PEG | • Biocompatible<br>• Hydrophilic<br>• Tuneable mechanical degradation properties<br>• Poor cell affinity | [119] |

The challenges associated with the utilization of natural and synthetic polymers (as shown in Table 2.2) have resulted in the introduction of composite scaffolds with various compositions in order to enhance the biological activity of synthetic polymers and improve the mechanical properties of natural polymers. Also, the resultant composite materials may have superior properties of the individual materials [36].

### 2.5.3 Composite Materials

It is well documented that composite scaffolds have been applied extensively in the fields of bone, nerve, ligament, cartilage and cardiac tissue engineering [120]. Numerous ranges of biomaterials have been tested for the fabrication of composite scaffolds to support and promote tissue regeneration and cellular activity. For example, due to poor mechanical strength and electrical properties of alginates, the application of the material has been limited toward skeletal and electroactive tissues [121]. In addition, it was reported that alginate has poor biological properties which could have a great effect on *in vivo* cellular and molecular signalling [122]. To address the problems, researchers have suggested the combination of alginate with other polymer and/or nanomaterials to construct effective 3D scaffolds. For instance, Kim et al, successfully fabricated PCL/alginate scaffolds with enhanced osteoblastic cellular behaviour in comparison with control samples based on pure PCL [121].

Furthermore, another alginate-based composite scaffold was developed by Wang et al using a freeze-drying method. The blended porous scaffold composed of silk fibroin and sodium alginate showed suitable integrity for cell culture purposes. It was demonstrated that the prepared scaffold has good biocompatibility along with improved proliferation which can be employed as a capable construct for repairing diseased/injured soft tissues [123]. In another work, a neural scaffold based on chitosan and alginate was produced by ionic interactions with high pores interconnectivity and hydrophilicity which resulted in enhanced neural proliferation [124].

In the field of neural tissue engineering, another alginate-based composite hydrogel was synthesized with the incorporation of hyaluronic acid and explored in terms of Schwann cell performance. It was shown that this 3D hybrid scaffold could support cellular activity and growth within its inner porous structure [122]. Furthermore, in a recent study by Yao et al, the chitosan/alginate composite scaffold was compared with pure chitosan- and alginate-based scaffolds in terms of capability to regenerate nerve fibers and repair rats with the injured spinal cord. It was observed that composite and alginate-only scaffolds failed to support the damaged tissue after implantation which could be due to the quick degradation rate [125].

### 2.5.4 Carbon-based Materials

Another example of biomaterials as tissue engineering scaffolds is carbon-based nanomaterials with favourable mechanical, chemical and biological properties. Several carbon-based derivatives such as graphene, carbon nanotubes, carbon dots, and nanodiamonds have been used as scaffold biomaterial to reconstruct a variety of tissues. These derivatives have been shown to affect cell morphology, migration, growth, proliferation, and differentiation which could eventually influence the tissue regeneration. In addition, their substantial stimulating effects on efficient nutrient delivery, suitable chemical properties to facilitate cell interactions, can be considered as merits of carbon-based scaffolds for biomedical applications [126]. For instance, Sitharaman et. al fabricated a porous nanocomposite scaffold based on polymer/ Single-walled carbon nanotubes (SWCNTs) for implantation in a rabbit model. The *in vivo* study revealed that the bone tissue growth was improved after the implantation of the prepared composite scaffolds compared to the individual polymer scaffolds [127]. In another study by Zhou et al, the morphological and electrical properties of PCLF scaffold was improved after incorporation of CNT. Also, the prepared conductive composite scaffolds have shown enhanced neural cell growth, neurite extension and differentiation [128]. Despite the advantageous properties of CNTs as tissue scaffolds, its application has been partially limited due to its uncertain biocompatibility, insolubility and nonbiodegradability [126, 129].

## 2.6 Graphene Characteristics

Among all nanostructured carbon materials, graphene is considered as the most emerging material for effective tissue regeneration in a number of applications. The suitable biocompatibility of graphene-based family has enabled their utilization in drug delivery, bioimaging, biosensor, antibacterial interfaces, cancer therapy, and tissue engineering applications [130]. Several studies have investigated the feasibility of graphene derivatives in creating nanocomposite scaffolds. Incorporation of graphene highly enhances the mechanical and electrical properties as well as the bioactivity of the resulted composite construct. In addition, studies have demonstrated the extensive potential of graphene in the fabrication of nanocomposite scaffolds due to its good mechanical properties and bioactivity. Being the most versatile nanomaterial, graphene with its exceptional characteristics can interact with various biomolecules including DNA and proteins resulted in employing graphene and its derivatives in a wide variety of regenerative medicine and tissue engineering applications during the past few decades. Owing to graphene's excellent optical, electrical and mechanical properties, developments in stem cell-based tissue engineering have greatly depended on graphene-based scaffolds, particularly in terms of inducing cell differentiation and proliferation [131, 132]. Additionally, the ability of graphene to be modified and functionalized easily has led the material to be employed in wider applications of the health care industry [133].

Various graphene derivatives including GO and rGO have been employed as tissue engineering scaffolds. Reduced graphene oxide (rGO) can be obtained using various reduction methods including hydrothermal, chemical, photocatalytic, electrochemical, green methods and solvothermal. This material is very attractive for electroactive tissue regeneration due to its good electrical conductivity. Most of the previous studies took advantage of the utilization of GO as a filler material due to high dispersibility compared to rGO. However, the conductivity of reduced graphene oxide-based composites provides a path for external electrical stimulation purposes [134].

Graphene production route significantly affects the properties of the produced structure, as a result, the outcome of cellular behaviour could be highly affected by fabrication parameters such as synthesis approach, washing steps, reducing reagents, the amount of surface oxygens, etc [135]. For instance, in one study, GO reduced using ascorbic acid as an alternative for hydrazine resulting in a more favourable structure for medical applications. Accordingly, the rGO with ascorbic acid coated on the collagen scaffold and showed excellent cell viability [136]. Overall, graphene could be physically and/or chemically modified to develop a competent platform for biomedical applications. As evidenced from the literature, solution blending was appeared to be the most preferred method for synthesis of graphene biocomposites comparing to other preparation methods including UV-assisted crosslinking synthesis, microwave-assisted synthesis and synthesis by the means of covalent bonding.

## 2.7 Graphene-based Scaffolds in Tissue Engineering

Many graphene-based materials are already being combined with other biomaterials to effectively improve their mechanical, electrical and biological properties and construct tissue engineering matrices. A number of these studies are dedicated to investigating the potential of graphene-based composites in tissue engineering applications. For instance, Shin et al [137] incorporated graphene oxide inside gelatin hydrogels and analysed its characteristics for 3D encapsulation of fibroblasts. This scaffold presented superior cellular viability, proliferation, spreading, and alignment comparing with pure gelatin methacrylate hydrogel. The addition of GO significantly enhanced mechanical and electrical properties as well as cellular interactions. In another study, high hydrophobicity and poor bioactivity of PDMS, colossal obstacles toward accomplishing tissue engineering scaffolds, have been ameliorated by reduced graphene oxide coating. The results of this study showed that the enhancement in the mechanical properties and improved growth and differentiation to osteogenic cell lineages on the 3D porous rGO-PDMS scaffold encouraged the further utilization of graphene-based composite scaffolds for osseointegrated implant [138].

In excitable tissues, design challenges of composite scaffolds involve mimicking and providing the electrical microenvironment and coupling with the targeted tissue. Therefore, conductive scaffolds attracted a great deal of attention in engineering of cardiac and nerve tissues to improve the transmission of electrical signals [139]. Among many materials, graphene-based materials are highly promising for the restoration of electrically excitable living tissues due to their excellent electrical properties [140]. In cardiac tissue engineering, graphene was used to make electrically conductive scaffolds. For instance, Jiang et al. [141] developed chitosan/graphene oxide scaffolds with suitable cell viability, porosity and swelling ratio for the culture of cardiac cells. It was observed that conductive scaffolds could give rise to the promotion of cell adhesion and cellular network formation. Besides, the prepared scaffolds provided a platform for further electrical stimulation. CVD-grown 3D porous graphene foams were prepared by Li et. al and seeded with NSCs in order to examine its potential in neuronal growth and differentiation *in vitro*. It is found that NSCs growth, proliferation and differentiation into astrocytes and neurons enhanced when cultured on 3D conductive graphene foam. It is also concluded that the excellent conductivity of the produced graphene foams can be further effective in electrical stimulation and neural prostheses [142]. In another study by Hong et al. CVD grown 2D graphene film showed suitable biocompatibility as well as good neurite outgrowth which is essential for repairing nerve gaps [143].

Furthermore, graphene-based materials showed good bioactivity for cell performance and tissue regeneration. In a recent study conducted in Australia [138], the coating of reduced graphene oxide on 3D PDMS scaffolds significantly improved bioactivity, cell differentiation and osteointegration. Also, the developed scaffold showed suitable mechanical properties and porous structure for stem cell growth and proliferation. Another study by Lalwani et al also suggested the utilization of 3D graphene scaffolds fabricated by crosslinking of graphene oxide nanoribbons. It is indicated that synthesized scaffolds not only support good cell viability and proliferation but also keep cell at metabolically active state with cells spreading through the scaffold pores [144].

Owing to the excellent mechanical properties of graphene, GO was added to PAA hydrogels to improve the mechanical stiffness and thermal stability of the hydrogel for a wide range of applications [145]. In another study, GO is incorporated inside GelMA hydrogels to enhance the mechanical strength and electrical properties for the construction of tissue replacements [137]. The results of the study revealed that hybrid hydrogel improved 3D cellular performance and proliferation.

It has been demonstrated that graphene-based materials combined with stem cells offer a facile microenvironment for neuronal differentiation and organized neuronal network formation to reconnect damaged nerves. For instance, Yang et al [146] showed that embryonic stem cells (ESCs) loaded on graphene oxide substrates notably improved differentiation into dopaminergic neurons for up to GO concentration of 100 µg/mL. Similarly, in another study [147], it is found out that MSCs cultured on functionalized graphene made an improvement in metabolic activities of cells and resulted in differentiation of these cells into neuronal cell lineages. In the case of NSCs, Park et al [148] initially demonstrated the role of graphene in human NSCs behaviours. The findings of the study suggested that graphene improves proliferation and neuronal differentiation compared with the control samples. In addition, Lalwani et al [144], took advantage of graphene oxide physiochemical properties to fabricate 3D composite scaffolds based on single- and multiwalled graphene oxide nanoribbons. These scaffolds showed suitable cytocompatibility, cell adhesion and proliferation when seeded with adipose-derived stem cells (ADSCs) and murine MC3T3 preosteoblast cells.

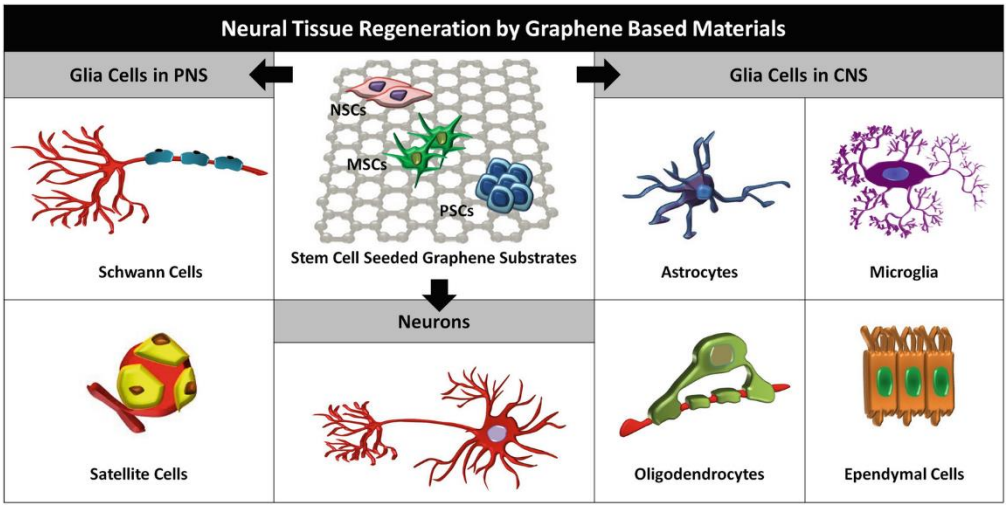


*Figure 2.4. Neural tissue regeneration on graphene-based materials [149]*

Graphene-based substrates have a promising potential in the differentiation of stem cell sources to neurons, as shown in Figure 2.4, which is important in successful neuronal regeneration.

Weaver et al. [150] reported on developing a conductive platform based on GO and PEDOT to improve neuronal differentiation. Also, it is evidenced the differentiation rate of oligodendrocytes improved on GO-coated PCL substrates compared to the control substrate with no coating. Similarly, Solanki et al have acknowledged that silica nanoparticles coated with GO promoted differentiation and axonal alignment [151]. Also, it is identified that graphene-based substrates are able to retain high cell viability during the stem cell differentiation process. The unique surface chemistry of graphene effectively induces stem cell differentiation which is very favourable in tissue engineering applications [152-154].

Additionally, it is confirmed that graphene-based materials can be effectively utilized in the electrical stimulation of neural cells to promote growth, proliferation, axonal growth and differentiation of neural lineage [155, 156]. Recently, the potential of 3D graphene scaffold was analysed using electrical stimulation to differentiate neural progenitor cells. Electrical stimulation could enhance cell growth and morphology. The excellent electrical conductivity of graphene scaffolds provides a valuable 3D culture system for electrical stimulation to enhance neuron maturation, while simultaneously facilitating therapy of neurological disorders in human [157]. Conductive porous graphene foams presented excellent performance under electrical stimulation of human neural stem cells which resulted in elongated and the directional growth of neural cells as well as enhancement of differentiation and proliferation [158]. In another similar study, graphene foams showed upregulating Ki-67 protein expression upon neural stem cell culture. The cells formed a connected 3D network through the macroporous scaffold which is important in cell attachment and growth. Cellular metabolism and communication have been improved in 3D graphene foams compared to 2D graphene substrates [142].

Due to modifiable topography and characteristics of graphene-based scaffolds through different fabrication conditions, graphene-based scaffolds contributed to proliferation and cell interactions of a wide variety of tissues, as listed in Table 2.3. Based on the previous research outcomes, although graphene-based scaffolds exhibited a great potential in creating tissue engineering scaffolds, the synthetic conditions which affect the properties of scaffolds have to be engineered to match the desired requirement by the targeted application [159-161].

*Table 2.3. Graphene-based scaffolds in tissue engineering applications.*

| No. | Scaffold | Graphene Synthesis | Scaffold Preparation Method | Response | Application | Ref |
|---|---|---|---|---|---|---|
| 1. | GO/Chitosan | Not specified | Freeze Drying | • Good cell viability<br>• Promoted cell attachment<br>• Intercellular network formation<br>• Upregulation of the cardiac-specific gene,<br>• Expression of protein involved in muscle conduction of electrical signals | Cardiac tissue Engineering | [141] |
| 2. | GO/Chitosan | Modified Hummers' method | Freeze drying | • Aligned porous 3D scaffolds resembling bone lamellae<br>• Improved mechanical strength and shape-memory<br>• Aligned cell guiding capabilities<br>• Enhanced protein adsorption ability | Bone tissue engineering | [162] |
| 3. | GO nanoflakes incorporated into a gelatin–hydroxyapatite (GHA) | Modified Hummers' Method | Freeze drying | • Improved compressive strength<br>• Yield strength and WOF of composite scaffolds with GO<br>• Enhanced osteogenic differentiation | Bone tissue engineering | [82] |

| | | | | | | |
|---|---|---|---|---|---|---|
| 4. | Graphene/HA hydrogels | Commercial GO (Graphene Laboratories Inc., Calverton, NY, USA) | Colloidal solution mixing, hydrothermal treatment and dialysis | • Excellent mechanical properties<br>• High electrical conductivity<br>• High SSA, and good cell compatibility | Bone tissue engineering | [163] |
| 5. | 3D Graphene Nanofiber | Not specified | Electrospinning method | • Recoverable electrical conductivity<br>• Excellent biocompatibility and physicochemical stability<br>• Improved growth and development of the primary motor neurons for cellular electrical stimulation | Neural tissue engineering | [164] |
| 6. | GO/PVA | Modified Hummers' Method | Electrospinning method | • Increased mechanical strengths after the addition of GO<br>• Good osteoblasts viability<br>• Improved cell adhesion and spreading | Bone tissue engineering | [165] |
| 7. | Single-layered graphene (SG) or multi-layered graphene (MG) and polycaprolactone (PCL) | Purchased from Graphene Technology (China) | 3D printing and layer-by-layer casting (LBLC) method | • Improved neural expression both *in vitro* and *in vivo*<br>• Promotion of axonal regrowth and remyelination | Neural tissue engineering | [166] |

| | | | | | | |
|---|---|---|---|---|---|---|
| 8. | 3D graphene foam | CVD-grown | Chemical vapor deposition method with Ni foam | • Improved electrical coupling between the scaffold and differentiated cells<br>• Enhanced 3D formation of neuronal networks | Neural tissue engineering | [142] |
| 9. | 3D rolled GO foam | Modified Hummers' method | Soft rolling the laminin-functionalized GOF layers | • Generating a neuronal fiber along the axis of the porous cylindrical-like scaffold | Neural tissue engineering | [158] |
| 10. | Chondroitin sulfate (CSMA)/PECA/GO | Modified Hummers' method | Heat-initiated free radical method and Freeze-drying | • Improved chondrocyte morphology, integration, continuous subchondral bone<br>• Thickened newly formed cartilage<br>• Improved porosity, elasticity, swelling ratio, electrical conductivity and rational degradable time | Cartilage tissue engineering | [167] |
| 11. | GO/PLGA | Modified Hummers' method | Electrospinning | • Enhanced hydrophilic performance, and protein- and inducer-adsorption ability of the nanofibers<br>• Accelerated cell adhesion, proliferation and osteogenic differentiation | Bone tissue Engineering | [168] |
| 12. | rGO/PDMS | Modified Hummers', | Solvent Casting | • Improved mechanical strength and pore sizes | Bone tissue engineering | [138] |

| | | | | | | |
|---|---|---|---|---|---|---|
| | | Reduction by L-ascorbic acid | | • Supported growth and osteogenic differentiation of human stem cells | | |
| 13. | PCL/graphene | Water-assisted liquid phase exfoliation | Melt blending | • Stimulated cell proliferation, and lowered immune response suggesting high potential for *in vivo* bone regeneration | Bone tissue engineering | [169] |
| 14. | 3D graphene-cellulose | Modified Hummers' Method | Solution Mixing | • Robust neurite outgrowths and possible synapse formation *in vitro* | Neural tissue engineering | [170] |
| 15. | GO/PCL nanoscaffold | Purchased from Sigma Aldrich | Integration Moulding | • Facilitated long-term nerve regeneration *in vivo*<br>• Enhanced neurite sprouting and angiogenic restoration | Neural tissue engineering | [171] |
| 16. | Starch-based NanoGO | Starch-derived GO | Electrospinning | • Improved cytocompatibility, osteo-bioactivity, and biodegradability | Bone tissue Engineering | [172] |
| 17. | rGO nanomesh | Improved Hummers' Method | Drop-casting method | • Improved chemical stability<br>• Enhanced cell proliferation and differentiation to neural cells | Neural tissue Engineering | [173] |
| 18. | TCP/Gel/CH/rGO | Purchased | 3D printing | • Improved calcium deposition<br>• Enhanced alkaline phosphatase (ALP) activity | Bone Tissue Engineering | [174] |

According to the reviewed literature, graphene derivatives demonstrate unique physical, chemical, mechanical and electrical properties which can promote stem cell behaviour and enhance tissue repair in a wide range of applications including cardiac, bone and neural tissue engineering. Particularly, key properties of graphene-based biomaterials in NTE can be listed as their morphological structure, electrical conductivity, biocompatibility, biodegradability, and ability to induce neural differentiation [175]. Among graphene-based materials, GO has attracted attention in tissue engineering field due to its hydrophilic nature, excellent water dispersibility, suitable biocompatibility, and bioactivity owing to multiple oxygen functional groups on its surface to absorb protein, growth factors and biomolecules [176]. As a result, studies have shown that GO can prominently enhance the proliferation and differentiation rate of cultured neuron cells as well as bioactivity and biocompatibility of the scaffold biomaterials [177]. Furthermore, they have demonstrated that graphene and rGO are considered as permissive materials play an effective role in astrocyte growth, neurogenesis and axonal growth in case of implantation for the nervous system disease [178, 179].

Overall, engineering of functional scaffolds for regeneration of tissues highly depends on different design parameters such as selection of materials, synthesis techniques, etc. Although there has been great research conducted in fabricating novel biomaterials for tissue engineering scaffolds, there is a huge need for research and development of biomaterials that mimic the mechanical properties of host tissue and retain the integrity of the scaffolds during treatment in neural tissue engineering applications. Moreover, directing the cell behaviour and regeneration process by scaffold materials is of prime importance.

## 2.8 Chapter Summary

The developments in tissue engineering have attracted researchers' attention and have employed materials science and bioengineering fields. In this chapter, some existing developments in scaffold materials and fabrication technologies in tissue engineering applications have been outlined. These developments have resulted in a deep understanding of the mechanism of how tissue engineering outcomes can be influenced by selected materials. The utilization of graphene in designing 3D scaffolds creates a revolutionary impact on providing a favourable microenvironment for tissue regeneration. This chapter highlighted that blending different materials can improve the properties of the scaffold. Moreover, it is critical to meet the specific tissue engineering scaffold requirements to achieve functional 3D tissues and incorporation into the host. Before *in vitro* culture of cells on the scaffolds, it is important to develop certain physiochemical characteristics of the scaffold biomaterials in accordance with the targeted tissue characteristics. The current research in the field is highly focused on improving the properties of graphene family materials to create composite or functional bioscaffolds for further utilization in clinical research. The impacts and mechanism of graphene in inducing cells in neural tissue engineering still need to be deeply investigated. In addition, further studies need to be conducted to illustrate the cytotoxic effects of graphene-based materials on tissue regeneration prior to clinical applications. The significant amount of research in the literature emphasizes the role of synthetic and fabrication conditions of biomaterials in the ultimate performance of tissue engineering scaffold.

The development of a new class of scaffold materials based on graphene to facilitate culturing cells with matched microenvironment for cell growth and interconnected pores for penetration and migration of cells is the next important subject which is discussed extensively in Chapter

3 utilizing a broad range of characterization techniques. Furthermore, optimizing the properties of the prepared scaffolds for neural tissue engineering applications are investigated in the next chapter.

# CHAPTER 3: FABRICATION AND CHARACTERIZATIONS OF 3D GRAPHENE-BASED COMPOSITE SCAFFOLDS

## 3.1 Abstract

Neural tissue engineering provides enormous potential for restoring and improving the function of diseased/ damaged tissues and promising opportunities in regenerative medicine, stem cell technology, and drug discovery. The conventional 2D cell cultures have many limitations to provide informative and realistic neural interactions and network formation. Hence, there is a need to develop 3D bioscaffolds to facilitate culturing cells with matched microenvironment for cell growth and interconnected pores for penetration and migration of cells. Herein, the synthesis and characterization of 3D composite bioscaffolds based on graphene-biopolymer with porous structure and improved performance for tissue engineering are presented. A simple and eco-friendly synthetic method is introduced and optimized for synthesis of this hybrid fibrous scaffold by combining Graphene Oxide (GO) and Sodium Alginate (Na-ALG) which are specifically designed to match the mechanical strength of the central nervous system (CNS) tissue and provide porous structure for connective tissue engineering. Properties of the initially developed scaffold in terms of the structure, porosity, thermal stability, mechanical properties, and electrical conductivity are characterized and presented. In the next step, scaffold's properties were fine-tuned using key synthesis conditions including GO concentrations, reduction process and crosslinking time. This developed material will be used in the following chapters as a scaffold to explore the enhancement of neuron cell interactions and act as nerve conduits for neurological diseases.

## 3.2 Introduction

The most critical step in NTE is the assembly of bioscaffolds loaded with nerve cell sources to produce a 3D tissue substitute for transplantation [180]. These approaches intend to develop treatments for nerve disorders through the help of biomaterials and cell transplantation methodologies [53]. An appropriate regenerated nerve requires appropriate scaffold materials with suitable structural, mechanical, biological, and physical features that give rise to neurite and axonal growth, prevention of scar formation, and axonal alignment to the lesion area [181]. Therefore, materials development of these scaffolds is a topical and pivotal area of research that has attracted significant research interests in recent years. Thus, there is a need for the development of a new class of materials to provide enhanced features for neural tissue engineering [96]. To address these requirements, 3D composite scaffolds have attracted great attention due to their versatile properties to overcome limitations of those prepared by a single material. The most noteworthy advantage of composite materials for tissue engineering is that their properties can be easily adapted by modifying the composition and structure of biomaterials according to characteristics of specific tissue [182]. A number of different methods have been employed to construct porous 3D structures including solvent casting, 3D printing, gas foaming, freeze-drying, and phase separation. The freeze-drying approach is considered as one of the most common well-established methods for fabricating porous materials with controllable architecture for medical applications [67]. This fabrication process does not involve toxic solvents and rinsing steps which is certainly safe for biomedical uses. One of the common scaffold biomaterials with a similar structure to ECM is alginate which is

considered as a very promising natural polysaccharide polymer that can be isolated from renewable sources such as brown algae or microorganisms with applications in bioengineering [123]. It has many advantages since it is non-toxic, biocompatible, biodegradable, relatively low-cost in comparison with other polymeric materials, easy gelation using calcium chloride and appropriate as biomaterials to help the recovery of the malfunction tissues [183]. The properties of crosslinked alginate can be tailored by various concentrations of crosslinker as well as the crosslinking time. Although alginate-based scaffolds suffer from some limitations such as lack of mammalian cell receptors, poor ability to have control over the internal architecture, low protein adsorption capability and excessive hydrophilicity, they hold the potentials for being applied in tissue engineering due to the ease of processability and delivery of growth factors and cells [184]. To address these limitations, alginate is combined with other materials to form biocomposites that offer biological benefits of alginate together with good mechanical strength and bioactivity of the reinforcing material. One of the main challenges in designing a 3D composite scaffold for excitable tissues is to mimic the electrical microenvironment in order to improve cellular response and create an electrical coupling with the host tissue. As a result, conductive scaffolds have been studied extensively in the form of hydrogels, microporous materials, nanofibers, and hybrid materials to enhance the transmission of electrical signals [139]. Among many materials, graphene and its derivatives have emerged to be extensively explored in tissue engineering, regenerative medicine and other biomedical fields owing to their exceptional electrical and mechanical properties [140]. Particularly, graphene derivatives demonstrate unique physical, chemical, and electrical properties which can promote stem cell behaviour and enhance tissue repair. Critical characteristics of graphene-based biomaterials in NTE can be listed as their morphological structure, electrical conductivity, biocompatibility, biodegradability, and ability to induce neural differentiation [175]. Among graphene-based materials, GO has attracted attention in tissue engineering field due to its hydrophilic nature, excellent water dispersibility, better biocompatibility, and bioactivity owing to multiple oxygen functional groups on its surface to absorb growth factors and biomolecules [176]. Studies have shown that GO can prominently enhance the proliferation and differentiation rate of cultured neuron cells as well as bioactivity and biocompatibility of the scaffold biomaterials [177]. Furthermore, they have demonstrated that graphene and rGO are considered as permissive materials playing an effective role in astrocyte growth, neurogenesis and axonal growth in case of implantation for the nervous system disease [178, 179]. In the pioneering study by Wan et al., a 3D GO–alginate composite hydrogel was prepared via the direct mixing method showing improved mechanical strength and Young's modulus compared to pure alginate scaffold [185]. However, the structure suffers from poor stability in aqueous media which is a fundamental property for cell culture purposes. The addition of crosslinker in the blend solution made the structure instantly dissociated in water within several minutes which has a high probability of quick-dissolving in vivo. Hence, unable to guarantee good healing of tissue damage. On top of that, Sinha et al. recently reported the synthesis of the 3D rGO-embedded alginate scaffold by reducing GO using reducing agents such as hydrazine [186]. However, due to the toxicity of hydrazine and its traces left in the prepared scaffold, this method is not acceptable for biomedical and tissue engineering applications [174]. Besides, the addition of rGO in the mixing solution usually causes a poor water solubility and undesired aggregation which can adversely affect cellular behaviour and fate [187]. To address these problems, the aim of the present study is twofold. Firstly, it attempts to improve the fabrication method of the 3D graphene–alginate composite scaffolds

that uses a simple, scalable and environmentally sustainable fabrication technique involving solution mixing, freeze-drying, crosslinking, and bio-reduction. This method could enhance the stability of the 3D matrix in culture media. Secondly, it is to optimize the properties of the prepared 3D scaffold in terms of morphological, mechanical, and electrical characteristics to meet challenging requirements in neural tissue engineering. To accomplish the first aim, the synthetic procedure was improved which enables the production of conductive scaffolds based on the in-situ reduction of GO/Na-ALG aerogels with gelatin (a biodegradable collagen-based biomaterial) which makes the structure more favourable for cell culture. The advantage of the proposed bio-reduction process with gelatin is to eliminate the use of toxic reducing agents, which eliminated the need for using dangerous reducing agents such as hydrazine resulting in no harmful residue for neuron cells. Besides, strong reducing agents make the structure hydrophobic. The reduction of GO with gelatin is a relatively mild reduction method which does not cause severe damage to the edge morphology of GO and highly stable 3D composite structures can be prepared.To achieve the second goal, the influence of GO concentration, reduction process, and crosslinking time of the 3D structure was explored to establish the optimised GO content and synthetic conditions in order to achieve proper physicochemical, mechanical and electrical properties of Graphene Oxide–Sodium Alginate (GO/ Na-ALG) nanocomposite scaffolds. The fabricated 3D scaffolds are characterized by a broad range of characterization methods such as Scanning Electron Microscopy (SEM), micro-CT scanning, Dynamic Mechanical Analysis (DMA), Thermogravimetric Analysis (TGA), Cyclic Voltammetry (CV), and Electrochemical Impedance Spectroscopy (EIS).

## 3.3 Experimental Section

### 3.3.1 Materials and Chemicals

Sodium alginate (Na-ALG) was purchased from AJAX Chemicals (Sydney, Australia). Type B gelatin powder, extracted from bovine skin was purchased from Sigma-Aldrich. Calcium chloride dried (molecular weight of 110.99 g $mol^{-1}$, Chem-Supply) was used as the crosslinking agent. Natural graphite flakes were purchased from a local mine (Uley, Eyre Peninsula, South Australia, Australia). Potassium permanganate ($KMnO_4$, Sigma-Aldrich), 98% sulphuric acid ($H_2SO_4$, Chem-Supply), 85% w/w phosphoric acid ($H_3PO_4$, Chem-Supply), and 30% hydrogen peroxide ($H_2O_2$, Chem-Supply) were used during GO synthesis. High purity Milli-Q water (18.2 MU $cm^{-1}$, pH of 5.6) was used throughout the study

### 3.3.2 Synthesis of Graphene Oxide (GO)

Graphene oxide (GO) was prepared via the modified Hummers' method from graphite flakes [188]. Briefly, concentrated acids including sulphuric acid ($H_2SO_4$) and phosphoric acid ($H_3PO_4$) with a ratio of 9:1 were mixed with 2 g of graphite and 18 g of potassium permanganate ($KMnO_4$). The mixture was stirred and heated to 50 °C for 16 hours. The obtained solution was cooled with 400 mL of ice cubes and hydrogen peroxide was added to it subsequently. The brownish-colour solution was then centrifuged for two hours and washed with 30% HCl and water in order. After discarding the supernatants, the resultant GO paste was kept in the fridge for further use.

### 3.3.3 Preparation of graphene oxide/sodium alginate composite

The GO/Na-ALG aerogel was fabricated through incorporating GO into alginate matrix by combining freeze-drying and ionic cross-linking process, as reported earlier [189] with slight modifications. Briefly, as summarized in Figure 3.1, the GO suspension was ultrasonic-dispersed for 15 min to obtain a homogeneous dispersion. Meanwhile, sodium alginate (4 wt.%) was dissolved in deionized water and was constantly stirred to form a transparent solution. Then, GO suspension was added into the solution to get the final ratios of 0, 0.5, 1, 3 and 5 mg $mL^{-1}$, with continuous magnetic stirring, until a homogeneous dispersion was obtained. The GO/Na-ALG mixture was poured into moulds, frozen, and freeze-dried. After that, the aerogel was immerged in 1 M $CaCl_2$ solution for two different time intervals (1 h and 3 h) to achieve the calcium ion-induced cross-linking process. After cross-linked by calcium ions, the aerogel was washed with deionized water several times to remove the unbound calcium ions and was freeze-dried again to obtain the cross-linked GO/Na-ALG aerogel. The obtained GO/Na-ALG scaffolds with 0, 0.5, 1, 3 and 5 mg $mL^{-1}$ of GO are named as Na-ALG, GO/Na-ALG0.5, GO/Na-ALG1, GO/Na-ALG3 and GO/Na-ALG5, respectively. The dimension of each sample is almost 14 × 12 mm. Three samples per each condition were synthesized to obtain the average value along with their standard deviation [190].

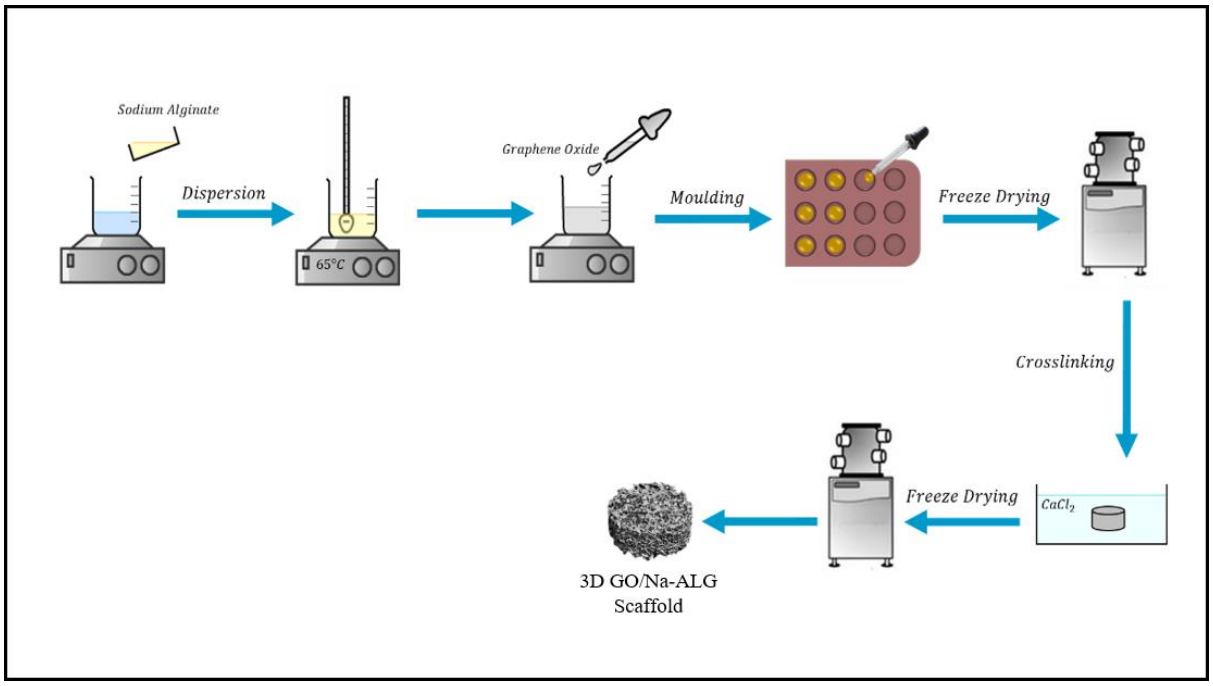


*Figure 3.1. Schematic diagram of the fabrication process of GO/Na-ALG scaffolds.*

### 3.3.4 Preparation of reduced graphene oxide/sodium alginate composite

As shown in Figure 3.2, the obtained GO/Na-ALG scaffolds with various concentrations of GO including 0.5, 1, 3, and 5 mg $mL^{-1}$ were incubated in 1 mg $mL^{-1}$ of gelatin at 95 °C. After 24 h, the samples are washed with deionized water and sent for freeze-drying in order to get reduced GO/Na-ALG (rGO/Na-ALG) samples named as rGO/Na-ALG0.5, rGO/Na-ALG1, rGO/NaALG3, and rGO/Na-ALG5.

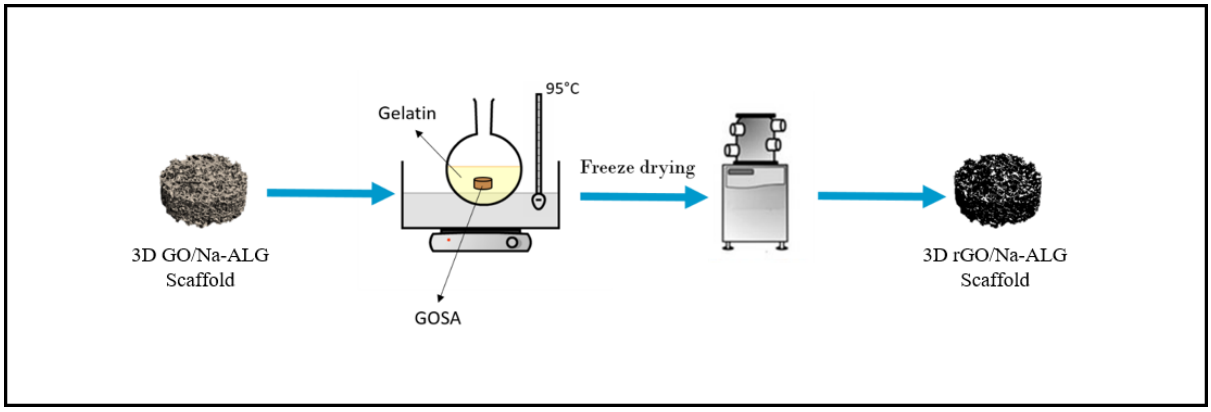


*Figure 3.2. Schematic diagram of the fabrication process of rGO/Na-ALG scaffolds.*

### 3.3.5 Materials Characterisation Techniques

**Raman Spectroscopy:** The Raman analysis was done by LabRAM Evolution, Horiba Jvon (Japan) with a laser excitation wavelength of 532 nm.

**Fourier Transform Infrared spectroscopy** (FTIR, Nicolet 6700): FTIR was used with a record between 4000 and 500 $cm^{-1}$.

**X-ray diffraction (XRD):** it was achieved by Rigaku MiniFlex 600 X-Ray Diffractometer (XRD) at the pipe voltage of 40 kV and the scan rate of 10 $min^{-1}$ to confirm the oxidation of GO. The measurement was performed in the $2\theta$ range from 5° to 60°. The cross-sectional area of scaffolds was cut using a blade and mounted on carbon tapes.

**Scanning Electron Microscopy (SEM):** SEM images were obtained (Hitachi, SU1510 high technologies) at an acceleration voltage of 30 kV to observe the porosity of samples. ImageJ software was utilized to analyse SEM images to measure pore sizes. The mean pore size and the standard deviations were calculated for at least 5 pores in each of the collected images (N=3) per scaffold type. These pores were selected randomly for both long and short pore axes.

**μ-CT Scan Images:** X-ray microtomography scans were carried out using a micro-CT scanner (SkyScan 1276, Bruker micro-CT, Belgium) operated at a source voltage of 55 kV and source current of 200 μA with 0.25 mm aluminium filter. The samples were rotated to 360° with a rotation step of 0.3° and a frame averaging of two. Then, the obtained images were reconstructed by NRecon software. The volume of interest was selected in the centre of the scaffold to measure scaffold structures only. 3D images and qualitative data of scaffold formation were achieved by CTAn and CTVol software, respectively.

**Thermogravimetric Analysis (TGA, Q500 TA instruments):** TGA in a nitrogeneous atmosphere was performed to study the thermal stability of the composite structure. During this test, samples (approximately 2.3 to 5 mg) were placed in platinum crucibles and heated from room temperature to 900° C at the rate of 10° C $min^{-1}$.

**Dynamic Mechanical Analysis (DMA):** The mechanical properties of porous scaffolds were tested with the TA Q800 DMA machine in the compression mode. The test was performed at ambient temperature with a controlled force rate of 1 N $min^{-1}$. All samples were kept hydrated

by storing them in distilled water 24 hours prior to the test. The height of the scaffolds was measured automatically at 0.1 N tare load.

**Contact Angle Measurements:** Wettability measurements were conducted at room temperature with Milli-Q water by the sessile drop method using a tensiometer (Attension Theta optical tensiometer). The mean contact angle was reported according to measurements of three different spots on each sample.

**Shear Rate Ramp Test:** The rheological properties of the cross-linked and uncross-linked samples before freeze-drying have been determined using an automated rheometer (MCR 301, Anton Paar) with a 49 μm cone and plate fixture.

**Porosity Measurements:** The density and porosity of the obtained scaffolds were calculated using the following equations [191]:

$$\varepsilon = \left(1 - \frac{\rho}{\rho_0}\right) \times 100\% \quad (2.1)$$

$$\rho_0 = \rho_{0,NA-ALG} \times w_{NA-ALG} + \rho_{0,GO} \times w_{GO} \quad (2.2)$$

where ε is the percentage of porosity, $\rho$ is the mass density of aerogel samples, $\rho_0$ is the theoretical mass density, and w is the weight fraction of each component of the material. The densities for graphite and sodium alginate were taken as 2.2 $gcm^{-3}$ and 1.6 g $cm^{-3}$, respectively.

**Swelling Ratio Measurements:** The swelling ratio of the scaffolds was determined by using the equation given below [192]. Briefly, the dried samples were weighed and noted as $W_0$. The scaffolds were then immersed in phosphate-buffered saline (PBS) and were incubated at 37 °C. At different time intervals, the weight of the scaffolds was measured and noted as $W_t$. The experiment was carried out in triplicates.

$$\text{Swelling index} = \left(\frac{W_t - W_0}{W_0}\right) \quad (2.3)$$

**Electrochemical Characterizations:** Both electrochemical measurements including cyclic voltammetry (CV) and electrochemical impedance spectroscopy (EIS) were taken using an electrochemical working station (HCH 850) with a three-electrode system in PBS. CV measurements were performed at a voltage range between 0 and 1.0 V with a scan rate of 100 mV $s^{-1}$. Regarding impedance measurements, compressed layers of conductive, rGO/Na-ALG, scaffolds were moistened in PBS and pressed between two gold electrodes. EIS was measured in the frequency range of 0.1 Hz to 0.1 MHz with a disturbance amplitude of 1 mV.

## 3.4 Results and Discussion

### 3.4.1 Characterizations of synthesized GO

Prepared GO was characterised by a series of characterization methods to confirm their properties which are summarised below. Figure 3.3 (a) shows FTIR spectrum of GO with its corresponding functional groups. A broad peak at 3309 $cm^{-1}$ and another peak at 1625 $cm^{-1}$ correspond to stretching and bending vibrations of OH groups in GO. The peaks at 1706 $cm^{-1}$ (C=O) and 1005 $cm^{-1}$ (C–O) are caused by carbonyl, carboxylic and epoxy groups. These oxygen-containing groups on GO spectra confirm the successful oxidation of graphite [193].

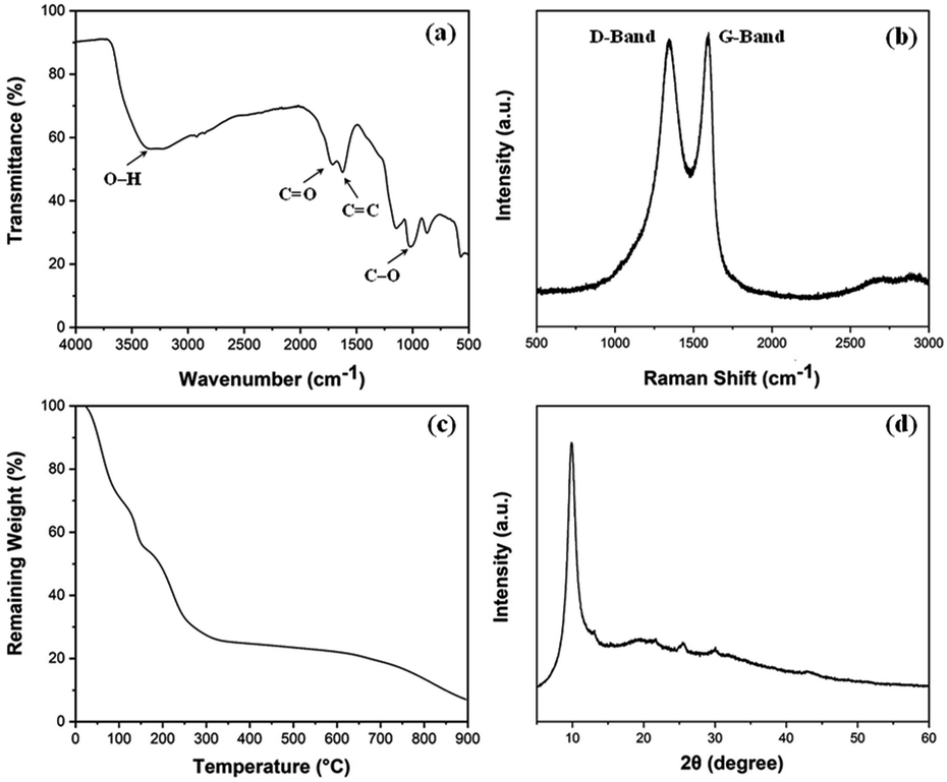


*Figure 3.3. (a) FT-IR plot, (b) Raman spectra, (c) TGA curve and (d) XRD pattern of the synthesized graphene oxide (GO).*

Figure 3.3 (b) shows the Raman spectrum of GO which defines its crystalline structure by considering the conjugated and carbon–carbon double bonds and structural defects. The high-intensity peaks can be observed at 1590 $cm^{-1}$ and 1346 $cm^{-1}$ which correspond to G-band and D-band, respectively. These typical peaks are indicative of significant structural disorders during the oxidation process. Also, the absence of the 2D (~2600 $cm^{-1}$) band points out that GO is dominated by the fully-disordered $sp^2$ bonding network [194]. The thermal stability of GO under nitrogen atmosphere up to 900 °C was investigated using TGA as shown in Figure 3.3 (c). The figure highlights the weight loss around 100 °C is related to the removal of water molecules trapped inside the GO structure. The major weight loss between 200 to 400 °C can be ascribed to the thermal decomposition and complete removal of residual oxygen functional groups [195]. The XRD measurement shown in Figure 3.3 (d) indicates the crystalline properties of prepared GO. The absence of the characteristic peak of graphite at ~26° and the existence of the GO peak at 9.88° validates the oxidation of graphite [196].

### 3.4.2 Morphology and structure of fabricated composite scaffolds

Figure 3.4 (a–c) displays the sponge-like feature of fabricated graphene composite aerogels with low density. This is attributed to the optimum concentration of both GO and Na-ALG which made the composite scaffold with a proper elastic property. This sponge-like property is beneficial for tissue engineering scaffolds to get squeezed and absorb water in culture media. So, in our experiment, the sponge was compressed a few times, in each case the structure remained almost the same with no change in structure, indicating a repeatable and reversible compressive deformability. Besides, no agglomeration or precipitation were observed, and colour of samples were homogenous. These tests are not meant to show any stiffness properties

as this has been discussed further in the mechanical properties of the Results and discussion section.

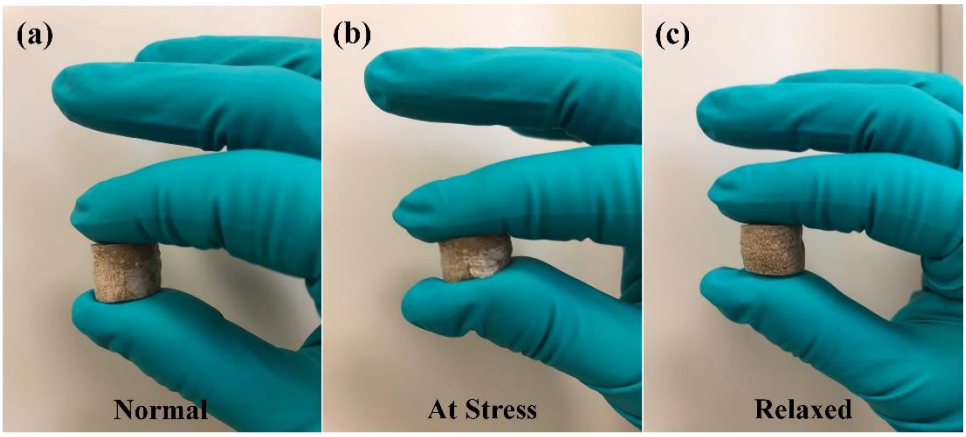


*Figure 3.4. Sponge-like property of GO/Na-ALG sample in a series of events; (a) normal, (b) under compressive stress and (c) relaxed.*

The proposed fabrication method which combines freeze-drying and crosslinking approaches suitable for tissue engineering applications improved the absorption capacities as displayed in Figure 3.5. The colour of GO/Na-ALG scaffolds turned to dark brown as the concentration of GO increases, as shown in Figure 3.6. Besides, the black colour of reduced samples is an indication of the GO reduction. There was no significant physical difference observed in rGO/Na-ALG samples with varying concentrations of GO except changing colours. Also, the excellent stability of scaffolds has noticeably improved with physical crosslinking which is ascribed to the reaction between alginate and calcium ions to harden the scaffold and make a robust 3D interconnected-network structure [197, 198].


*Figure 3.5. (a) Initial, (b) transition, and (c) final stage of the quick absorption and percolation of water droplet by the prepared GO/Na-ALG scaffold.*

The microstructure of fabricated GO/Na-ALG and rGO/Na-ALG scaffolds was tested using SEM technique and summarized in Figure 3.6 (a–j). These images revealed homogeneous 3D structures with interconnected porosity of all samples regardless of GO concentration and reduction process. The average pore size decreased from 162.5 ± 37.2 to 85 ± 16.9 μm as the GO concentration increased from 0.5 to 5 mg $mL^{-1}$ in the GO/Na-ALG scaffolds (as tabulated in Table 3.1), showing the dependency of GO/Na-ALG composite on GO content. This is explained by the fact that the hydrogen bonding interaction between GO sheets and alginate resulted in increasing the resistance of forming larger ice particles in the freeze-drying method [55].

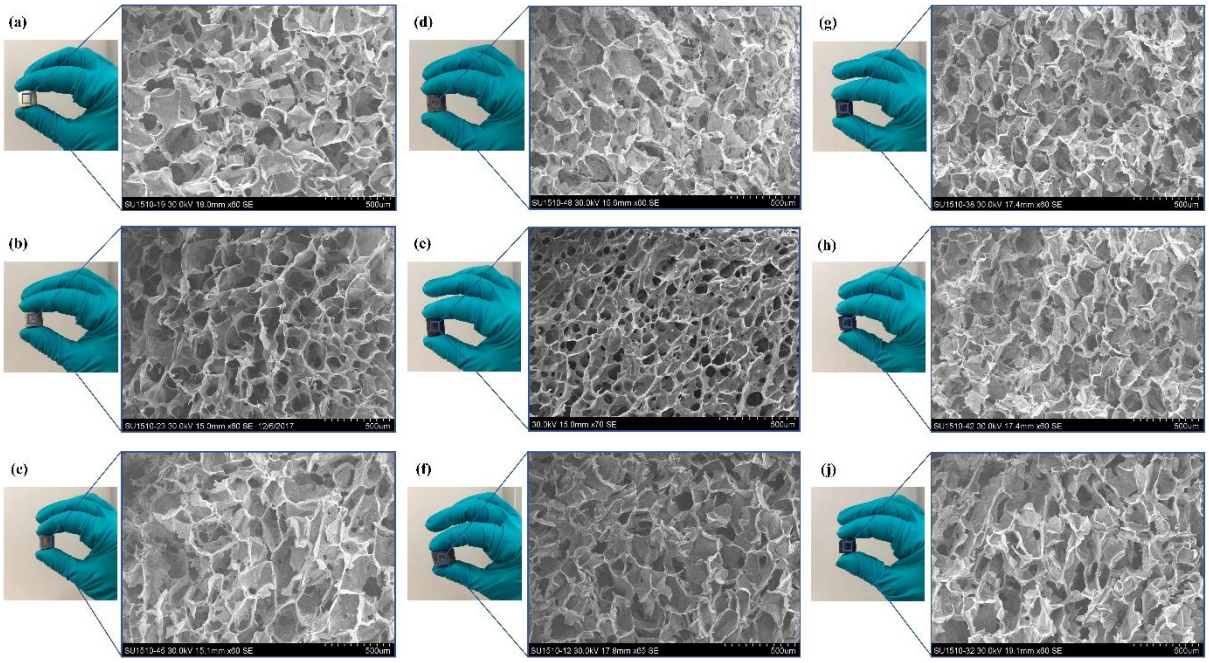

*Figure 3.6. Digital photographs of fabricated graphene-based composite scaffolds with their corresponding SEM images: (a) Na-ALG, (b) GO/Na-ALG0.5, (c) GO/Na-ALG1, (d) GO/Na-ALG3, (e) GO/Na-ALG5, (f) rGO/Na-ALG0.5, (g) rGO/Na-ALG1, (h) rGO/Na-ALG3, and (i) rGO/Na-ALG5 porous scaffolds (scale bar of all images is 500 μm).*

It should be noted that, at 5 mg $mL^{-1}$ of GO concentration, a non-homogeneous dispersion and pore-clogging were observed and resulted in a non-spherical pore network. Unlike GO/Na-ALG composites, the average pore size remains constant for different rGO/Na-ALG scaffolds. However, a well-established porous structure, as well as pore thickness, were observed in the rGO/Na-ALG scaffolds after the reduction process.

*Table 3.1. Pore diameter and porosity of the fabricated graphene-based composite scaffolds at different GO concentrations*

| Sample | GO (mg $mL^{-1}$) | Pore size (μm) | Mean pore size (μm) | Porosity (%) |
|---|---|---|---|---|
| Na-ALG | 0 | 132–228 | 162.5 ± 37.2 | 97.2 ± 2.3 |
| GO/Na-ALG | 0.5 | 112–158 | 147.4 ± 17.5 | 97.5 ± 3.5 |
| GO/Na-ALG | 1 | 102–183 | 142.5 ± 28.5 | 98.0 ± 2.7 |
| GO/Na-ALG | 3 | 89–150 | 122.6 ± 14.3 | 99.0 ± 3.1 |
| GO/Na-ALG | 5 | 47–103 | 85.0 ± 16.9 | 99.3 ± 3.2 |
| rGO/Na-ALG | 0.5 | 93–184 | 116 ± 8.1 | 99.05 ± 3.5 |
| rGO/Na-ALG | 1 | 89–220 | 114.7 ± 16.1 | 99.18 ± 2.3 |
| rGO/Na-ALG | 3 | 82–183 | 98.5 ± 5.5 | 99.15 ± 3.4 |
| rGO/Na-ALG | 5 | 80–205 | 112.4 ± 24.1 | 99.71 ± 2.1 |

Overall, in order to provide a general insight about the morphological properties of the prepared freeze-dried scaffolds comprising of alginate and graphene, the morphology of all prepared graphene-based scaffolds is regular with an average pore size of 120 ± 24 μm and high porosity ≈ 99% (±0.3%). The effective porous structure in all fabricated graphene-based scaffolds reported to be beneficial in the proliferation and migration of neuron cells, considering the fact that desirable pore size for neuron culture is greater than 50 μm [56]. It could be concluded that the porous structure has been improved by the addition of GO which has also been illustrated previously [199]. Therefore, this facile preparation method renders the spongy graphene-based

scaffold a more attractive cell culture platform due to cell penetration ability. The suggested method produces lyophilized porous scaffolds that provide stable 3D structure for cell culture and biological characterization purposes.

The micro-CT cross-sectional images were obtained to quantify the pore's interconnectivity and distribution of the prepared graphene-based scaffolds for cell migration and growth, as indicated in Figure 3.7. Not only no skin layer was observed on both scaffolds' surface, but also uniform pores were existent from the surface through to the centre which is favourable for cellular activity by facilitating the exchange of nutrients and oxygen during tissue development. There was no significant difference observed between GO/Na-ALG and rGO/Na-ALG scaffolds in terms of μ-CT images. Therefore, the established sphere-shaped macropores allow cell colonization inside the scaffold [200].

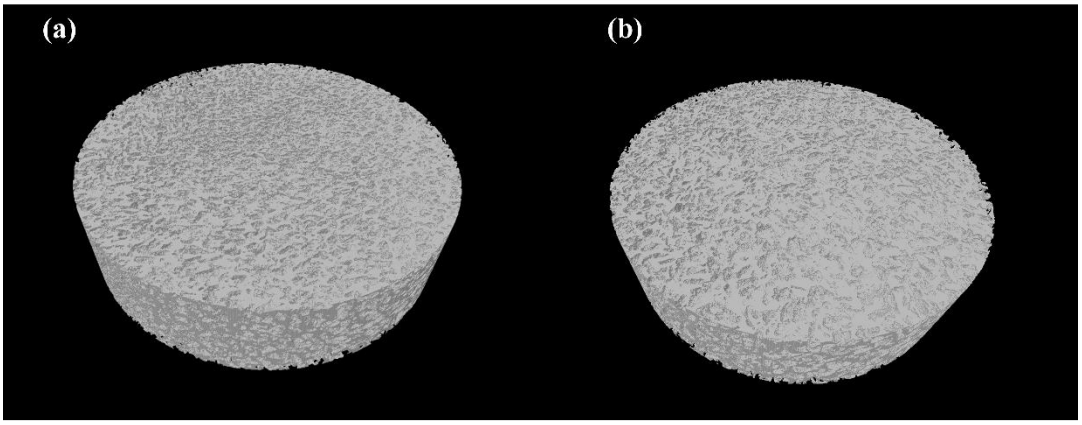


*Figure 3.7. Micro-CT scan 3D models of composite (a) GO/Na-ALG0.5 and (b) rGO/Na-ALG0.5 scaffolds.*

### 3.4.3 Chemical composition, rheological, thermal and interfacial properties of fabricated composite scaffolds

Figure 3.8 presents the EDAX analysis and mapping of elements of GO/Na-ALG and rGO/Na-ALG scaffolds to have clear insights about chemical composition and homogeneous distribution of elements throughout the composite. The main elemental peaks (C, O, and Na) corresponding to graphene and Na-ALG can be undoubtedly observed from the spectra in Figure 3.8 (a, b). Besides, calcium and chloride peaks presented in EDAX spectra indicate the diffusion of these ions in the 3D network. In addition, the elemental peaks corresponding to oxygen drops after reduction in gelatin solution, confirming the successful reduction of GO in the Na-ALG matrix [201].

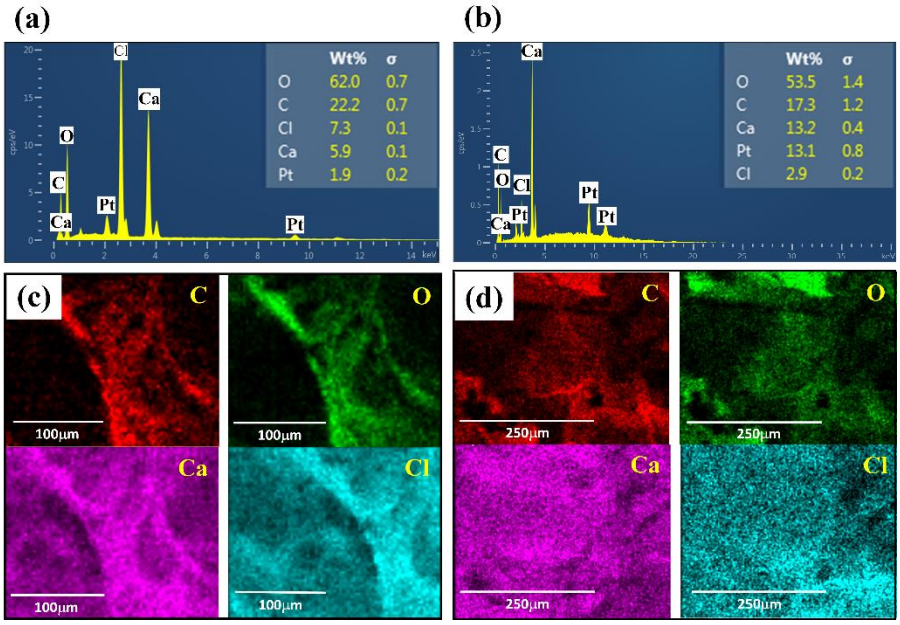


*Figure 3.8. EDAX spectrum showing the elemental compositions of cross-linked (a) GO/Na-ALG and (b) rGO/Na-ALG scaffolds and mapping analysis of (c) GO/Na-ALG and (d) rGO/Na-ALG composites.*

Zeta potential is another important method to estimate the performance of scaffold's material in cell culture as negative-charged surfaces are apposite for cell adhesion. The zeta potentials of prepared GO and commercial Na-ALG were about −45 mV and −17 mV, respectively. Therefore, the synthesized GO can be incorporated into Na-ALG chains in order to develop its characteristics for tissue engineering applications [202].

FTIR analysis was specifically performed to determine the interactions between GO and Na-ALG. The spectrum basically compares the characteristic absorption peaks related to the Na-ALG, GO/Na-ALG and rGO/Na-ALG materials. As shown in Figure 3.9, the asymmetric stretching vibration of –OH and –COO– in Na-ALG caused the formation of bands at 3442 and 1597 $cm^{-1}$. For the GO/Na-ALG sample, the peak at 1005 $cm^{-1}$ which is attributed to C–O–C stretching is considerably stronger. Besides, the presence of particular bands at 3316 and 1607 $cm^{-1}$ confirms the interaction mechanism between GO and Na-ALG chains via intermolecular hydrogen bonds. The physical bonding between GO and alginate matrix provided a homogeneous dispersion of GO in the composite structure. Furthermore, FTIR spectrum is used to study the evolution of functional groups during the self-assembly and reduction process. The most prominent and broad peak of rGO/Na-ALG was observed at 3245 $cm^{-1}$, which corresponded to the stretching vibration of –OH bond. Meanwhile, it could be realized that Na-ALG matrix and the rGO filler had interactions through hydrogen binding as the vibration peak became broader in the composite samples. In addition, oxygen-functioning groups were less prominent after the reduction process. From the spectra, the peaks at 1593 $cm^{-1}$, 1413 $cm^{-1}$, and 1023 $cm^{-1}$ which are presented in all samples can be attributed to the vibration absorption peak of the C=O, C=C and C–O bonds, respectively [191].

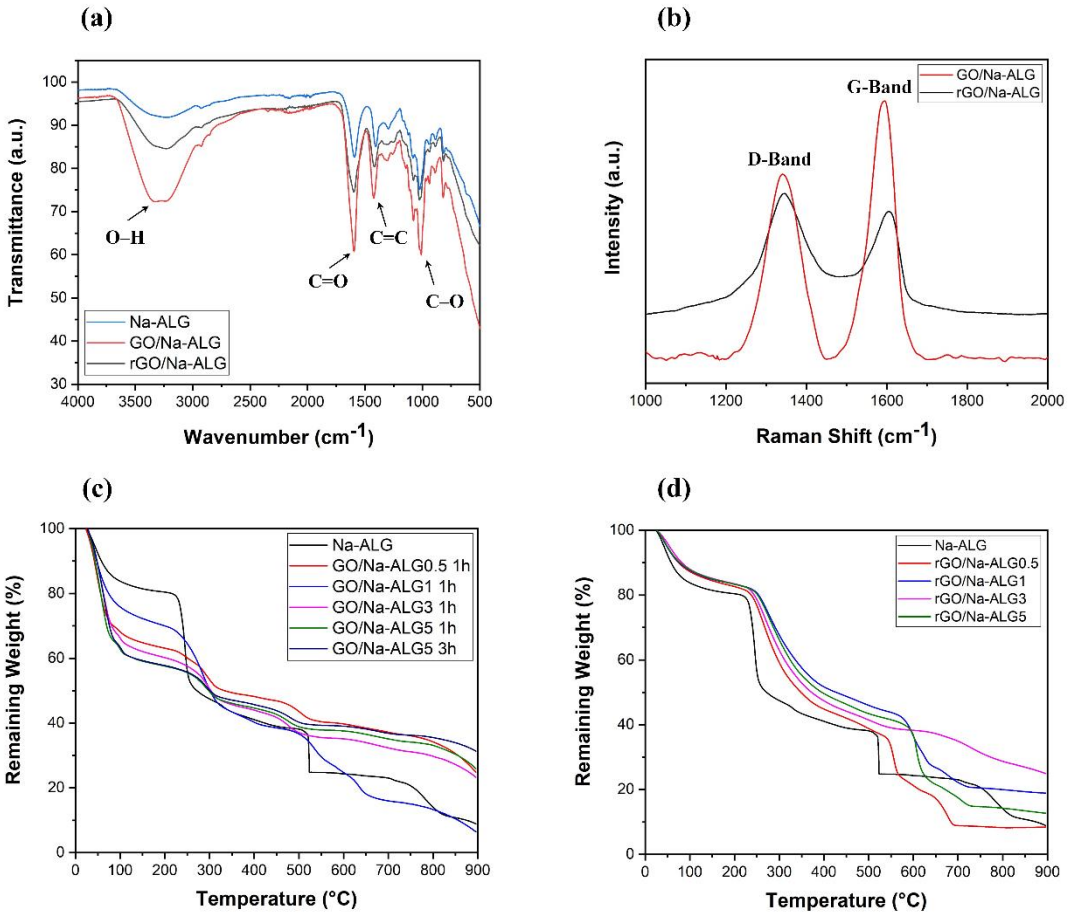


*Figure 3.9. (a) FTIR spectra of composite and control samples, (b) Raman spectra of prepared composite scaffolds, TGA curves of (c) GO/Na-ALG and (d) rGO/Na-ALG scaffolds compared with control group.*

Figure 3.9 (b) shows the Raman spectra of composite samples before and after the reduction process. It can be seen that, both samples exhibit a prominent D-band (1340 $cm^{-1}$) and G-band (1595 $cm^{-1}$) in the spectrum which used to characterize carbon structure and defects. The ID/IG intensity ratio usually indicates the GO reduction. Increased value of $I_D/I_G$ from 0.71 of GO to 1.12 of rGO confirms the removal of oxygen-containing groups [203]. The spectrum clearly confirms the reduction of the GO embedded in the composite by gelatin treatment.

Figure 3.9 (c) compares the thermal properties of GO/Na-ALG with various concentrations of GO at two different crosslinking times. Theoretically, the amount of water in the composite scaffold increases with a higher concentration of GO. It is expressed that the cause for all samples experienced the first weight loss of around 100 °C is due to the loss of absorbed moisture and trapped water. This could be due to the superior thermal conductivity of GO aiding bond cleavage [204]. Based on analysing TGA curves, Na-ALG started to thermally degrade between 200 and 300 °C which is attributed to fracture of glycosidic bonds and removal of carboxyl and carbonyl groups of the alginate. Hence, the TGA graph confirms that GO/Na-ALG scaffolds have lower mass loss in comparison with the control group. Overall, with the addition of GO, the thermal performance of the prepared samples has improved due to hydrogen-bonding interactions between oxygen functional groups of GO and Na-ALG. As seen in Figure 3.9 (c), samples crosslinked for a longer time period possessed higher thermal stability, which could be due to the presence of covalent bonds, as reported previously [205].

As indicated in Figure 3.9 (d), the curve of all the composite samples containing rGO ran above the Na-ALG aerogel since heating, which is an indication of better thermal stability of composites. All samples experienced a major mass loss at about 150 °C due to the evaporation of water molecules trapped in the nanofiber. Additionally, all scaffolds with rGO demonstrated a rapid weight loss in a similar temperature range. Overall, increasing the rGO content in the composite structure could result in a decrease in weight loss. This could be due to the better thermal stability of graphene-based materials which makes the rGO-containing scaffolds to degrade at higher temperature [206]. It should be emphasised that the major weight loss took place at temperatures above the biological system temperature, which implies that all these structures will be very stable under human body conditions.

The flow curves over a range of shear rates before and after the addition of GO and calcium chloride to alginate are illustrated in Figure 3.10. The pure Na-ALG shows a shear-thinning behaviour. Moreover, the addition of GO apparently enhanced the viscosity of the control sample. After crosslinking, it can be admitted that the viscosity of the cross-linked solution significantly improved by two orders as a result of a strong physical crosslinking between Na-ALG and calcium chloride, which was also reported previously [207]. It should be highlighted that immersion of various samples in the crosslinking solution could not be further analysed in terms of rheological properties. Instead, a comprehensive analysis of samples regarding mechanical properties had to be performed by means of a mechanical test machine which will be covered in the following section.

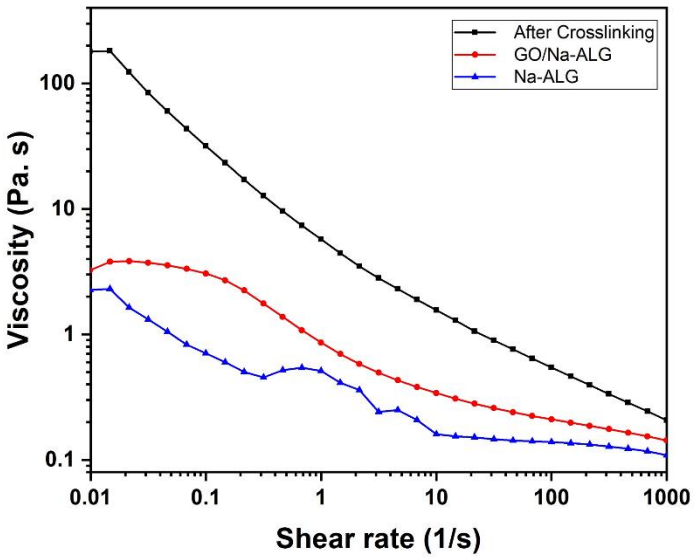


*Figure 3.10. Viscosity as a function of the shear rate before/after the addition of GO and crosslinker.*

As previously reported [206], an appropriate hydrophilic surface of the scaffold could give rise to the improvement of cellular affinity and adhesion. The apparent water contact angle on prepared scaffolds with different contents of GO is given in Figure 3.11(a, b). According to Figure 3.11 (a), the water contact angle on the surface of composite GO/Na-ALG scaffolds decreases with the increase of GO concentration, which corresponds to the hydroxyl groups and carboxylic groups on the GO surface. For instance, the contact angle reached its minimum value of 30.9 ± 5.7° in GO/Na-ALG5 scaffold which has the highest GO content. As a result, the control samples with no GO have been improved in terms of surface morphology and wettability for better cell adhesion and proliferation. Thus, in agreement with previous works,

the addition of GO could enable the interactions with biological molecules owing to its proper hydrophilicity [84]. In the case of rGO/Na-ALG scaffolds, as indicated in Figure 3.11 (b), reduction of samples impacted the wettability of the composite scaffolds where the hydrophilicity decreases with the increment of rGO concentration (from 91.07 ± 2.6° to 110.24 ± 18.4°). This effect could be attributed to the surface nanostructure of rGO layers [139]. Hence, the hydrophilicity of the prepared rGO-based composite is still in a safe range for cell culture purposes. Comparing the hydrophilicity of scaffolds before and after reduction, it can be seen that scaffolds had a significant increase in contact angle after reduction of GO due to the removal of some oxygenated groups during the reduction process.

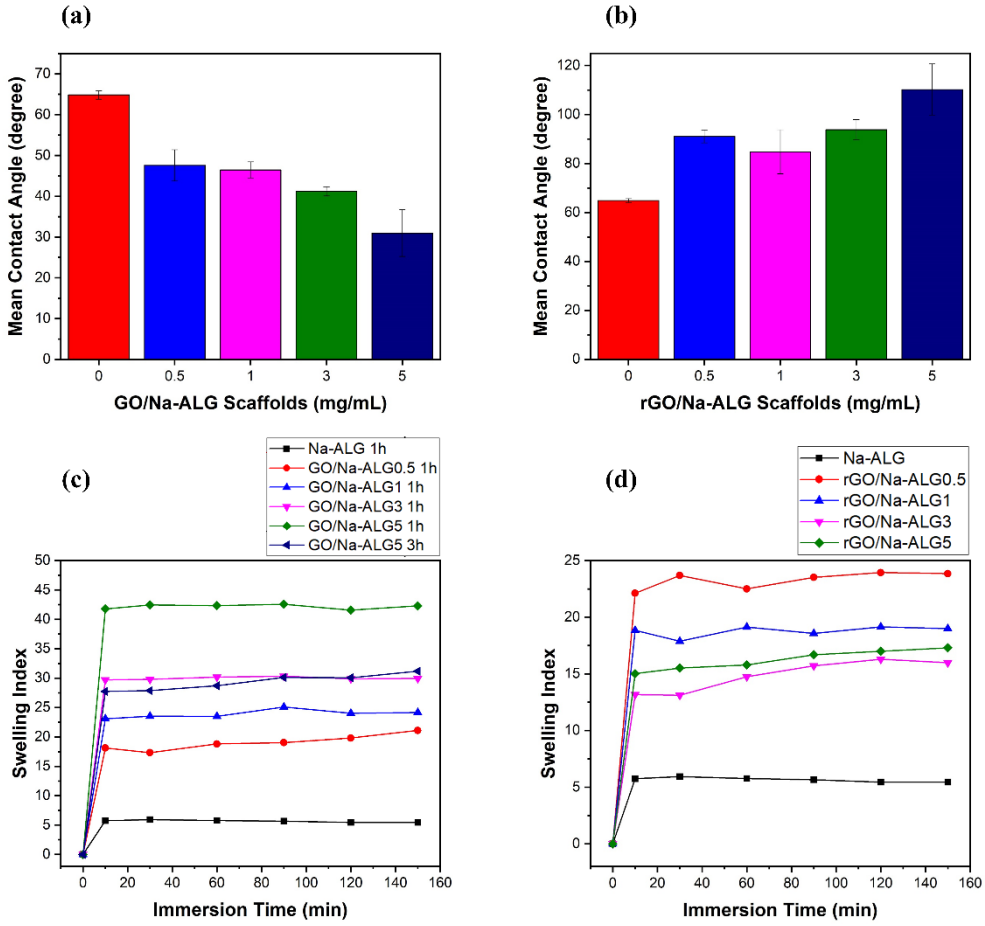


*Figure 3.11. Water contact angle measurements of (a) GO and (b) rGO-based scaffolds, swelling behaviour of (c) GO/Na-ALG and (d) rGO/Na-ALG scaffolds against time.*

As an efficient biomaterial in tissue engineering, once the scaffolds are placed in culture media, they should swell and maintain the body fluid in their 3D network. Figure 3.11 (c, d) indicate the water absorption capability of 3D GO/Na-ALG and rGO/Na-ALG scaffolds at 37 °C at various time intervals. In the case of GO/Na-ALG scaffolds, incorporation of GO considerably increase the water uptake ability of Na-ALG from 5 up to 42 when mixed with 5 mg $mL^{-1}$ of GO. This could be due to the hydrophilicity of GO nanosheets. On the other hand, reduction of GO/Na-ALG caused the swelling ratio of rGO/Na-ALG scaffolds to decline when GO concentration increases, which is ascribed to removing some of the oxygen-containing groups during gelatin and thermal treatment. The swelling index of the rGO composites found to be varied from 15 to 44, depending on the GO content. Also, crosslinking time is inversely associated with a swelling ratio of fabricated scaffolds, as expected. Moreover, all fabricated

composite scaffolds could clearly swell to equilibrium without dissolving, which is a critical feature for cell culture purposes. To sum up, the swelling behaviour of the prepared scaffolds could be controlled by the incorporation of graphene and reduction process.

### 3.4.4 Electrical and mechanical properties of fabricated composite scaffolds

The characterization for electrical properties presented in a recent study by Shin et al. is adopted in the following electrical impedance measurement [208]. Figure 3.12 (a), in which the EIS curve is illustrated, compares the conductivity of prepared samples over a frequency range. The control sample containing Na-ALG showed the highest electrical impedance value over the frequency range with a maximum value of ~18 kΩ. Meanwhile, the addition of 0.5 mg $mL^{-1}$ of GO could significantly decrease the impedance by half. Also, there is a significant drop in impedance value from 17.6 kΩ of pure Na-ALG to 6.2 kΩ of rGO/Na-ALG3. The impedance measurements were noticeably lower for samples after the reduction process due to the excellent conductivity of graphene sheets. Moreover, as the concentration of GO increased in the composite scaffolds, the conductivity is further increased which is expected and consistent with previous studies [208]. However, there is a certain limit for the addition of GO sheets depending on their dispersion in the alginate matrix to develop the electrical conductivity. This fact has been similarly revealed in previous research works, stating that there exists a crucial concentration of GO, known as percolation threshold, which is a deciding factor in maintaining the balance between GO nanosheets and GO-matrix interactions to improve the electrical conductivity [209].

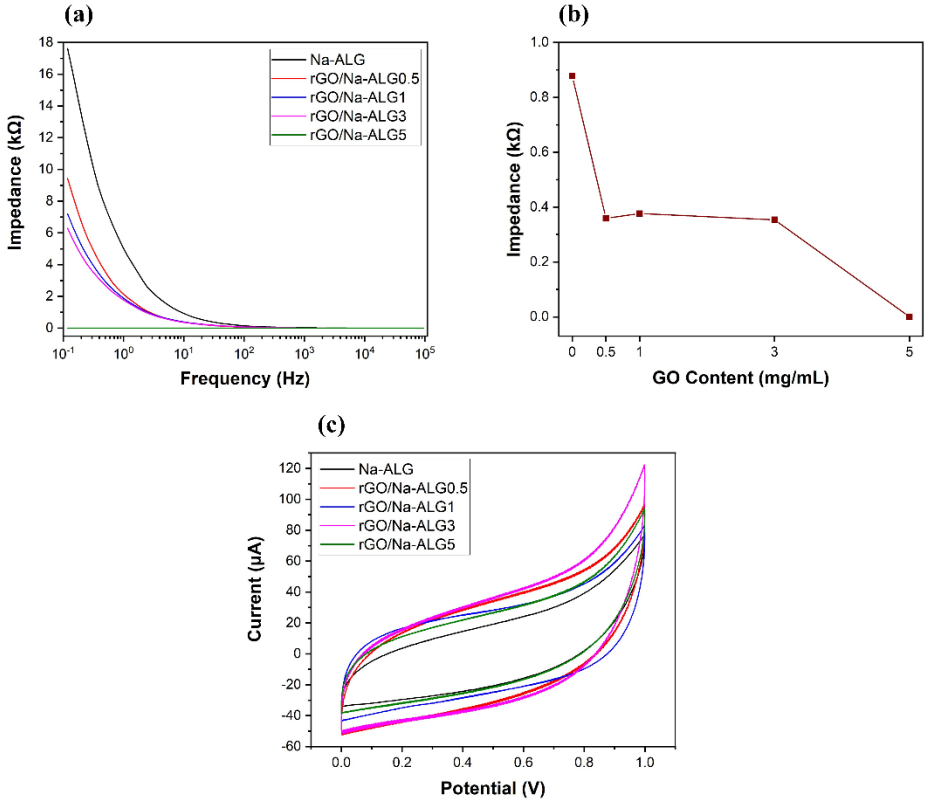


*Figure 3.12. (a) A comparison of the impedance magnitudes of conductive rGO/Na-ALG scaffolds, (b) impedance vs. GO concentration of scaffolds at the frequency of 10 Hz, and (c) the CV curves obtained for rGO-based scaffolds containing 0 to 5 mg $mL^{-1}$ of GO.*

In order to explore the effect of GO concentration on electrochemical properties of scaffolds, the impedance values were plotted at a constant frequency of 10 Hz and presented in Figure 3.12 (b). This figure illustrates that the increment of GO content from 0.5 to 3 mg $mL^{-1}$ in the nanocomposite scaffolds led to a major increase in conductivity, which could be helpful in signal propagation and electrical coupling between neural cells and the scaffold within injured nerve tissue. On the other hand, the addition of more GO content abruptly decreased the impedance value to $3.14\times10^{-4}$ kΩ for GO/Na-ALG5 scaffold. At this condition, the agglomeration and formation of resistant path in the structure can probably result in an overestimated impedance value [210].

The electrochemical properties of fabricated conductive scaffolds in PBS buffer are indicated in Figure 3.12 (c) by cyclic voltammetry curves. It can be seen that the current is delivered mainly through charging/discharging the interfacial double layer. Additionally, the current densities associated with the rGO scaffolds are evidently higher than that of the control scaffold which is indicative of higher double-layer capacitance due to a larger specific surface area. Therefore, the incorporation of graphene in the matrix could cause a stronger charge injection ability which is an effectual factor for neural stimulation [142].

From the mechanical point of view, every scaffold in tissue engineering must have proper mechanical characteristics, according to biomechanical properties of the targeted tissue, not only to support tissue regeneration but also, to maintain satisfactory integrity at the site of implantation during cell growth. The mechanical properties of the samples were investigated to first study the influence of the reduction process and different biomaterials used on the compressive modulus of the microfabricated scaffolds and secondly assess the exact match with the mechanical strength of the spinal cord. The typical compressive stress–strain curves of the prepared scaffolds with different GO weight ratios are displayed in Figure 3.13 (a, c) and the compressive modulus was determined as the slope of the linear region of the curve. From the stress–strain curves, it can be observed that the stress of all prepared scaffolds has a sharp increase which is due to the solidification of hydrated porous samples exposed to a strong compressive force [211]. Thus, the calculated compressive modulus values at 10% strain before the porous structure is damaged are plotted in Figure 3.13 (b, d). It can be concluded that the addition of GO and increased crosslinking time enhance the mechanical performance of the scaffold. It is worth noting that, the compressive modulus of scaffold crosslinked for 3 h (0.873 kPa) had a negligible improvement compared to that of crosslinked for 1 h (0.850 kPa). The composites containing 1 mg $mL^{-1}$ of GO, both before and after reduction, showed the highest mechanical improvement compared to other samples. This result is consistent with other studies utilizing graphene-based nanocomposites with optimum GO content of 1 mg $mL^{-1}$ [212]. Also, the measurements confirmed that compressive strength decline to increase for GO at higher concentrations because of agglomeration. This deterioration of compressive modulus could be attributed to the defects or aggregation of GO during the fabrication procedure. This has been similarly reported in a recent study by Abzan et al., which concluded that enhanced elastic modulus of graphene-based scaffolds is greatly depended on the dispersion of GO nanosheets in the composite matrix [213].

Our results reveal that the mechanical characteristics of GO/Na-ALG and rGO/Na-ALG scaffolds can be adjusted by controlling the GO concentration or graphene/alginate ratio. In addition, the nervous system tissue has a unique mechanical characteristic that meaningfully affects neural cell behaviour and tissue regeneration. It has been reported that the elastic

modulus of the spinal cord varies from approximately 3–300 kPa [214, 215]. This indicates that the mechanical property of fabricated scaffolds matches up with the native tissue which is needed to support neuron growth. Although the mechanical stiffness of high molecular weight pure Na-ALG-based porous scaffold is adequate to match the neuron microenvironment, the incorporation of GO has brought excellent biological, chemical and physical features to the composite scaffold while keeping the elasticity in the proper range for neural tissue engineering. Furthermore, the scaffold strength could be significantly reduced due to the hydrated condition of measurements as a large amount of water deteriorates the structure's resistance to external force [216].

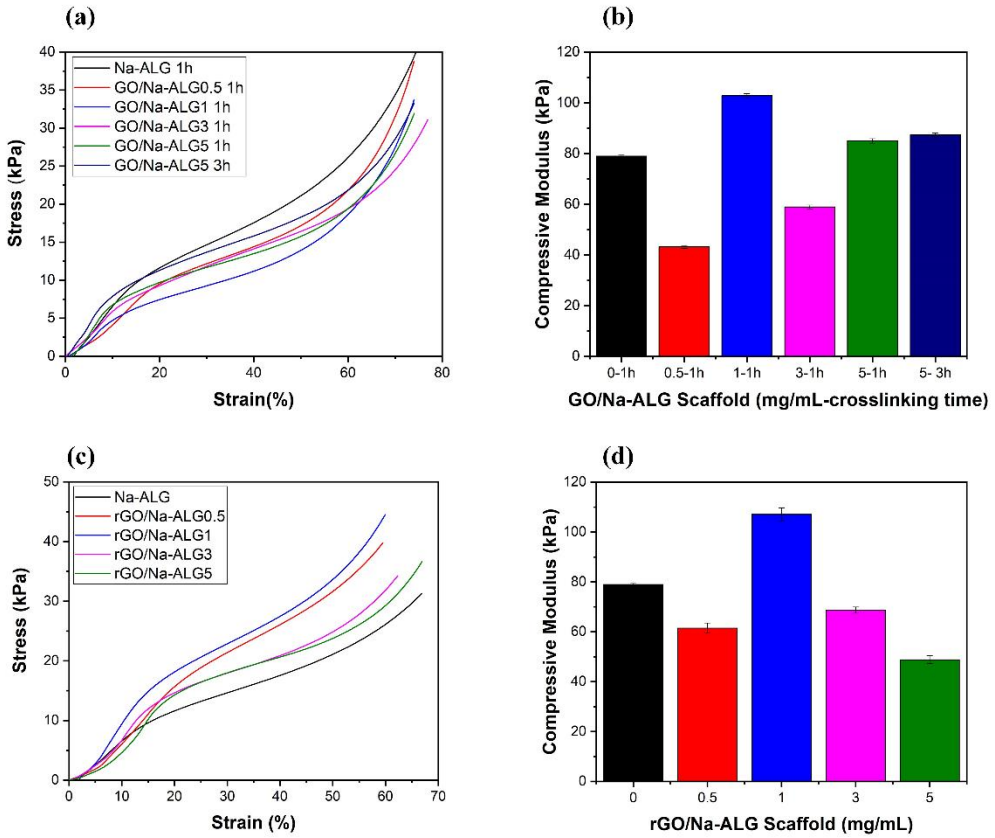


*Figure 3.13. Stress–strain curves of (a) GO/Na-ALG and (c) rGO/Na-ALG scaffolds, and the corresponding compressive modulus of (b) GO/Na-ALG and (d) rGO/Na-ALG scaffolds prepared from different blending ratio.*

Overall, aggregation was observed in higher concentrations of GO, more than 3 mg $mL^{-1}$, for GO/Na-ALG and rGO/Na-ALG composites in which the graphene sheets were not able to fully exfoliate in the matrix. It has been observed from previous studies that the extent of improvement upon addition of GO mainly depends on the level of dispersion of graphene sheets in the matrix. Thus, the concentration of GO in the plating solution can play a significant role in generating homogeneous distribution of graphene sheets in the composite. Also, a certain concentration of GO leads to a stable dispersion owing to the van der Waals interaction of monolayers. On the other hand, an excessive amount of GO could undesirably affect the composite properties because of graphene sheets agglomeration causes a dramatic reduction in the suitable ratio of the reinforcement. A proper concentration of GO in the composite material is expected to decrease the tendency of flakes to restack and develop the permeability [217, 218].

*Table 3.2. Comparing the previous relevant composite scaffolds for neural tissue engineering with the fabricated scaffolds in the current study.*

| Material | Interconnected porous structure | Conductive | Matched mechanical properties with the targeted tissue | Ref |
|---|---|---|---|---|
| Chitosan/gelatin/hyaluronic acid/heparan sulfate | ✓ | × | N/A | [219] |
| Collagen/chondroitin sulphate | ✓ | × | N/A | [220] |
| Polypyrrole (PPy) doped by butane sulfonic acid | × | ✓ | N/A | [221] |
| PVV/PANi | × | ✓ | ✓ | [222] |
| PLGA/PEG | ✓ | × | N/A | [223] |
| PANi/PEGDA | ✓ | ✓ | N/A | [224] |
| PPY and PDLLA | × | ✓ | N/A | [225] |
| PCL/PANI and PLGA/PANI | ✓ | ✓ | N/A | [226] |
| GO/Na-ALG and rGO/Na-ALG | ✓ | ✓ | ✓ | Current Study |

In general, interconnected porous structure, matched mechanical strength with neural tissue and electrical conductivity of bioscaffolds make them more suitable for neural tissue engineering applications [227]. Table 3.2 summarizes properties of the most relevant composite scaffolds in neural tissue engineering as well as the graphene-based hybrid scaffold presented in this study. There are a number of studies that uses conductive polymers for the fabrication of neural constructs. However, poor interaction with cells and biodegradability are some of the key challenges associated with using conductive polymer-based scaffolds [228]. In addition, the mechanical strength of the fabricated scaffold should match the nervous system tissue that is going to be engineered. This can greatly impact cell fate, nerve regeneration, and transplantation outcome. Therefore, the prepared graphene-based scaffold reported here, which can be rendered to a conductive platform for electrical stimulation purposes, with integrated porous structure and matched mechanical strength to the spinal cord opens possibilities for further biological experiments.

## 3.5 Chapter Summary

In chapter 3, the fabrication and characterization of composite sponge scaffolds composed of Na-ALG and GO are described. The fabrication process uses solution mixing, freeze-drying and crosslinking which results in an improved, simple, eco-friendly, high yield strength and integrity 3D scaffold structure with desirable pore sizes greater than 50 μm needed for neuron cell culture. The experimental results showed that although the composite scaffold has water uptake ability, the integral composite scaffold can float on the liquid surface. Results showed that prepared scaffold properties depend on several key parameters such as scaffold materials, concentration of composite ratio, crosslinking condition, and GO concentration which can be tuned to achieve the best characteristics needed from an application point of view. In addition, the incorporation of GO improved the hydrophilicity of 3D composite scaffolds in which the

water contact angle was decreased from 64.8° to 30.9° when the concentration of GO was increased from 0 to 5 mg $mL^{-1}$, respectively.

Furthermore, electrical measurements have shown that when GO content in the composite structure increased, the conductivity of the prepared rGO/Na-ALG scaffolds significantly increased during the reduction process, which can be helpful in signal propagation for electrical stimulation purposes. Also, the compressive modulus of the scaffolds has improved to more than 100 kPa after the addition of 1 mg $mL^{-1}$ of GO. This reported value of compressive modulus is in the reported range of mechanical strength of human neural tissue. Further, the crosslinking time can be used to tune the mechanical strength and water adsorption capacity of scaffolds according to the engineered tissue requirements. Overall, the introduction of graphene, apart from physical, electrical and chemical properties improvements, provides favourable properties for neural tissue engineering. These results suggest that the obtained porous scaffold could serve as a suitable matrix to support cellular responses for the three-dimensional culture of neural cell types. Investigation of the detailed study of biological reactions of the fabricated scaffolds is the next important subject which will be covered in the next chapter to confirm the effective capability of the scaffolds in neural induction.

# CHAPTER 4: *IN VITRO* BIOLOGICAL EVALUATION OF FABRICATED GRAPHENE-BASED SCAFFOLDS

## 4.1 Abstract

The primary goal of neural tissue engineering is to produce CNS/PNS tissue substitutes using a biocompatible matrix for the development of neural cells. Scaffolds should have suitable biocompatibility with minimum toxic effects on seeding cells and ultimately forming tissue. It is believed that minor changes in biomaterials composition, internal porous structure, and mechanical strength of 3D scaffolds can impact cellular behaviour such as migration, growth, and adhesion. 3D GO/Na-ALG scaffolds have been found to have the capability of neural cell infiltration and culture. Besides, *in vitro* biodegradation study reveals that the addition of GO enhanced degradation rate of the composite GO/Na-ALG and RGO/Na-ALG scaffolds, suggesting that as GO concertation increases weight loss increases as a result of the increase in hydrophilicity. The aim is to investigate *in vitro* biological effects of graphene-based 3D scaffolds on dental pulp stem cells (DPSCs) in terms of proliferation, cell viability, and cytotoxicity. The AB assay showed that DPSCs viability cultured onto Na-ALG and GO/Na-ALG scaffolds was higher than that of 2D controls. This can clearly express the desirable initial cell adhesion to the scaffolds' surface followed by cell spreading through pores. Besides, the LDH release measurements confirmed that DPSCs toxicity on the GO/Na-ALG and RGO/Na-ALG scaffolds was comparable to that obtained on the 2D surface in the absence of the biomaterial. Regarding coating materials, PLL was the most robust reagent that improved cell-matrix adherence and affected metabolism activity of DPSCs, being superior to combined PLL+LAM coating. The incorporation of graphene into the composite scaffold did not elicit significant cytotoxic effects after 2 days of DPSCs culture and supported higher DPSCs viability and function. In particular, the GO-enriched scaffolds exhibited cytotoxicity of 15–27% during 48h of culture, suggesting that these materials are biocompatible with DPSCs which is ascribed to unique surface chemistry, good mechanical properties, high surface area, and excellent physicochemical properties of graphene-based nanomaterials. The cytotoxicity of GO/Na-ALG and RGO/Na-ALG scaffolds in serum-rich media is increased comparing to the serum-free condition which can be explained by the good capability of graphene-based materials to adsorb serum proteins. The findings from the current study suggest that proposed composite 3D graphene-based scaffolds had a favourable effect on the biological responses of DPSCs.

## 4.2 Introduction

In general, biocompatibility can be widely defined as the appropriate biological response of material without the likelihood of introducing toxic contaminants to the living system. This appropriateness may differ from the specifications of one application to another. Therefore, one material can be biocompatible in general or for a particular application but may cause adverse effects or systematic toxicity if not designed in accordance with the characteristics of the targeted application [229]. Hence, the assessment of biological effects of a material in terms of *in vitro* cytotoxicity and bioactivity is crucial to identify suitable candidates for biomedical applications and clinical trials [230, 231]. Ideal biocompatible materials require a functional integration with the host tissue with no inflammatory reaction to trigger a number of biological

responses. For instance, a failure to match the elastic moduli between biomaterials and the targeted tissue has created a barrier in full integration to create functional tissues [229]. In particular to neurology demands, the safety of designed biomaterial to expose brain cells and neuronal circuits is the primary consideration for diverse neurological therapeutic approaches.

Another important consideration of designing tissue engineering scaffold is the biodegradability of scaffold biomaterials which highly influences the structural stability, cellular behaviour and tissue formation [232]. Besides, the biomaterials degradability should match the tissue regeneration and be in line with the mechanical properties of the scaffold. Controlled and gradual biodegradability of scaffold ensures proper regeneration of the tissue. The degradation and resorption kinetics of the scaffold depend on scaffold composition, structure of materials, porosity geometry, and hydrophilicity [233-235]. Since the initial discovery of graphene, a question that needs significant attention is the biodegradability and biodistribution of graphene-based materials. While graphene attracted researchers' attention as a novel biomaterial for tissue engineering applications, it is highly important to elucidate graphene-based scaffold biodegradation behaviour [175].

## 4.3 Biocompatibility/Toxicology of Graphene-based Materials

Owing to the unique surface chemistry of graphene-based nanomaterials, it has been demonstrated that graphene-based surfaces can encourage protein adhesion, cell anchorage, migration and proliferation which resulted in the development of tissue engineering scaffolds [152, 236, 237]. While graphene derivatives seem to offer numerous advantages with potential use in commercial biomedical applications, thorough analysis to evaluate their interactions with biological systems should not be neglected. Besides, the assessment of *in vitro* cytotoxicity is the fundamental stage towards *in vivo* studies. In transition of cell culture system from 2D to 3D cultures, cellular responses including cell toxicity, cell-type specific function and gene expression are more challenging than traditional cell culture. The success of tissue engineering products highly depends on the biological response of the scaffold which is impressed by cell adhesion, cell viability and material biocompatibility. Suitable biocompatibility of graphene-based scaffolds encourages their further utilization for 3D tissue engineering [132, 238, 239]. Consequently, various studies have reported the toxicity of graphene family nanomaterials on various cell lines and animal models including stem cells [240, 241], HeLa cells [242, 243], HepG2 cells [244, 245], rats [246], mice [247] and etc. Contradictions in the biocompatibility profile of graphene-based nanomaterials can be mainly attributed to the different physicochemical properties of the material used. Accordingly, two materials with the same name of "graphene" might be completely different in terms of lateral dimensions, thickness, degree of oxidation, and formulations which significantly results in different toxicity responses [248, 249]. Thus, the importance of the extent of biodistribution and safety of prepared graphene-based materials should be highlighted for their utilizations in tissue engineering applications. The studies on biocompatibility assessment of graphene family nanomaterials revealed that the toxicological profile, accumulation and biodegradation highly depends on several parameters including physiochemical properties (shape, size, concentration, oxidative state, surface chemistry, degree of dispersion), routes of administration, purity, synthesis technique, exposure dose, and cell type [250-253]. These complex factors may cause different cellular responses which are key determinant factors in the fate of biomaterials. However, these properties could be altered by further functionalization or adsorption of

proteins/biomolecules which ultimately influence the biological performance of the material [254]. Moreover, Yuan et al. studied the potential cytocompatibility of graphene oxide *in vitro* [255]. Human hepatoma cells treated with 1 µg/mL of GO expressed 6% mitochondrial damage, 8% increase in generation of Reactive Oxygen Species (ROS) and no significant cell apoptosis. The moderate protein level variations for cells cultured with GO suggested that GO could be promisingly utilized in biomedical applications. Another study investigated the neural cell behaviour of 3D bioscaffold based on rGO and porcine acellular dermal matrix (PADM). Addition of graphene has improved the mechanical strength and conductivity of the scaffold which can be highly beneficial in neural tissue engineering. In addition, excellent electrical properties of rGO can promote the charge transport and maturation of neural cells. The prepared scaffold exhibited excellent biocompatibility and enhanced neurite sprouting and outgrowth [256]. In this regard, recent studies have been compiled to discuss and compare toxicological aspects of different graphene-based materials using various viability assays in tissue engineering applications.

Table *4.1* summarises the toxicity assessment of graphene-based materials at various experimental conditions.

In a study by Zhang et al., cytotoxic impacts of graphene with various concentration and SWCNTs was evaluated on PC12 cells. LDH and MTT assays showed no cell death for graphene with concentration of 0.01–10 μg/mL and almost 15–20% cell death was measured at 100 μg/mL [257]. However, SWCNTs at 100 μg/mL caused more than 70% cell death. The resultant cytotoxic effects and apoptosis of graphene at higher concentrations was ascribed to agglomeration and generation of reactive oxygen species. Besides, Vallabani et al. examined the interactions of graphene oxide at a concentration range of 10–100 μg/mL with human lung cells [258]. After 24 and 48 hours of cell culture, a significant concentration-dependent increase in cell toxicity was observed. In another study, Mbeh et al. investigated the cytotoxicity of graphene oxide nanoribbons functionalized by albumin [259]. Although more than 85% cell viability was observed for the functionalized graphene oxide nanoribbons with concentrations less than 50 μg/mL, the higher concentration (100 μg/mL) inhibited cell proliferation which resulted in cell apoptosis. In another similar study by Akhavan et al., cell cytotoxicity was measured for reduced graphene oxide nanoribbons (rGONRs) and reduced graphene oxide sheets (rGOSs) [260]. Accordingly, significant cell toxicity upon human MSCs was noticed for 10 μg/mL of rGONRs after only one hour of cell culture, whereas the same toxicity was observed for 100 μg/mL of rGOSs after 96 hours exposure. The toxicity of rGONRs was induced by cell membrane damage and DNA fragmentation, even after short culturing time of 1 h. Moreover, the generation of oxidative stress was considered as the main reason for the cytotoxic effects of the rGOSs. Therefore, it was demonstrated that the shape of graphene-based materials as well as the concentration are playing an extremely critical role in their interaction fate with stem cells and biological systems. Talukdar et al. has also studied the MSCs cytocompatibility and differentiation upon exposure to different morphologies of graphene nanomaterials including GONRs, graphene oxide nanoplatelets (GONPs) and graphene nanoonions (GNOs) [261]. Cytotoxicity effects for different concentrations from 5 to 300 μg/mL were assessed up to 72 hours using Alamar Blue and Calcein AM viability assays. The results confirmed that various 2D graphene materials at concentrations of more than 50 μg/mL could not be potentially safe doses for labelling of MSCs.

*Table 4.1. Cytocompatibility of graphene-based materials.*

| **Material** | **Synthesis method** | **Concentration** | **Assay** | **Cell line** | **Remarks** | **Ref** |
|---|---|---|---|---|---|---|
| 3D rGO-collagen | Modified Hummers' method followed by reduction with ascorbic acid | 1mg | LIVE/DEAD | Rat BMSCs | • Up-regulation of Nestin, Tuj1 and MAP2 protein and gene expression<br>• Promoted neurite sprouting and outgrowth | [256] |
| Graphene, SWCNT | Radio Frequency catalytic CVD | 0.01–100 µg/mL | MTT, LDH, ROS, Caspase3/7 | PC-12 | • Dose- and shape-dependent cytotoxicity for graphene and SWCNT | [257] |
| GO | Modified Hummers' method | 10-100 µg/mL | MTT, caspase-3 | H-SY5Y cell | • No obvious cytotoxicity at low concentration (<80 µg $mL^{-1}$)<br>• Dose- and time-dependent cell viability at higher concentrations | [262] |
| GO | Purchased from China | 0.02 and 0.1 mg/mL | CCK-8 | MSCs | • Proliferation and osteogenic differentiation showed concentration-dependent behaviour | [263] |
| GO | Hummers' method | 1, 5, and 10 µg/mL | MTT, LIVE/DEAD | NSCs | • GO-NPs at concentrations below 5 µg $mL^{-1}$ are generally biocompatible with hfNSCs | [264] |
| rGO | Modified Hummers' method, Reduction by hydrazine | 100, 10, 1.0, 0.1 or 0.01 µg/mL | Fluorescein diacetate (FDA) | MSCs | • The interaction of graphene sheets with stem cells depends on the lateral size of the sheets. | [265] |

| | | | | | | |
|---|---|---|---|---|---|---|
| PEG-GO | Modified Hummers method | 10–100 μg/mL | CCK-8 | human lymphoma cells | • Excellent dispersion in biological solutions and the low toxicity with lymphoma cells | [266] |
| GO | Modified Hummer method | 10, 25, 50, 100 and 200 μg/mL | CCK-8 | A549 cell line | • GO can cause dose-dependent oxidative stress in cell and induce a slight loss of cell viability at high concentration. | [267] |
| Graphene incorporated Polycaprolactone | Purchased from Sigma Aldrich (powder, 15-20 sheets, 4-10% edge-oxidized) | 0.1% and 0.5% (w/w) GO | Live/dead, WST-1 assay | Murine preosteoblast cell line (OB6) | • Scaffolds possessed good bioactivity, and graphene oxide increased the cell attachment and differentiation | [268] |
| GO/alginate | Purchased from Graphene Supermarket NY, USA (solution, 6 mg $mL^{-1}$) | 0, 0.05, 0.25, 0.5, and 1.0 mg $mL^{-1}$ | LIVE/DEAD, Alkaline phosphatase (ALP) | hMSCs | • High cell viability of MSCs printed with alginate/GO scaffolds | [269] |
| 3DG Foam | CVD | N/A | MTT assay | Mouse NSCs | • Enhanced NSC attachment and proliferation<br>• Enhanced differentiation to astrocytes | [270] |
| 3DGONR | Unzipping of CNTs | N/A | LDH Assay, LIVE/DEAD | Human adipose-derived stem cells (ADSCs) And murine MC3T3 preosteoblast cells | • Good cell viability (comparable to PLGA controls) | [144] |

Another study by Wojtoniszak et al. reported the effects of GO and rGO dispersions (at 3.12–100 µg/mL) with various surfactants (such as PEG, Pluronic P123 and DOC) on the cytocompatibility of fibroblast cells [271]. The results from WST-1 assay proved that toxicity level highly depends on the surfactant and treatment concentrations in which GO and rGO at concentrations between 3.125–12.5 µg/mL showed suitable cell viability. In addition, Lv et al. acknowledged that GO showed no significant cytotoxicity or cell apoptosis at concentrations of 80 µg/mL or below for 96 h [262]. However, cell viability of human neuroblastoma cell lines decreased at higher concentrations. Remarkably, GO increased the differentiation rate of SH-SY5Y cells as well as neurite length which can be applied for the treatment of neurodegenerative diseases. Overall, all of these studies indicated a dose-dependent cell viability trend that highly depends on the morphology of the graphene-based nanomaterial.

Another important parameter which could decisively affect the cytotoxicity of graphene nanoparticles is lateral size dimensions. For instance, Akhavan et al. have studied human mesenchymal stem cells viability on rGO nanoplatelets in different sizes including 11±4 nm, 91±37 nm and 418±56 nm [265]. The cytotoxic effects of rGO nanoplatelets were measured with FDA, ROS and Comet assays. It was found that rGONPs with a concentration of 100 µg/mL and size of 11±4 nm had the lowest cell viability (<5%). While almost 20% cell death was observed for the GO sample with the largest lateral size dimensions of 3.8±0.4 µm. In another study, Chang et al. analysed cytotoxic effects of GO in three different sizes including 160±90 nm, 430±300 nm and 780±410 nm on human lung cells (A549) using CCK-8 assay [267]. After 3 days of cell culture, it was observed that GO sheets with the lowest size had higher cytotoxicity compared with GO sheets with size of 780±410 nm. On the other hand, the highest amount of ROS generation was recorded for GO sheets of size 780±410 nm compared to other dimensions. Thus, it was concluded that cell viability, as well as ROS generation, are potentially dependent of graphene sheet size. In addition, graphene oxide nanoribbons (GONRs) were examined in a study by Dasgupta et al. in terms of cytotoxicity of breast cancer cells (MCF-7) as well as human lung cells (A549) [272]. Various sonication times have been performed on the GONRs to modify the nanoparticles size. It was indicated that probe sonication disrupted nanoribbons structure following the creation of carbonaceous debris, which could be the reason for the cytotoxic effect. Thus, it was reported size-dependent effects on cytocompatibility. In another similar study by Yue et al., the cell viability of six different cell lines on 350nm and 2 µm GO sheets were analysed after 2 days of incubation [273]. It was shown that cellular behaviour and inflammatory response is highly dependent on lateral dimensions of GO, in which the micron-sized GO caused a stronger inflammatory response and cytokines release. Additionally, the authors claimed that the removal of manganese, which was used during synthesis of GO, directly affected cell viability. Thus, purification steps and chemicals used during GO synthesis can significantly impact cellular responses. Another example of contamination from processing and synthesis methods is the reduction routes for producing rGO-based samples. For instance, hydrazine has been utilized for the reduction of GO by many researchers, but it was found that hydrazine and its residues are highly toxic to cells and carcinogenic [274, 275]. Therefore, alternative reducing agents must be employed in biomedical applications without introducing toxic contaminants to biological components. Generally, highly toxic chemical compounds involved in the production of graphene-based materials should be replaced with benign alternatives to prevent their highly negative impacts on the biological response. If substitution is not possible, a complete washing and purification

process of the final graphene-based materials is required to guarantee the removal of the toxic trace of residues [249, 276].

Cytocompatibility of graphene nanomaterials could be dependent on cell type. For instance, Mullick-Chowdhury et al. measured the level of toxicity of graphene oxide nanoribbons (GONRs), synthesized from CNTs, on four different cell lines (including mouse fibroblast cells (NIH-3T3), Henrietta Lacks cells (HeLa) derived from cervical cancer tissue, Michigan cancer foundation-7 breast cancer cells (MCF7), and Sloan Kettering breast cancer cells (SKBR3)) within 24–72 h using various assays [277]. It was shown that all cells showed dose-dependent cell toxicity. However, the degree of cell viability differed significantly across different cell lines in which higher cell viability was observed in MCF7 or SKBR3 cells (78–100%) compared to HeLa cells (5-25%). HeLa cells exposed to a low concentration of GONRs (10 μg/mL) showed a significant cell death. However, these results indicated a totally different cytotoxicity profile compared to GONRs produced by the modified Hummer's method.

The cell viability assay protocol is another significant factor in producing accurate and reliable results about the cytotoxic effects of the studied materials. In addition, the viability assessment protocol is crucial in obtaining relevant predictions about *in vivo* adverse effects of materials [278-280]. The common cytotoxic assays as listed in

Table *4.1* include MTT, WST and LDH assays. It is reported that measuring the toxicity of graphene-based nanomaterials using colourimetric assays is challenging. For instance, several studies have shown that GO and carbon nanotubes have possible interference with MTT reagent which make it not a good assay for graphene-based materials. The reactivity of GO may cause inconsistent optical density, untrue cytotoxic effects and large errors in final outcomes [281-283].

Overall, before employing graphene-based products in any biomedical application, the potential mechanism of cytotoxicity induced by the proposed graphene-based materials should be investigated comprehensively to develop desirable scaffolds for clinical studies. More importantly, feasible toxicity assays must be selected concerning the 3D culture system and biomaterials specifications.

## 4.4 Materials and Methods

### 4.4.1 Materials

Sodium alginate (Na-ALG) and Calcium chloride dried was purchased from Chem-Supply. Alpha-MEM (Gibco, Life Technologies, Australia, Cat. No. 12561056) was supplemented with fetal bovine serum (FBS, USA origin, Life Technologies, Australia), penicillin /streptomycin (Gibco), L-ascorbic acid-2-phosphate (Sigma-Aldrich), and 100X L-Glutamine (Life Technologies, Australia). Natural mouse Laminin (Gibco-Life Technologies) and 0.01% Poly-l-lysine (PLL) solution (Sigma) were used as coating reagents. Trypsin-EDTA was supplied by Gibco Life Technologies, Australia. Clear-bottom 24-well and 96-well plates (Costar®, Corning, NY, USA) used throughout the study. The cytotoxicity assay was performed following the manufacturer's protocol using LDH kit from Promega Corporation (WI, USA). The AlamarBlue™ cell viability reagent was supplied by Invitrogen–ThermoFisher Scientific, USA.

### 4.4.2 *In vitro* Biodegradation Study

The *In vitro* biodegradation study aims to investigate the biodegradation rate of prepared scaffolds [284]. Briefly, each scaffold (n=3) with known weight ($W_0$) was incubated at 37°C in alpha-MEM culture media containing 1% (v/v) penicillin/streptomycin to prevent bacterial growth. At specific time points, scaffolds were rinsed with dd$H_2O$. Then, samples were dried under vacuum and weighed ($W_1$). The extent of biodegradation was calculated using the following formula.

$$\textit{In vitro}\ \text{Biodegradation}\ (\%) = \frac{W_0 - W_1}{W_0} \times 100$$

### 4.4.3 Cell Culture

Before cell seeding, the scaffolds were sterilized with 80% ethanol for 24 hours, then allowed to dry overnight and washed two times with DPBS. One ECM protein named as laminin (LAM) and one poly-amino acid named as poly-l-lysine (PLL) were used to coat the wells and scaffolds before cell seeding. In brief, scaffolds were incubated at room temperature in PLL (10 μg/mL) overnight followed by incubation at 37 °C in LAM solution (10 μg/mL) overnight.

Non-coated (NC) scaffolds, which were wetted but not incubated with any coating material, served as control.

The donor DPSCs were cultured in Alpha modification of Eagle's medium (α-MEM) supplemented with 10% fetal bovine serum (FBS), 0.5% penicillin/streptomycin, 100 μM L-ascorbic acid 2-phosphate, and 2 mM L-glutamine at 37 °C in 5% $CO_2$ humidified atmosphere. The cells reaching 80–90% confluency was harvested using 0.05% (w/v) trypsin/ethylenediaminetetraacetic acid solution and seeded onto scaffolds in 24-well culture plates. Five cell densities were analysed in triplicate: 1, 2, 4, 8, and 16 × $10^4$ cells per scaffold/well. The scaffolds were incubated for 3 hours to allow diffusion of cells through the network of pores before adding culture media (550 μL/well). Wells with no scaffolds were used as 2D control samples.

### 4.4.4 Flow Cytometry

After 24 hours of cell seeding, cells were detached from the scaffolds using 0.05% w/v trypsin-EDTA solution for 10min. During this time, scaffolds were shaking gently at 37 °C to get complete cell detachment from pores. Then, the suspended cells were centrifuged (300 rpm, 5 min) and the supernatant was discarded followed by addition of 300 μL of DPBS per reaction tube. Next, 5 μL of 7-aminoactinomycin D (7-AAD) per 100 μL of cells was added and mixed well and the test was conducted via a flow cytometer.

In order to perform H191 staining, after cells were detached from scaffolds and centrifuged (300 rpm, 5 min), the supernatant was discarded followed by adding 300 μL of blocking solution and incubating in the ice for 20 min. After 20mins, centrifugation was repeated for another 5 min at 300 rpm followed by discarding the supernatant. Then, 50 μL of primary antibody was added and incubated in ice for 45 min. Afterwards, in order to remove antibodies, the cells were mixed well with 500 μL of 5% FBS solution (in DPBS), and precipitated by centrifugation (300 rpm, 5 min), and the supernatant was discarded. 400 μL of DPBS and FBS was again added to reaction tubes, followed by addition of 1 μL of secondary antibody (1:400), and incubated in the ice. After 15 min, the cells were centrifuged (300 rpm, 5 min), and the supernatant was removed, and 300 μL of DPBS was added to each tube. In order to perform the test, 15 μL of 7-AAD was added to each tube. After the fluorescent dye was incubated for five minutes on ice, the cells in each sample were measured using a flow cytometer. Then, FlowJo software was used for further data analysis.

### 4.4.5 Alamar Blue (AB) Assay

The Alamar Blue (AB) assay was used to quantitively measure the metabolic activity of living cells on the scaffolds by detecting the oxidation-reduction rate of AB reagent [285]. The effects of cell seeding density, coating condition and utilization of 3D porous scaffolds on the viability of DPSCs were evaluated. Briefly, after 24 and 48 hours of cell seeding on scaffolds, 1 mL of 10% Alamar Blue (AB) solution was added to each well. The plates were shaken gently (200 rpm) for 5 min and incubated for 4h at 37 °C with 5% $CO_2$. After incubation, 100 μL of each sample was transferred to a 96-well plate and the fluorescence intensity was recorded at the excitation wavelength of 540 nm and emission wavelength of 600 nm using a spectrophotometer. Scaffolds without cells were used as negative control and the fluorescence

intensity values were subtracted as blank. The experiment was performed two times in triplicates.

### 4.4.6 Lactate Dehydrogenase (LDH) Assay

To evaluate the cytotoxic effects of the scaffolds, DPSCs were cultured on the scaffolds for up to two days under proliferation conditions, and the level of toxicity was measured by lactate dehydrogenase (LDH) kit according to manufacturer's instructions in which the number of viable cells is investigated by quantitatively measuring cytosolic lactate dehydrogenase enzyme leakage into the culture medium as a result of cell membrane damage [144]. Briefly, 50 µL of cell culture media was collected from 24-well plates after 24 and 48h and transferred into a fresh 96-well plate. After that, 50 µL of LDH assay mixture was added to each well and incubated at room temperature in dark. After 30 min, the reaction was stopped with HCl (1 N, 10 vol %) and the absorbance values were obtained at 490 nm (GloMax® Discover Microplate Reader) using a 96-well plate reader. DPSCs grown without scaffolds were incubated with lysis solution for 45 min and used as positive controls (100% dead). The cytocompatibility performance of the scaffolds was analysed by comparing the absorbance of the experimental group and the control group. Cytotoxicity data are presented as the average of three replicates.

### 4.4.7 Statistical Analysis

Data are graphically reported as mean value and the standard error mean of at least three independent samples. Statistical analysis was performed by two-way analysis of variance (ANOVA) with a significance level of 0.05 followed by post hoc Dunnett test. The analysis was carried out on GraphPad Prism software. The correlation between cell viability and mean pore size was determined by the Spearman Rank Order Correlation test.

## 4.5 Results

### 4.5.1 Biodegradation Study

The percentage of scaffolds' weight losses was measured as the biodegradation and the results are presented in Figure 4.1. To evaluate the effect of GO addition on the degradation rate of composite scaffolds, the GO/Na-ALG and RGO/Na-ALG scaffolds containing different percentage of GO were analysed in a period of 3 weeks. After 3 days of the study, all graphene-based scaffolds degraded gradually up to about 20% of their initial weight whereas Na-ALG scaffolds showed degradation percentage of about 31%. However, from 7th day onwards, the difference in the degradation rate of the composite scaffolds is clearly visible. The difference between all GO-based scaffolds and the Na-ALG scaffold (No-graphene control) was statistically significant ($p < 0.0001$) in 2nd, 3rd, 7th and 21st days. From *in vitro* biodegradation pattern (Figure 4.1), the mean weight loss was approximately 24.86%, 32.42%, 23.19%, and 31.42% for GO/Na-ALG0.5, GO/Na-ALG1, RGO/Na-ALG0.5, and RGO/Na-ALG1 scaffolds at the end of the period, respectively. The Na-ALG scaffold containing no graphene showed the highest weight loss of $\approx 44.02\%$ after 21 days. All hybrid scaffolds displayed a stable weight loss trend after 7 days.

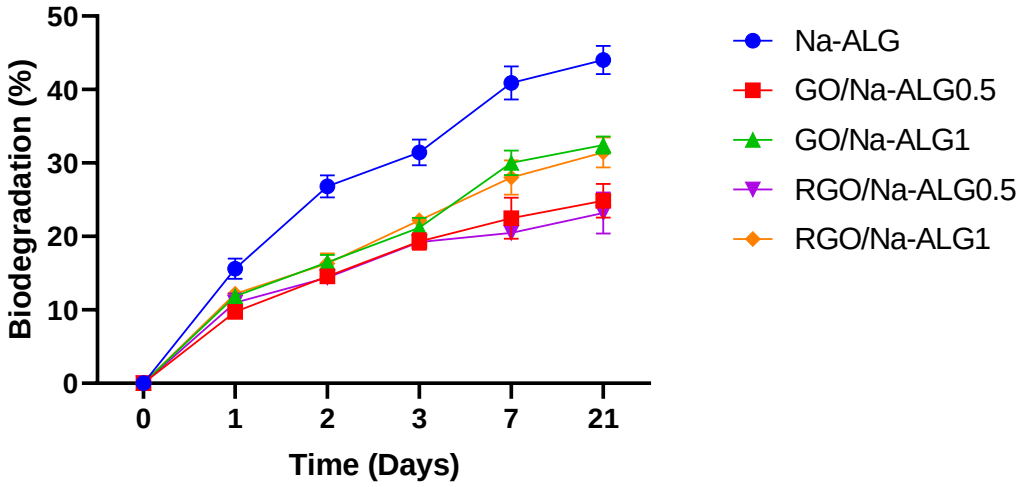


*Figure 4.1. The biodegradation rate of the Na-ALG, GO/Na-ALG0.5, GO/Na-ALG1, RGO/Na-ALG0.5 and RGO/Na-ALG1 scaffolds as a function of time within 3 weeks. Na-ALG scaffolds showed the quickest biodegradation rate comparing to all composite scaffolds.*

### 4.5.2 Cell Viability using Flow Cytometry

Cell viability was assessed using flow cytometry by labelling cells with 7-AAD staining to determine the effects of 3D scaffolds in DPSCs viability and apoptosis. The primary challenge was to acquire reliable data from adherent DPSCs detached from 3D bioscaffolds. Figure 4.2 (a-c) shows flow cytometry dot plots of cell population on the 2D surface at density 1, 3 and 5. The ungated cells were analysed based on their forward scatter and side scatter populations. It can be seen from Figure 4.2 (c) that more than 80% of DPSCs are viable when cultured on control 2D surface.

Furthermore, regarding flow cytometry analysis of 3D scaffolds, the percentage of viable cells cultured on Na-ALG scaffolds were found as 48.84%, 51.43%, and 49.04% for cell density 1, 3 and 5, respectively (as shown in Figure 4.3 (a-c)). However, cell viability was measured as 48.67%, 58.15%, 29.40% for GO/Na-ALG1 scaffolds with a seeding density of 1, 3 and 5, respectively (Figure 4.4 (a-c)).

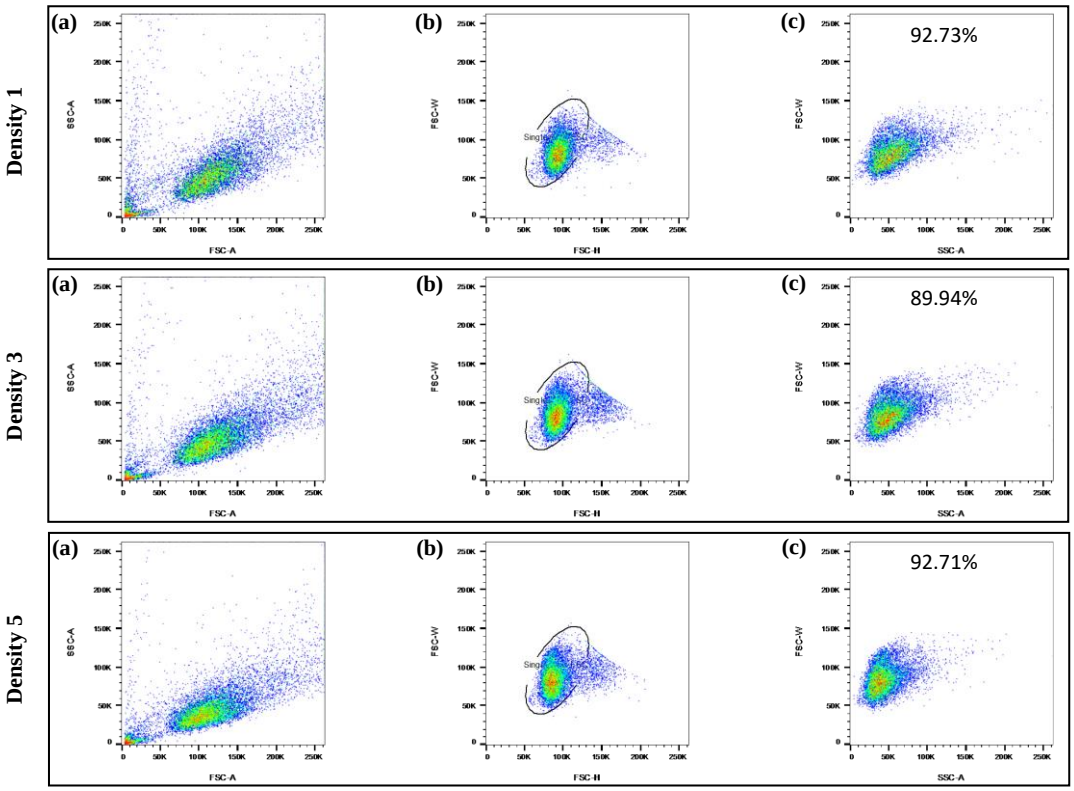


*Figure 4.2. Representative flow cytometry plots, 7-AAD staining, of DPSCs viability on the 2D surface (No Scaffold) at different cell seeding densities showing forward scatter (FSC) and side scatter (SSC) profiles: (a)Ungated, (b) Viable cells, and (c) Single cells are shown. Percentage of viable cells are shown for each condition.*

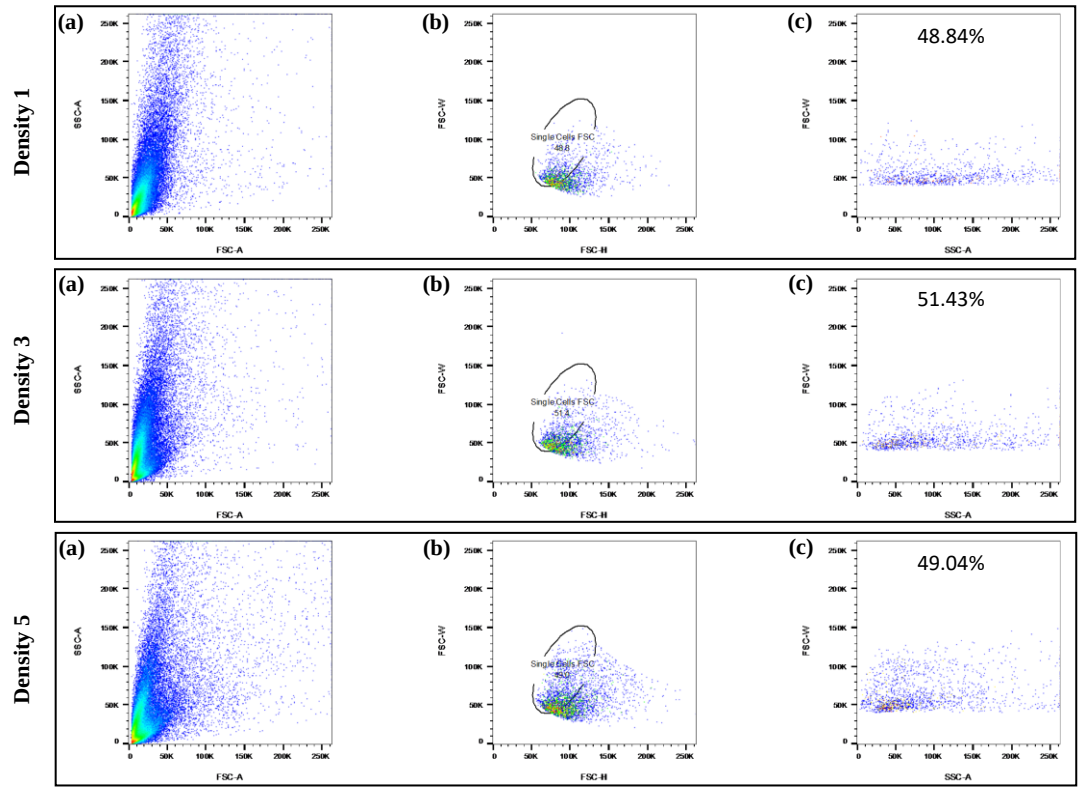


*Figure 4.3. Representative flow cytometry plots, 7-AAD staining, of DPSCs viability on 3D Na-ALG Scaffolds at different cell seeding densities showing forward scatter (FSC) and side scatter (SSC) profiles: (a)Ungated, (b) Viable cells, and (c) Single cells are shown. Percentage of viable cells are shown for each condition.*

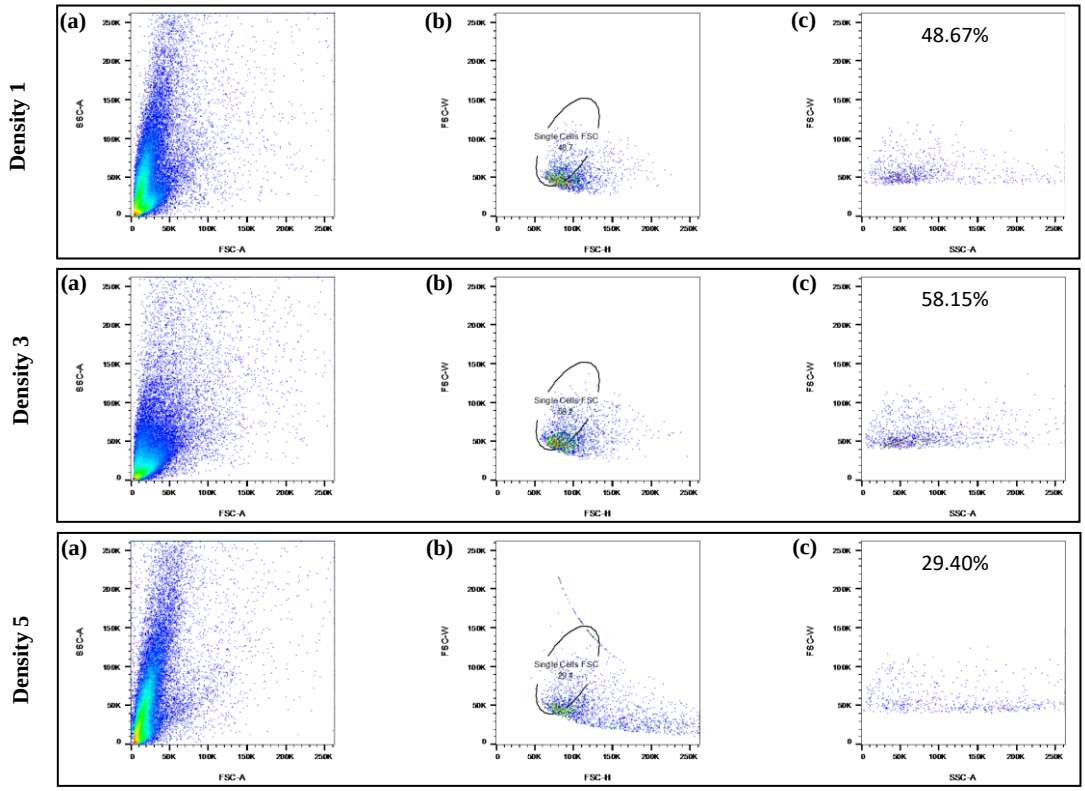


*Figure 4.4. Representative flow cytometry plots, 7-AAD staining, of DPSCs viability on 3D GO/Na-ALG1 Scaffolds at different cell seeding densities showing forward scatter (FSC) and side scatter (SSC) profiles: (a)Ungated, (b) Viable cells, and (c) Single cells are shown.*

Regarding staining of DPSCs with H191, flow cytometry data in Figure 4.5 shows more than 98% of cell viability for cells cultured on the 2D environment (No scaffold) at all experimented densities.

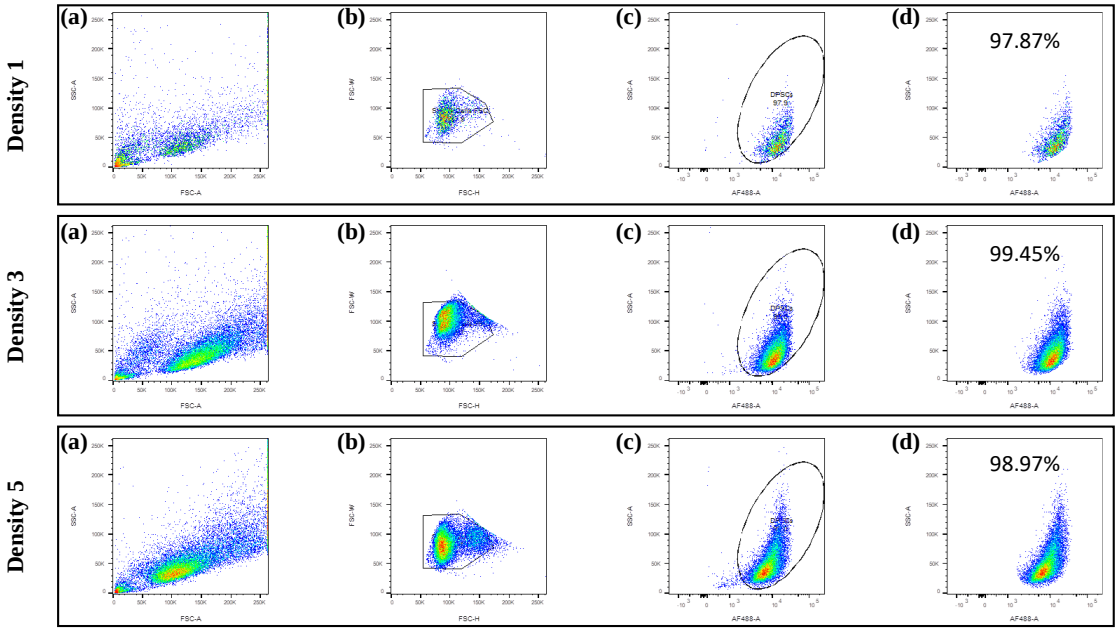


*Figure 4.5. Representative flow cytometry plots, 7-AAD and H191 staining, of DPSCs viability on the 2D surface (No Scaffold) at different cell seeding densities showing forward scatter (FSC) and side scatter (SSC) profiles: (a)Ungated, (b) Viable cells, (c) Single cells, and (d) DPSCs are shown. Percentage of viable cells are shown for each condition.*

Cell viability of DPSCs seeded on 3D Na-ALG and GO/Na-ALG1 scaffolds decreased dramatically following H191 staining as illustrated in Figure 4.6 and Figure 4.7, respectively. The highest percentage of viable cells was recorded at density 5 for both scaffolds. Over 86% of cultured cells on Na-ALG scaffolds were dead, as shown in Figure 4.6 (d). Besides, DPSCs on GO/Na-ALG1 scaffolds showed maximum 15.39% viability, showing a drastic reduction in cell viability in comparison to Figure 4.4.

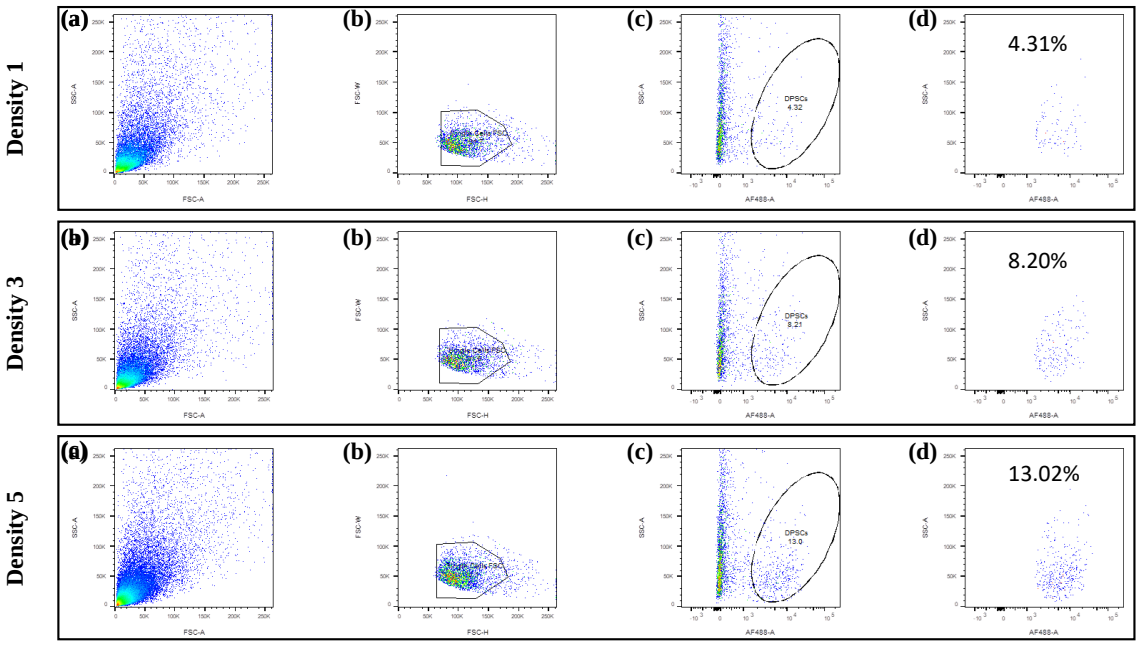


*Figure 4.6. Representative flow cytometry plots, 7-AAD and H191 staining, of DPSCs viability on 3D Na-ALG Scaffolds at different cell seeding densities showing forward scatter (FSC) and side scatter (SSC) profiles: (a)Ungated, (b) Viable cells, (c) Single cells, and (d) DPSCs are shown. Percentage of viable cells are shown for each condition.*

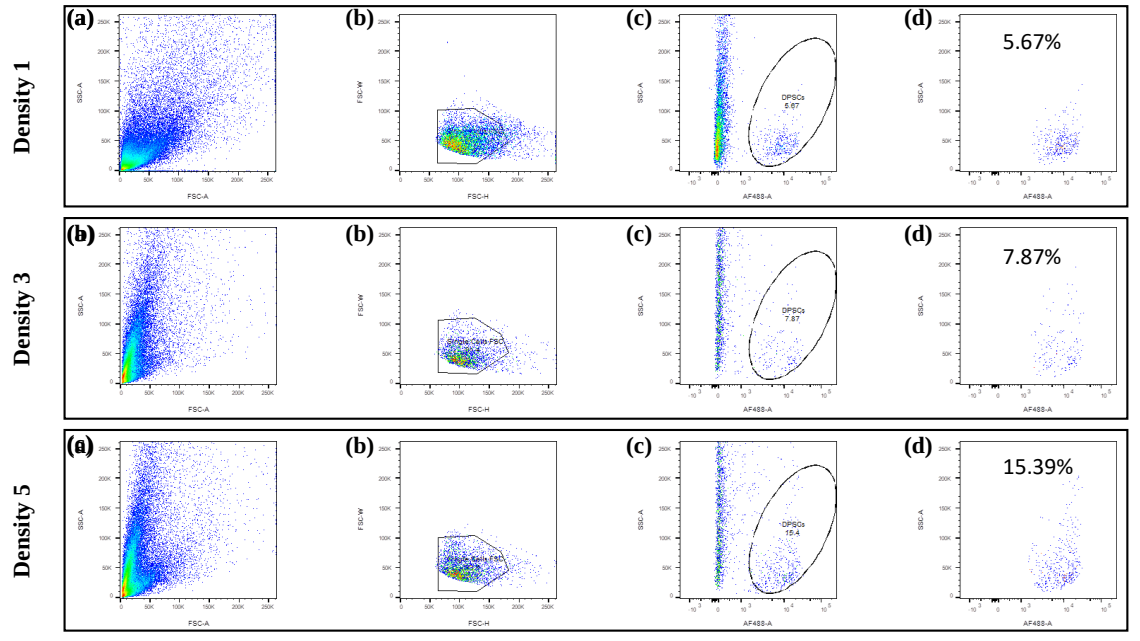


*Figure 4.7. Representative flow cytometry plots, 7-AAD and H191 staining, of DPSCs viability on 3D GO/Na-ALG1 Scaffolds at different cell seeding densities showing forward scatter (FSC) and side scatter (SSC) profiles: (a)Ungated, (b) Viable cells, (c) Single cells, and (d) DPSCs are shown. Percentage of viable cells are shown for each condition.*

### 4.5.3 Cell Viability using AB Assay

#### 4.5.3.1 Comparison based on 2D vs 3D Culture System

The viability of DPSCs grown in 2D or 3D scaffold was assessed using the AB assay. After 24 h of cell culture (Figure 4.8), there was a significant increase in the cellular activity of Na-ALG and GO/Na-ALG scaffolds seeded with DPSCs comparing to DPSCs grown in the 2D environment at all cell densities (P <0.0001). Cells seeded directly on the surface have an average degree of AB reduction of 53.7±1.00% across all five seeding densities. It is also shown that cells on 3D scaffolds were more viable compared to no scaffold (2D) condition which implies good cell adhesion on 3D scaffolds.

#### 4.5.3.2 Comparison based on Cell densities

After 24h of cell culture, both scaffolds (Na-ALG and GO/Na-ALG) supported cell viability across various cell densities with no negative effect on seeding efficiency (Figure 4.8). It is shown that AB reduction increased significantly, as an indication of metabolic activity, in Na-ALG and GO/Na-ALG1 scaffolds at all five cell densities.

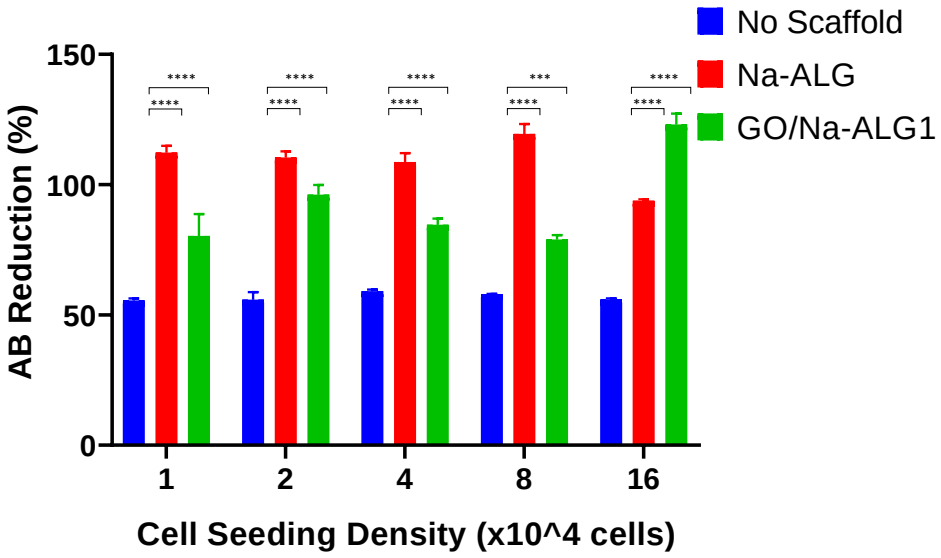


*Figure 4.8. 24-hour Alamar Blue reduction (%) of 2D surface (No Scaffold), Na-ALG and GO/Na-ALG1 scaffolds at five cell seeding densities; * indicates statistical significance (***p <0.001, ****p <0.0001).*

#### 4.5.3.3 Comparison based on Coatings

As DPSCs viability was not affected by seeding density conditions, density 1, 3 and 5 were selected to conduct 24- and 48-hour AB assay. In order to determine the effects of coating conditions on seeded DPSCs, three different coating conditions including NC, PLL, and PLL+LAM were used. The effect of cell seeding densities was impacted by various coating conditions within the first day of DPSCs culture. Significantly higher AB reduction percentage was observed for Na-ALG and GO/Na-ALG scaffolds at all three densities comparing to the 2D control condition (Figure 4.9 (a-c)). After 48 h of DPSCs culture, statistically significant differences were determined in the proliferation profile of cells growing in 2D and 3D in various coating conditions (Figure 4.9 (d-f)). In addition, PLL coating significantly increases the cellular activity of GO/Na-ALG scaffolds at all three cell densities within two days of DPSCs culture (Figure 4.9).

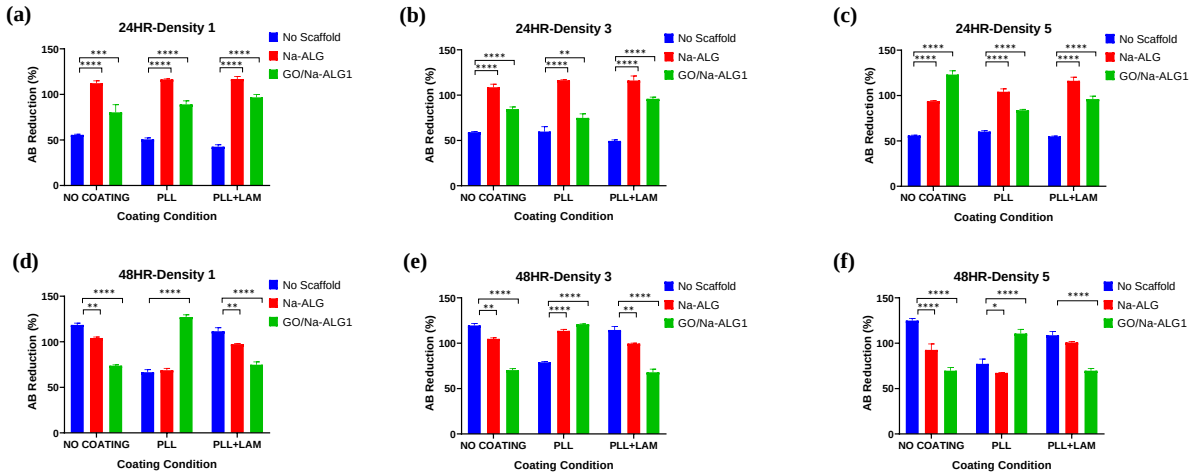


*Figure 4.9. (a-c) 24- and (d-f) 48-hour change in Alamar Blue reduction percentage of No scaffold, Na-ALG and GO/Na-ALG1 scaffolds across (a, d) Density 1 ($1\times10^4$cells/scaffold), (b, e) Density 2 ($4\times10^4$cells/scaffold), and (c, f) Density 5 ($16\times10^4$cells/scaffold); * indicates statistical significance (**p <0.01, ***p <0.001, ****p <0.0001).*

### 4.5.3.4 Comparison based on Scaffold Compositions

The metabolic activity of cultured DPSCs on various scaffolds was measured using the AB assay to explore the effects of scaffold biomaterials on cellular functions. Cellular activity in Na-ALG scaffolds showed no significant change in comparison with 2D cell culture (Figure 4.10). Moreover, the cell viability was significantly increased on GO/Na-ALG1, RGO/Na-ALG0.5 and RGO/Na-ALG1 scaffolds compared to SA only scaffolds across all coating conditions. A significantly higher degree of reduction of the AB dye by the DPSCs grown on PLL-coated graphene-based scaffolds was observed than those cultured on the 2D surface, which implies the importance of PLL coating (as previously proved in coating conditions). The highest AB reduction percentage was recorded for PLL-coated RGO/Na-ALG1 as 93.66±5.88%.

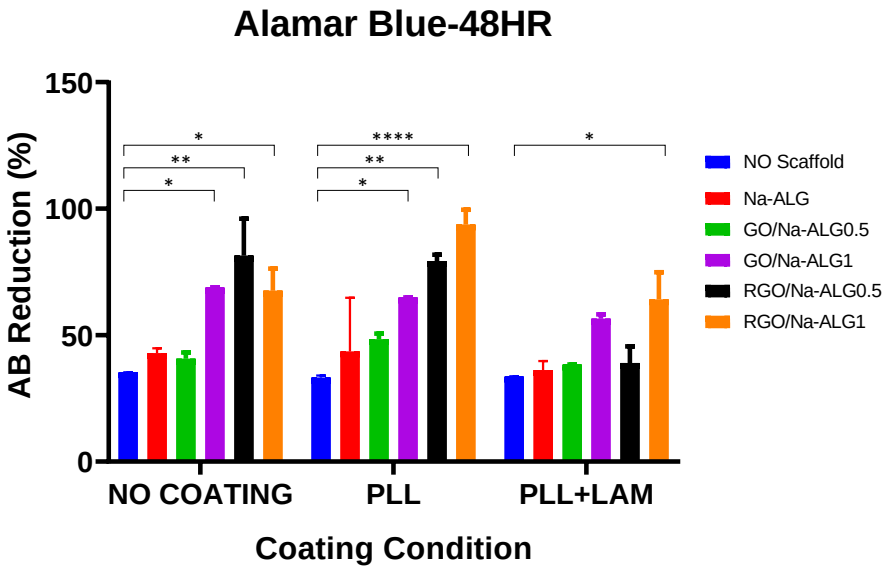


*Figure 4.10. 48-hour Alamar Blue assay of DPSCs seeded on 2D surface (No scaffold), Na-ALG, GO/Na-ALG0.5, GO/Na-ALG1, RGO/Na-ALG0.5 and RGO/Na-ALG1 scaffolds; * indicates statistical significance (*p <0.05, **p <0.01, ****p <0.0001).*

### 4.5.4 Cell Toxicity using LDH Assay

The cytotoxicity of fabricated scaffolds was studied using analysis of lactate dehydrogenase (LDH) release in culture media induced by DPSCs with damaged membrane. At 24 hours of DPSCs culture, all biomaterials have a relatively low level of released LDH (Figure 4.11 (a)). However, significant increased LDH levels of DPSCs have been observed for uncoated Na-ALG (41.65±7.35%) and PLL-coated GO/Na-ALG0.5 (34.31±5.31%) scaffolds after one day of cell culture. It is interesting to note that, after 48 hours of culture, DPSCs toxicity on graphene-based scaffolds were not significantly higher than the 2D surface (Figure 4.11 (b)). However, DPSCs cultivated onto pure Na-ALG scaffolds displayed the highest levels of cytotoxicity as compared to 2D control (no scaffold) ($p<0.0001$).

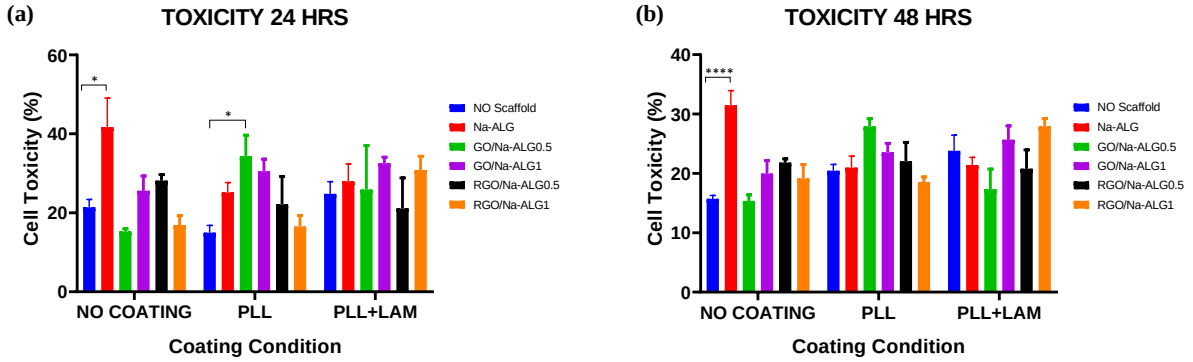


*Figure 4.11. The cell cytotoxicity of the scaffolds measured by LDH assay in no coating, PLL and PLL+LAM coating conditions after (a) 24 and (b) 48 hours of DPSCs culture; * indicates statistical significance (*p <0.05, ****p <0.0001).*

#### 4.5.4.1 Effects of mean pore size on cellular behaviour in scaffolds

The results of AB and LDH assays were utilized to observe the effects of scaffolds' pore size on cellular behaviour. As mean pore size increases on PLL-coated scaffolds, cellular activity decreases (Figure 4.12 (a)). The lowest AB reduction percentages were measured for PLL+LAM coated Na-ALG and GO/Na-ALG0.5 scaffolds with the largest mean pore sizes as 36.12% and 38.33%, respectively. Accordingly, the relatively lowest cytotoxicity was observed for RGO/Na-ALG0.5 (116.0 μm) and RGO/Na-ALG1 (114.7 μm) scaffolds with smaller mean pore sizes comparing to Na-ALG and other composite scaffolds (Figure 4.12 (b)). Overall, a negative correlation (Spearman R = −0.83) between the mean pore size of scaffolds and cellular activity (obtained by AB assay) and a positive correlation (Spearman R = 0.06) between the mean pore size of scaffolds and cell cytotoxicity (obtained by LDH assay) was observed, showing that increasing mean pore size induces a decrease in DPSCs activity and an increase in DPSCs toxicity.

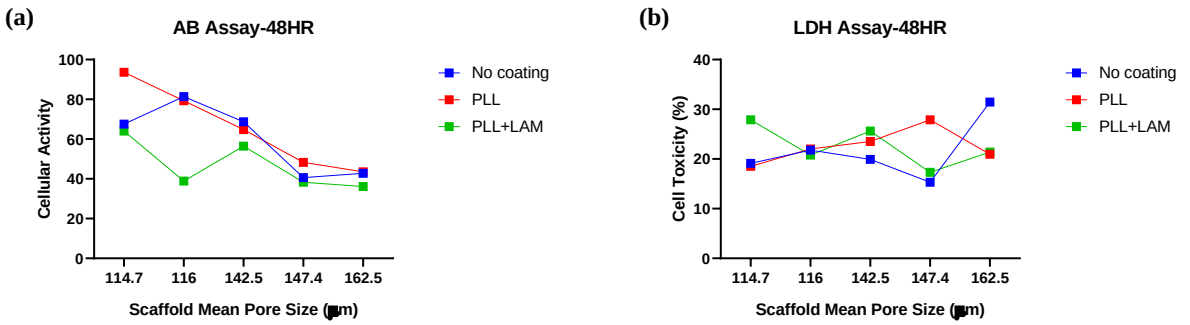


*Figure 4.12. Effect of mean pore sizes on (a) cell activity and (b) cell toxicity within various scaffolds (n=3) 48h after incubation (mean pore sizes: Na-ALG=162.5 µm, GO/Na-ALG0.5=147.4 µm, GO/Na-ALG1=142.5 µm, RGO/Na-ALG0.5=116.0 µm and RGO/Na-ALG1=114.7 µm). There is a strong negative correlation between cellular activity and mean pore size (Spearman R = −0.83) as well as a positive correlation between the cell toxicity and mean pore size (Spearman R = 0.06), that is, the enlargement of mean pore size leads to increase in cellular activity and decrease in cell toxicity.*

### 4.5.4.2 Effects of serum-supplemented scaffolds on cytotoxicity

Figure 4.13 (a) shows that after 24 h of DPSCs culture in serum-free media, all graphene-based scaffolds had significantly lower cytotoxicity levels comparing to cell only (2D) control, irrespective of coating conditions. The figure also highlights higher cell toxicity of Na-ALG scaffolds, across all coatings, comparing to both GO/Na-ALG1 and RGO/Na-ALG1 scaffolds. The highest LDH released (70%) under expose of DPSCs with PLL+LAM-coated Na-ALG scaffolds.

Besides, Figure 4.13 (b) indicates that DPSCs seeded in serum-supplemented media on PLL+LAM-coated 3D scaffolds showed significantly higher toxicity values than those cultured on a 2D surface. In PLL coatings, Na-ALG scaffolds (26.55±3.28%) showed significantly higher cell toxicity whereas GO/Na-ALG1 and RGO/Na-ALG1 scaffolds had no higher significant toxicity comparing to 2D culture system (13.40±2.19%). No-coated scaffolds showed no significant difference with no-scaffold control. After 24h of cell culture, serum-containing medium groups showed higher levels of cell toxicity in all experimental conditions (Figure 4.13 (a, b)).

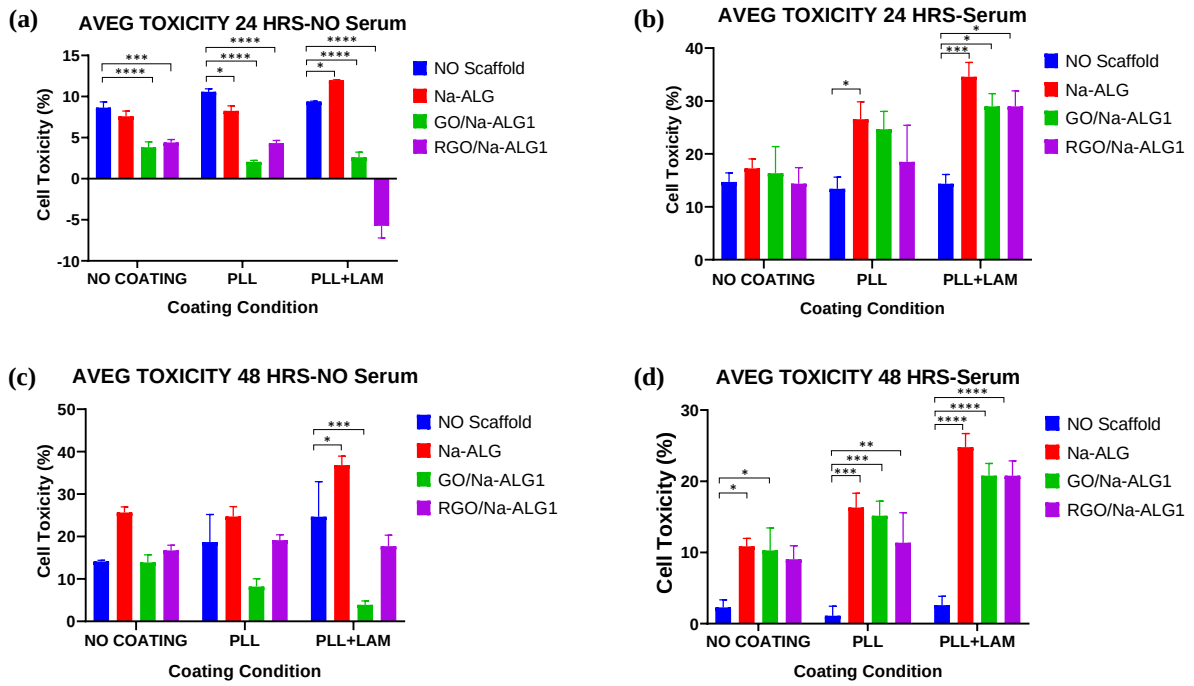


*Figure 4.13. Comparative evaluation of LDH assay by DPSCs (derived from Donor 1) grown on Na-ALG, GO/ Na-ALG1 and RGO/Na-ALG1 scaffolds at (a, b) 24- and (c, d) 48-hours post-seeding in (a, c) serum-free and (b, d) serum-containing media; * indicates statistical significance (*p <0.05, **p <0.01, ***p <0.001, ****p <0.0001).*

There are no significant increases in the percentage of cell toxicity of DPSCs exposed to coated and uncoated GO/Na-ALG1 and RGO/Na-ALG1 scaffolds comparing to 2D control (Figure 4.13 (c)). However, a significant elevation of LDH release was detected when DPSCs cultured on PLL+LAM-coated Na-ALG scaffolds with serum deprivation. After 48 h of cell culture with no serum, the cell toxicity percentage of almost all evaluated samples have been increased compared to 24 h time point.

When DPSCs in serum-rich media are seeded onto fabricated 3D scaffolds, cell toxicity of scaffolds increases significantly in comparison with no scaffold culture system, regardless of coating conditions (as indicated in Figure 4.13 (d)). Besides, after 48 h of cell culture with serum, the cell toxicity percentage of all evaluated samples have been reduced compared to 24 h time point.

Quantitative LDH activity measurements in Figure 4.14 (a) and (b) show that no significant differences were found, after 24 hours, between all 3D scaffolds seeded with DPSCs using serum-free or serum-containing media comparing to 2D control. These cytotoxic effects were not influenced by coating conditions. However, after 48h of cell culture with no serum (as shown in Figure 4.14 (c)), the percentage of viable cells on Na-ALG scaffolds was the highest among other analysed scaffolds across all coating conditions. Meanwhile, DPSCs cultured on GO/Na-ALG1 and RGO/Na-ALG1 scaffolds with no serum had not have any significantly higher cell toxicity values than those grown on the 2D surface, showing that GO is able to influence cell responses and release low LDH levels. The cell viability for all graphene-based scaffolds without serum was higher than 80%. However, the lowest cell viability was revealed for PLL+LAM-coated Na-ALG scaffolds 35.6 %.

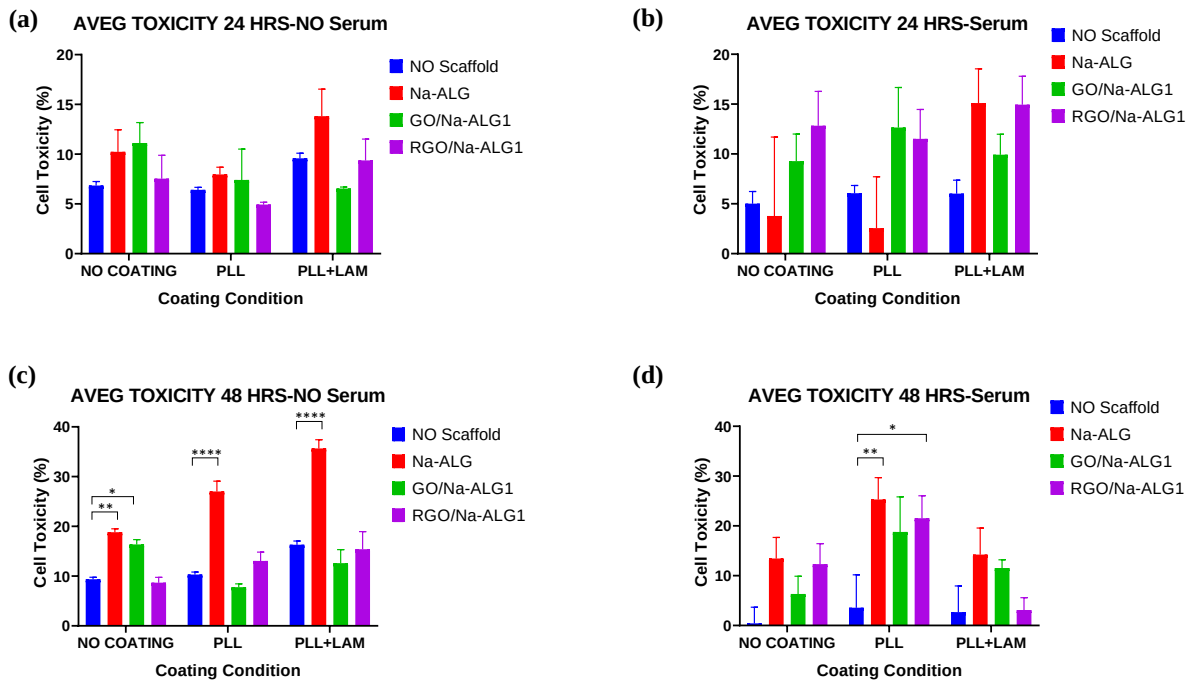


*Figure 4.14. Comparative evaluation of LDH assay by DPSCs (derived from Donor 2) grown on Na-ALG, GO/ Na-ALG1 and RGO/Na-ALG1 scaffolds at (a, b) 24- and (c, d) 48-hours post-seeding in (a, c) serum-free and (b, d) serum-containing media; * indicates statistical significance (*p <0.05, **p <0.01, ****p <0.0001).*

After 48 h of culturing DPSCs in serum-containing media, comparison with the 2D control disclosed no significant cell toxicity for 3D scaffolds under no coating and PLL+LAM conditions (Figure 4.14 (d)). However, significantly higher toxic effects were observed for SA (25.27±4.41%) and RGO/Na-ALG1 (21.51±4.52%) scaffolds when coated with PLL.

## 4.6 Discussions

The interaction between cells and engineered scaffolds is a complex process affected by several aspects including cell type, biomaterial properties, scaffold characteristics and experimental factors. Therefore, the objective of this study was to evaluate the capability of GO/Na-ALG and RGO/Na-ALG scaffolds to support DPSCs culture.

The biodegradation of scaffolds should take place in accordance with the growing tissue. The results of *in vitro* biodegradation study reveal that the composite GO/Na-ALG scaffolds with a higher concentration of the GO relatively lost more weight through easier accessibility of water molecules to the network. As discussed in the water contact angle measurements in our previous paper [286], the incorporation of GO increased the interaction of composite scaffolds with water. Therefore, as hydrophilicity accelerates with higher GO concentration, the water-mediated degradation of the scaffold increases, which is also indicated in another study [287]. After the reduction of GO/Na-ALG scaffolds, no significant changes observed in terms of weight loss. The reduced degradation rate of the nanocomposite scaffolds is assumed to be beneficial for the tissue regrowth [288]. Overall, incorporation of GO could control the quick degradation rate of Na-ALG scaffolds, and these results confirmed that the composite 3D scaffolds have adjustable degradability that can be controlled by the graphene content.

As determined by flow cytometry, there is a huge difference in apoptosis rates between 2D and 3D cultures. Lower cell viability on 3D scaffolds was observed comparing to 2D control which could be due to difficulties in detachment of cells from scaffold biomaterial during the flow cytometry procedures. Therefore, the primary challenge is to assess the cell viability of DPSCs detached from 3D scaffolds while minimizing the scaffold debris. To discern between scaffold debris and actual cell events, the H191 staining was performed. Less than 15.39% of total events were detected as DPSCs on 3D scaffolds as measured by flow cytometry plots. The presence of autofluorescent scaffold debris had caused complications in flow cytometric analysis of cells after seeding onto scaffolds. The debris particles clogged the fluidics system and obscured cellular events, causing non-realistic events detected by flow cytometry resulted from the generation of debris through enzymatic digestion of scaffolds and entrapment of some cells deep inside the network of pores. As a result, the most efficient methodology to measure cell viability of 3D scaffolds is to use the supernatant after cells are incorporated onto fabricated scaffolds which eliminate difficulties of cell detachment and generation of scaffold debris. Thus, AB and LDH assays which are based on cell culture supernatant were utilized to analyse DPSCs viability.

The AB analysis showed the importance of using a 3D matrix seeded with DPSCs which acts as a delivery system and also facilitates cellular functions in comparison to the 2D environment. In particular, the DPSCs viability cultured onto Na-ALG and GO/Na-ALG scaffolds was higher than that of culture plates in the absence of the biomaterial. This clearly signifies the desirable initial cell adhesion to the scaffold surface and further cell spreading. The increase in total metabolic activity of cell-seeded scaffolds provides good support for cell growth and proliferation. Thus, the use of artificial 3D scaffold is a good way to mimic the natural architecture of DPSCs. It is known that cellular behaviour is highly affected by the dimension of the culture model [289]. As a result, the proliferation rate increases in 3D matrices when cells infiltrate through a network of pores and colonize pores. This can clearly highlight the importance of 3D DPSCs culture in the outcome of cell viability studies. Thus, if DPSCs are cultured on 3D scaffolds, they can regain their actual biological properties which result in better proliferative ability. In contrast to 2D culture, the interaction of cells with each other and with the matrix in 3D cell culture systems extremely influence cellular functions including viability, migration and proliferation [290]. For instance, a study showed that 3D polymer-based scaffolds seeded with liver cells had less cytotoxic effects than those cultured in 2D [291]. In another relevant study, it is reported that the 3D culture of dental stem cells supported their neuronal characteristics and maintained the cell phenotypes [292]. Thus, the superior proliferative ability of DPSCs can be obtained when cultured on 3D porous scaffolds.

Regarding cell seeding density, it is shown that when cells are seeded on scaffolds at all densities, the cell proliferation significantly increases in comparison with cells seeded on the 2D surface. Moreover, increasing seeding density in 3D scaffolds did not exert cytotoxic effects. In this study, it was shown that the addition of graphene in 3D composite scaffolds improved cellular behaviour across all seeding densities of DPSCs. The cellular activity did not differ significantly between different cell densities, which implies no negative effects of 3D scaffolds on the distribution of cells and seeding efficiency even at high cell densities. High seeding densities might have different effects when increasing the length of culturing days.

Regarding coating reagents, it is revealed that PLL+LAM coating did not affect the cell viability of all tested samples and displayed similar AB reduction percentage trend with

uncoated samples. After 48 hours of DPSCs culture, laminin and no coating conditions decreased the cell viability on both Na-ALG and GO/Na-ALG scaffolds, which could be due to low adherence of DPSCs. It was reported in another study that laminin coating caused cell aggregation which led to decreased cell proliferation [293]. However, PLL was the coating reagent that improved robust cell-matrix adherence. This enhancement can be due to the increased number of cationic sites offered by PLL coating on the surfaces of our samples. Our results showed that coating reagents could affect metabolism activity of DPSCs, with PLL being superior to laminin coating which is in agreement with another study [293]. The effect of all three coating conditions on DPSCs was not impacted by alterations in the cell seeding density.

The AB assessments show that DPSCs responses on the fabricated scaffolds can be regulated by scaffold biomaterial composition. Na-ALG, GO/Na-ALG and RGO/Na-ALG scaffolds exhibited higher AB reductions as compared to the no scaffold control suggesting that these materials are not toxic with DPSCs. Also, it can be concluded that the composition of scaffold materials has a direct effect on the factors that influence the fate determination of these cells. The results suggest that different scaffolds with varying material properties (such as blend ratio, swelling index, microstructure) induce various effects on DPSCs behaviour. The observed increase in cell viability upon the incorporation of graphene in composite scaffolds is consistent with some other studies [285, 294]. The outstanding surface properties and adsorption capacity of graphene-based nanomaterials are the main factors which contributed to promoting DPSCs responses. However, excellent electrical properties of graphene in RGO/Na-ALG scaffolds can be further exploited for electrical stimulation and stem cell differentiation.

The AB reduction percentage decreased by the increment of mean pore size in fabricated scaffolds. Lower level of AB reductions in Na-ALG (97.2%) scaffolds were observed comparing to graphene-based scaffolds including GO/Na-ALG0.5 (97.5%), GO/Na-ALG1 (98.0%), RGO/Na-ALG0.5 (99.05%), and RGO/Na-ALG1 (99.18%). The differences in AB reduction across various graphene-based scaffolds could be explained by variations in the porosity of scaffolds. Scaffolds with higher porosity (RGO/Na-ALG $\approx$ 99%) are able to accommodate a higher number of viable cells when compared to scaffolds with low porosity (GO/Na-ALG $\approx$ 97%). Besides, it was shown that the scaffolds with smaller mean pores induce relatively less toxicity. This can be explained by the available surface area of scaffolds for cultured cells. The mean pore size and specific surface area are inversely proportional. The specific surface area and mean pore size of a scaffold affect initial cell adhesion and ensuring cell proliferation and migration [295]. It is well-known that the lowest levels of cell adhesion are observed on the scaffolds with larger pore size and less specific surface area [296, 297]. As a result, the available specific surface area per unit volume for cell adhesion of each fabricated scaffolds can be calculated using mean pore sizes [54]. Accordingly, the normalized specific surface area of GO/Na-ALG and RGO/Na-ALG scaffolds, as shown in Table 1, can be obtained by dividing the mean pore size of each scaffold by mean pore size of Na-ALG scaffold (3D control). As a result, higher AB reduction of RGO/Na-ALG1 scaffolds can be explained by the higher specific surface area comparing to GO/Na-ALG1 and Na-ALG scaffolds. Therefore, a larger surface area is available for cells to adhere and proliferate on RGO/Na-ALG scaffolds which resulted in enhanced cellular activity. These data show that higher pore size better facilitates DPSCs migration and proliferation, which is consistent with another study on culturing DPSCs into 3D scaffolds [298]. Also, the mechanical properties of the scaffolds with

too large pores are compromised. Higher cellular proliferation within large pore sizes can have effective implications for differentiation [299].

*Table 4.2. The estimate of the specific surface area of scaffolds relative to Na-ALG scaffold.*

| Sample | Mean pore size (μm) | Normalized Specific Surface Area |
|---|---|---|
| Na-ALG | 162.5 | 1 |
| GO/Na-ALG0.5 | 147.4 | 0.907 |
| GO/Na-ALG1 | 142.5 | 0.876 |
| RGO/Na-ALG0.5 | 116.0 | 0.713 |
| RGO/Na-ALG1 | 114.7 | 0.705 |

Thus, these results showed a strong influence of pore size, material composition and substrate dimensionality on cell viability which are also shown by Domingos et al. [300].

LDH measurements showed a significantly higher level of DPSCs toxicity of uncoated Na-ALG scaffolds which can be attributed to poor ability and lack of efficient sites of alginate scaffolds to support cell adhesion and proliferation. This has been shown in another study and that is the reason why other materials are mixed with alginate to create biocomposites [301]. However, the incorporation of GO in GO/Na-ALG scaffolds did not elicit significant cytotoxic effects after 2 days of DPSCs culture. Not only GO in the composition of scaffold materials did not lead to higher cell toxicity, but also has positive effects on cell functions in long term DPSCs culture, which is also revealed in other studies on GO layer cultured with mesenchymal stromal cells and GO/chitosan scaffolds seeded with human adipose-derived stem cells [302, 303]. Overall, the GO-enriched scaffolds exhibited cytotoxicity of 15–27% after 48h of culture, suggesting that these materials are biocompatible with DPSCs.

The variability in using serum-free or serum-rich culture media for biological assays is still a matter of debate [304]. The associated clinical problematic issues with the use of fetal bovine serum (FBS) include immune rejection, batch to batch variations, unidentified growth factors and proteins, and viral contamination [305]. For example, there is clear evidence about the positive effects of serum-free neuronal media on retaining stemness of DPSCs [306, 307]. In another study, serum-free cultured DPSCs within chitosan scaffolds expressed stem cell markers (nestin and Sox2) and were survived successfully after transplantation into SCI models which could have neural therapeutic capability [308]. Therefore, it has been demonstrated whether serum depletion can facilitate attachment of DPSCs onto the scaffolds. Hence, the adhesion of DPSCs onto the fabricated scaffolds was facilitated by coating conditions. It is showed that cytotoxicity of DPSCs cultured in serum-rich media onto 3D scaffolds increased significantly in comparison with 2D control. This could be due to the formation of protein corona on the GO surface which influences the toxicity level of GO-based materials [309, 310]. Furthermore, studies have been pointed that the amount of serum proteins can highly interfere with the way nanoparticles interact with cells and biological molecules [311-313]. Accordingly, Lesniak et al. [312] demonstrated that various protein corona on silica nanoparticles have modified cell adhesion, cellular uptake, and toxicity, which is determined by the serum concentration. It was shown that serum-containing media resulted in lower cell adhesion and internalization efficiency of silica nanoparticles. Besides, our results showed that DPSCs can be seeded in serum-free media onto GO/Na-ALG and RGO/Na-ALG scaffolds with no cytotoxic effects, showing promising potential for human translation as cellular transplants are typically serum-free.

The available specific surface area by the microstructure of scaffolds lead to more protein adsorption and therefore increase scaffold-cells interactions. Meanwhile, surface properties of graphene have a considerable effect on protein adsorption ability of scaffolds [314]. In particular, RGO and GO, with their unique surface chemistry, have impressive surface interactions with serum proteins due to their oxygenated functional groups, hexagonal structure and hydrogen bonding [315]. Thus, the effects of serum on cytotoxicity of DPSCs have been tested using 2D and 3D culture systems across three different coating conditions at a cell density of 4 × 104 cells/sample. It is shown that there is a correlation between the serum starvation of cell culture medium and the LDH release. The increased level of cytotoxicity of graphene-based scaffolds in the serum-containing medium could be due to the capability of GO and RGO to adsorb FBS owing to their surface oxygen content compared to Na-ALG scaffolds and well-plate surface. Besides, the presence of serum significantly caused higher cytotoxic behaviour of PLL-coated scaffolds which could be due to lack of cell attachment on the scaffold surface. These findings are in agreement with results from another study [316]. The combination of PLL and LAM coatings (in the presence of serum) on the 3D structures have led to lower available surface area of scaffold biomaterials for cell receptors to be attached, which subsequently caused poor cell adhesion. In contrast, PLL+LAM-coated 2D surface was found to result in better attachment of DPSCs which is due to the unfavourable bare tissue culture surface. Regardless of coating conditions, results show that while in both donors GO/Na-ALG and RGO/Na-ALG scaffolds have comparable cytotoxic levels in the absence of serum, scaffolds did not exhibit significantly higher LDH release to control cell only condition. Taken together, these results showed that the deprivation of serum decreased cell toxicity of DPSCs cells on the fabricated scaffolds.

There are significant differences observed between the percentage of LDH released in two different donor types, for all scaffold types under all coating conditions. However, these cell viability and toxicity results are demonstrating a behaviour in accordance with intrinsic characteristic and variability of donors. Similarly, Miyagi et al. showed that DPSCs obtained from different donors have variations in ECM proteins which could cause various cell adhesion behaviour [317].

## 4.7 Chapter Summary

The implantable scaffolds should have in-line biodegradability with mechanical integrity and new tissue formation. The results of *in vitro* biodegradation study showed that the composite GO/Na-ALG scaffolds with a higher concentration of the GO relatively lost more weight according to the wettability of composite scaffolds. Besides, no significant changes observed in degradation rates of RGO/Na-ALG in comparison to GO/Na-ALG. The fabricated porous 3D scaffolds have controlled biodegradability which is effective in therapeutic tissue engineering.

The biocompatibility of designed scaffolds is a pre-requisite for generating functional tissue engineering constructs. This chapter started with an extensive review of toxicology studies of graphene-based materials with the focus of the synthesis method and viability assays. In this chapter, it is shown that the biocompatibility of graphene-based nanomaterials is highly dependent on their concentration, size, shape, synthesis method and cell type. It is significant to evaluate the potential cytotoxic effects of graphene-based products to develop the desired clinical outcomes. Moreover, the feasibility of selected toxicity assays is a crucial step in

acute toxicity prediction of the analysed materials. While it has been shown that the proposed graphene-based scaffolds in Chapter 3 are able to serve as appropriate platforms to support stem cell fate for neural tissue engineering applications, this chapter explored the bioactivity and *in vitro* cytotoxicity of the fabricated scaffolds for neural induction. In order to achieve this, DPSCs were cultured in the prepared 3D scaffolds as well as 2D control environment. Then, AB colourimetric and LDH assays were used to analyse cell activity and viability after 24 and 48 h of culture across three different coating conditions. The AB assay confirmed the important role 3D matrices loaded with DPSCs in supporting cellular functions. Particularly, the DPSCs viability cultured onto Na-ALG and GO/Na-ALG scaffolds was higher than that of on 2D controls thus signifying the desirable initial cell adhesion to the scaffolds' surface followed by cell spreading through pores. Besides, the DPSCs toxicity, as a result of LDH release, on the GO/Na-ALG and RGO/Na-ALG scaffolds was comparable to that obtained on the 2D surface in the absence of the biomaterial.

Regarding coating materials, PLL was the most robust reagent that improved cell-matrix adherence and affected metabolism activity of DPSCs, being superior to laminin coating. However, the effects of all coating conditions on DPSCs were not impacted by changes in the cell seeding densities. The incorporation of graphene into the composite scaffold did not elicit significant cytotoxic effects after 2 days of DPSCs culture. As a result, GO supported higher DPSCs viability and function. In particular, the GO-enriched scaffolds exhibited cytotoxicity of 15–27% during 48h of culture, suggesting that these materials are biocompatible with DPSCs. This favourable effect is mainly due to unique surface chemistry, good mechanical properties, high surface area, and excellent physicochemical properties of graphene-based nanomaterials. The cytotoxicity of GO/Na-ALG and RGO/Na-ALG scaffolds in the presence of serum are increased in comparison to serum-free condition. This was explained by the capability of graphene-based materials to adsorb serum proteins owing to their surface oxygen content compared to the control groups. In addition, there were some differences observed in cell viability and toxicity levels of analysed samples between two different DPSCs donors. These discrepancies could be due to variations in ECM proteins and/or donor intrinsic characteristics such as age and gender. The findings from the current study suggest that proposed composite 3D graphene-based scaffolds had a favourable effect on the biological responses of DPSCs. In the next chapter, a summary of all tasks, contributions, and conclusion are presented. Moreover, recommendations for future continuation of this work are presented.

# CHAPTER 5: CONCLUSIONS AND FUTURE DIRECTIONS

## 5.1 Introduction

Treatment of SCI using cell transplantation imposes a number of limitations on the effectiveness in providing regenerative therapy at the spinal lesion cavity due to a number of factors, these include poor axonal regeneration and extension, low cell adhesion due to the existence of cerebrospinal fluid, and poor survival rate of cells because of inhibitory post-SCI environment. Tissue engineering has emerged as a promising alternative therapeutic strategy to conventional treatments based on guiding tissue regeneration using engineered scaffolds. Despite the multidisciplinary nature and vast challenges of the tissue engineering field, the opportunities for improving the quality of human life are enormous. In the field of NTE, the role of scaffolds (as shown in Figure 5.1) involves the delivery of stem cells, promoting nerve repair, supporting aligned axonal regrowth, and bridging of the lesion site [318, 319]. Graphene with excellent electrical conductivity, suitable biocompatibility, good mechanical properties, and high surface area has significantly contributed to the fabrication and design of NTE scaffolds. In recent years, an increasing number of researches has combined graphene-based materials with other polymers to fabricate nanocomposites as promising candidates for stimulating neural behaviour. However, the current challenge in the treatment of SCI is to develop biomaterial scaffolds that can fulfil multiple requirements including mimicking *in vivo* microenvironment, modulating cellular behaviour and functions, supporting regenerative growth and functional recovery of damaged neural tissues, and providing axonal regeneration and network connection. Thus, the aim of this current work is to engineer graphene-based composite scaffolds that interact with neural cells and induce nerve regeneration in the spinal cord. Furthermore, it introduces a new 3D graphene-based scaffold loaded with dental pulp stem cells (DPSCs) in order to promote stem cell fate.

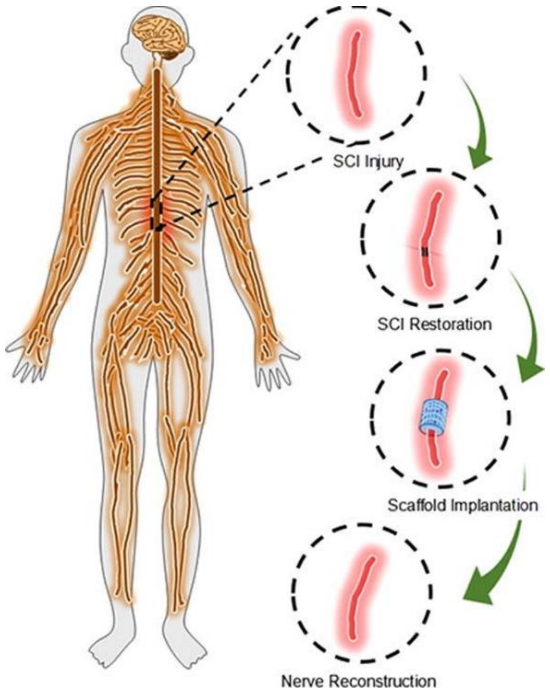


*Figure 5.1. Application of scaffolds in treatment of SCI [319].*

## 5.2 Summary of Research Contributions and Significance

The following points summarise the contributions of the current research.

- **A detailed review of the different approaches to SCI repair using biomaterials and stem cells:** In Chapter 1, after an introduction to the CNS diseases focusing on SCI, the conventional treatment options and NTE as a promising therapeutic strategy are described in details. It is believed that a combination of stem cell technology and tissue engineering strategies excellently fulfil the expectations of treatment of nervous system disorders. However, the success of this combinational approach highly depends on the utilization of a 3D scaffold to mimic the natural environment of neural tissues and provide synergistic cell guidance cues to assist tissue recovery. Besides, the important design elements in the fabrication of nerve conduits are given in Section 1.4. In this section, the major studies on the repair of the injured spinal cord using biomaterial scaffolds and stem cells are discussed and compared in detail. As a result, despite the numerous attempts and proven improvements over the recent years, a new class of multi-functional scaffold biomaterials to enhance the functional recovery of patients suffering from SCI after transplantation is necessitated.
- **A thorough review of previously developed graphene-based scaffolds and their outcomes:** In Chapter 2, after highlighting several commonly-used materials for designing scaffolds, pros and cons of common fabrication methods are discussed. Among current scaffold materials, graphene is identified as a highly attractive scaffold material for a various range of organs including cartilage, bone, skin, and brain owing to its porous morphology, great surface area, excellent mechanical strength, and good electrical conductivity. In Section 2.7, the potential of graphene-based nanomaterials in tissue engineering is discussed providing a review of previously developed graphene-based scaffolds and their outcomes. Iterating the advantages and shortcomings of tissue engineering scaffolds, the research gap is recognized, and the scope of the proposed research is outlined. It is reported that the utilization of graphene in designing 3D scaffolds creates a revolutionary impact on providing a favourable microenvironment for tissue regeneration. However, further studies need to be conducted to illustrate the cytotoxic effects of graphene-based materials on tissue regeneration outcomes. Then, this chapter concluded that fabrication of graphene-based composite scaffolds with tuneable properties could meet the specific tissue engineering requirements to achieve functional 3D tissues and their potential incorporation into the host. Besides, one of the most critical steps in the development of scaffold materials is to match the physiochemical characteristics of the scaffold biomaterials with the targeted tissue characteristics. Therefore, there is a need for the development of 3D graphene-based composite scaffolds to mediate culturing cells with matched microenvironment for cell growth and interconnected pores for penetration and migration of cells.
- **Development of the 3D scaffold using graphene oxide and sodium alginate:** In Chapter 3, the development of the proposed 3D scaffold, called GO/Na-ALG, is carried out through combining GO and Na-ALG. A simple and eco-friendly synthetic method is introduced and optimized to match the mechanical strength of the CNS tissue and provide a porous structure for connective tissue engineering. The fabrication process used solution mixing, freeze-drying and crosslinking which resulted in an improved, high yield strength and integrity 3D scaffold structure with desirable pore size greater

than 50 μm needed for neuron cell culture. Besides, the key synthetic conditions including GO concentrations, bioreduction process and crosslinking time are considered. The bioreduction procedure has developed conductive RGO/Na-ALG scaffolds which are effective for neural regrowth.

- **Development of scaffolds with favourable physical, chemical mechanical and electrical properties of the developed sponge scaffolds:** The proposed GO/Na-ALG scaffolds presented in Chapter 3 aim to regulate neural cell behaviour and tissue progression. Following the successful fabrication of highly integrated 3D graphene-based scaffolds, optimizing their properties for NTE applications are investigated and reported in this chapter. Physical, chemical, mechanical and electrical properties of the developed sponge scaffolds in terms of the structure, porosity, thermal stability, mechanical stiffness, and electrical conductivity are characterized and presented. The experimental results showed that although the composite scaffold has water uptake ability, the integral composite scaffold could float in water, which clearly confirms that scaffold can hold its structure during cell culture. The introduction of graphene, apart from physical, electrical and chemical properties improvements, provides favourable properties for the formation of neural pathways. For instance, the incorporation of GO improved the hydrophilicity of 3D composite scaffolds in which the water contact angle was decreased by increasing the concentration of GO. In addition, electrochemical characterizations have shown that when GO content in the composite structure increased, the conductivity of the prepared scaffolds significantly increased, which can be employed later for electrical stimulation purposes. Regarding meeting the mechanical strength requirements, the compressive modulus of the proposed scaffolds has improved to more than 100 kPa after the addition of 1 mg $mL^{-1}$ of GO. The fabrication and characterization results suggested that the obtained porous scaffolds could serve as suitable platforms to support cellular responses for the 3D structure when combined with stem cells culture. However, there is a need to explore cell-matrix and cell-cell interactions on the GO/Na-ALG scaffolds, allowing greater understating of biological reactions of scaffold biomaterials.
- **Development of scaffolds with favourable biodegradability:** Once the physicochemical properties of the fabricated scaffolds have been characterized in Chapter 3, further *in vitro* biological evaluation is required. Hence, Chapter 4 examined the biodegradability of prepared graphene-based scaffolds to confirm their suitability for tissue engineering applications. The addition of GO in the composite scaffolds ameliorated the quick degradation rate of Na-ALG scaffolds which is beneficial for new tissue formation. Besides, the results of biodegradation study are in line with hydrophilicity measurements of the prepared scaffolds (in Chapter 3).
- **Evaluation of scaffolds biocompatibility with DPSCs:** The first step of scaffolds validation for NTE is the investigation of cytotoxicity and biocompatibility of the developed biomaterials. Therefore, the *in vitro* biological effects of the scaffold materials with DPSCs are also analysed in this chapter. Assessing cell interactions with scaffolds requires identification and selection of important experimental parameters such as sterilization, seeding and viability evaluation methods which are also covered in Chapter 4. Toxicity tests showed that the graphene-based composite scaffolds did not induce any cytotoxicity and are biocompatible with DPSCs, while the results of LDH assay exhibited cytotoxicity of 15–27% during 48h of culture on different GO-based 3D scaffolds. This favourable biocompatibility is attributable to unique surface

chemistry, good mechanical properties, high surface area, and excellent physicochemical properties of graphene-based nanomaterials.

- **Experimental validation of the proposed 3D scaffold with 2D scaffold as control:** DPSCs cultured on tissue culture surfaces were used as 2D controls to find out the effects of using 3D matrices on cellular behaviour. In order to achieve these, AB colorimetric and LDH assays were employed to estimate cell activity and viability within 48h of DPSCs culture across three different coating conditions and five different cell densities. The AB results showed that 3D scaffolds seeded with DPSCs effectively supported cellular functions and attachment. The DPSCs viability on Na-ALG and GO/Na-ALG scaffolds are significantly higher than that of on the 2D surface, which indicates desirable cell adhesion and infiltration through scaffold network. In addition, the measured LDH releases on 3D GO/Na-ALG and RGO/Na-ALG scaffolds are comparable to that obtained on 2D control.
- **Demonstrated the effectiveness of the proposed 3D structure robustness as bioscaffold using PLL coating:** Regarding coating reagent, PLL is recorded as the most robust coating material which enhanced cell adhesion and resulted in higher DPSCs activity. In particular, significantly higher degree AB reductions is observed by the DPSCs grown on PLL-coated graphene-based scaffolds than those cultured on 2D surface. This is due to the increased number of cationic sites offered by PLL coating on the surfaces of our samples. Therefore, our results show that coating reagents could affect metabolism activity of DPSCs. However, the effects of coating conditions on DPSCs are not impacted by changes in the cell seeding densities.
- **Demonstrated the effects of serum-containing media on the toxicity of DPSCs-seeded scaffolds:** The LDH assay findings indicated that the toxicity of DPSCs cultured on GO/Na-ALG and RGO/Na-ALG scaffolds in serum-containing media is increased in comparison to serum-free condition, which can be due to good protein adsorption capability of graphene owing to its surface oxygen content compared to Na-ALG and 2D surface. Besides, the combined PLL and LAM coatings (in the presence of serum) on the 3D scaffolds have caused a lower available surface area of scaffolds for cell receptors to be attached, which subsequently caused poor cell adhesion. Overall, the findings from this chapter suggest that the proposed composite porous 3D graphene-based scaffolds can potentially be utilized for the construction of neural networks and nerve regeneration. The fabricated scaffolds can provide 3D DPSCs culture for neural growth and promote the formation of tissue function.

## 5.3 Recommendations for Future Work

The current research work established the scientific and engineering foundation for the development of neural bioscaffolds. The scaffold composition and fabrication technique were developed to be highly simple, eco-friendly, mechanically robust, and reproducible. Graphene with its unique topographical, chemical, and electrical characteristics incorporated to bridge nerve defects and promote neural regeneration. The 3D composite scaffolds containing SA and GO are fabricated with high integrity in liquid by optimizing synthetic conditions. Besides, microporous structure, good hydrophilicity, and suitable mechanical strength have been achieved. The potential of combining stem cells and biomaterial scaffolds for NTE applications is demonstrated by utilizing DPSCs in 3D culture systems.

- **Electrical stimulation strategies using conductive RGO/Na-ALG scaffolds:** Most importantly, graphene-based scaffolds as conductive platforms can provide cues to affect cellular mechanisms through electrically stimulating cells, thus opening a new scenario for therapeutic neural regeneration applications. External electrical stimulation

can take a significant part in the development and enhancement of nerve tissue reconstruction. Regarding the cellular level, a wide range of cellular responses, particularly in excitable cells, are highly affected by internal electrical signals as well as external stimuli. Therefore, electroactive scaffolds could mediate electrical stimulation of membrane potential to improve cell alignment, proliferation, migration, and differentiation [320, 321]. With increasing research, the combined application of electrical stimulation with suitable conductive scaffolds is attracting researchers' attention in tissue engineering and regenerative medicine. However, the consequences of different stimulation models have to be considered carefully before these signals will be incorporated into cell-loaded scaffolds for enhanced *in vivo* performance. Hence, the future direction can be directed toward further application of electrical stimulation strategies using conductive RGO/Na-ALG scaffolds to evaluate their potential in enhancing neural and axonal regeneration.

- ***In vivo* investigation of the engineered scaffolds:** Another area of importance in tissue engineering is to conduct an entirely *in vivo* investigation after biocompatibility of the scaffold materials has been analysed (Chapter 4). This could involve employing the composite scaffold within SCI contusion to direct neurite extension and compensate neuronal loss along the scaffolds. The *in vivo* study of engineered scaffolds is a critical step toward the development of cell-based therapies and clinical applications. As a result, future studies concentrating on the efficacy of long-term usage of DPSCs-seeded GO/Na-ALG scaffolds in SCI animal models are highly necessary. Besides, in order to facilitate clinical treatments, the potential *in vivo* distribution and degradation behaviour of scaffold materials must be evaluated with a focus on their organ accumulation and excretion through the body [322]. Hence, the enzymatic biodegradation kinetics of the fabricated graphene-based scaffolds should be accurately obtained through *in vivo* experiments and match with the growth rate of the neural tissue.
- **Incorporation of therapeutic drugs with the engineered scaffolds:** One of the main goals in the field of NTE is to reduce the inhibitory environment at the site of injury in a controlled, and localized manner. To achieve this goal, scaffolds could be engineered to incorporate therapeutic drugs or ECM proteins for functional recovery after SCI. In addition, preventing infection and host immune response upon scaffold implantation by incorporating antibiotic drugs is a desirable tissue engineering requirement [323]. Therefore, novel approaches using targeted drug delivery through fabricated scaffolds with high efficiency and controlled drug release provide hints for future perspectives.

# References


[1] P. Rea, Essential clinical anatomy of the nervous system. Academic Press, 2015.

[2] H. Lodish, A. Berk, S. L. Zipursky, P. Matsudaira, D. Baltimore, and J. Darnell, "Overview of neuron structure and function," Molecular Cell Biology, vol. 4, 2000.

[3] A. M. Avellino, D. Hart, A. T. Dailey, M. Mackinnon, D. Ellegala, and M. Kliot, "Differential macrophage responses in the peripheral and central nervous system during wallerian degeneration of axons," Experimental neurology, vol. 136, no. 2, pp. 183-198, 1995.

[4] K. Tsao and L. R. Putnam, "Tissue engineering and cell-based therapeutics for repair of myelomeningocele," in Cellular Therapy for Neurological Injury: CRC Press, 2016, pp. 278-293.

[5] C. E. Schmidt and J. B. Leach, "Neural tissue engineering: strategies for repair and regeneration," Annual review of biomedical engineering, vol. 5, no. 1, pp. 293-347, 2003.

[6] J. He, X.-M. Wang, M. Spector, and F.-Z. Cui, "Scaffolds for central nervous system tissue engineering," Frontiers of Materials Science, vol. 6, no. 1, pp. 1-25, 2012.

[7] Z. Su, W. Niu, M.-L. Liu, Y. Zou, and C.-L. Zhang, "In vivo conversion of astrocytes to neurons in the injured adult spinal cord," Nature communications, vol. 5, p. 3338, 2014.

[8] E. Tamariz and A. Varela-Echavarría, "The discovery of the growth cone and its influence on the study of axon guidance," Frontiers in neuroanatomy, vol. 9, p. 51, 2015.

[9] L. Tian, M. P. Prabhakaran, and S. Ramakrishna, "Strategies for regeneration of components of nervous system: scaffolds, cells and biomolecules," Regenerative biomaterials, vol. 2, no. 1, pp. 31-45, 2015.

[10] P. DeSaix, J. G. Betts, E. Johnson, J. E. Johnson, O. Korol, D. H. Kruse, B. Poe, J. A. Wise, and K. A. Young, "Anatomy & Physiology: OpenStax," 2018.

[11] M. E. Schwab, "Repairing the injured spinal cord," Science, vol. 295, no. 5557, pp. 1029-1031, 2002.

[12] E. Y. Snyder and Y. D. Teng, "Stem cells and spinal cord repair," New England Journal of Medicine, vol. 366, no. 20, pp. 1940-1942, 2012.

[13] H. Nomura, B. Baladie, Y. Katayama, C. M. Morshead, M. S. Shoichet, and C. H. Tator, "Delayed implantation of intramedullary chitosan channels containing nerve grafts promotes extensive axonal regeneration after spinal cord injury," Neurosurgery, vol. 63, no. 1, pp. 127-143, 2008.

[14] S. Yoshii, M. Oka, M. Shima, A. Taniguchi, Y. Taki, and M. Akagi, "Restoration of function after spinal cord transection using a collagen bridge," Journal of Biomedical Materials Research Part A, vol. 70, no. 4, pp. 569-575, 2004.

[15] S. Stokols and M. H. Tuszynski, "Freeze-dried agarose scaffolds with uniaxial channels stimulate and guide linear axonal growth following spinal cord injury," Biomaterials, vol. 27, no. 3, pp. 443-451, 2006.

[16] Y. Suzuki, M. Kitaura, S. Wu, K. Kataoka, K. Suzuki, K. Endo, Y. Nishimura, and C. Ide, "Electrophysiological and horseradish peroxidase-tracing studies of nerve regeneration through alginate-filled gap in adult rat spinal cord," Neuroscience letters, vol. 318, no. 3, pp. 121-124, 2002.

[17] B. J. Cummings, N. Uchida, S. J. Tamaki, D. L. Salazar, M. Hooshmand, R. Summers, F. H. Gage, and A. J. Anderson, "Human neural stem cells differentiate and promote locomotor recovery in spinal cord-injured mice," Proceedings of the National Academy of Sciences, vol. 102, no. 39, pp. 14069-14074, 2005.

[18] P. Lu, L. Jones, E. Snyder, and M. Tuszynski, "Neural stem cells constitutively secrete neurotrophic factors and promote extensive host axonal growth after spinal cord injury," Experimental neurology, vol. 181, no. 2, pp. 115-129, 2003.

[19] D. L. Salazar, N. Uchida, F. P. Hamers, B. J. Cummings, and A. J. Anderson, "Human neural stem cells differentiate and promote locomotor recovery in an early chronic spinal cord injury NOD-scid mouse model," PLoS One, vol. 5, no. 8, 2010.

[20] W. Z. Ray and S. E. Mackinnon, "Management of nerve gaps: autografts, allografts, nerve transfers, and end-to-side neurorrhaphy," Experimental neurology, vol. 223, no. 1, p. 77, 2010.

[21] X. Gu, F. Ding, Y. Yang, and J. Liu, "Construction of tissue engineered nerve grafts and their application in peripheral nerve regeneration," Progress in neurobiology, vol. 93, no. 2, pp. 204-230, 2011.
[22] A. M. Moore, W. Z. Ray, K. E. Chenard, T. Tung, and S. E. Mackinnon, "Nerve allotransplantation as it pertains to composite tissue transplantation," Hand, vol. 4, no. 3, pp. 239-244, 2009.
[23] W. Niu and X. Zeng, "The Application of Stem Cell Based Tissue Engineering in Spinal Cord Injury Repair," Journal of Tissue Science & Engineering, vol. 2015, no. 03.
[24] R. Midha, "Emerging techniques for nerve repair: nerve transfers and nerve guidance tubes," Clinical neurosurgery, vol. 53, p. 185, 2006.
[25] H. Cao, T. Liu, and S. Y. Chew, "The application of nanofibrous scaffolds in neural tissue engineering," Advanced drug delivery reviews, vol. 61, no. 12, pp. 1055-1064, 2009.
[26] S. Jaganathan, A. John, M. Vellayappan, A. Balaji, H. Mohandas, and A. Subramanian, "Carbon nanotubes and graphene as emerging candidates in neuroregeneration and neurodrug delivery," International Journal of Nanomedicine, vol. Volume 10, no. 1, pp. 4267-4277, 2015.
[27] X. Wang, J. He, Y. Wang, and F.-Z. Cui, "Hyaluronic acid-based scaffold for central neural tissue engineering," Interface Focus, vol. 2, no. 3, pp. 278-291, 2012.
[28] M. Tsintou, K. Dalamagkas, and A. M. Seifalian, "Advances in regenerative therapies for spinal cord injury: a biomaterials approach," Neural regeneration research, vol. 10, no. 5, p. 726, 2015.
[29] A. Espinosa-Jeffrey, K. Oregel, L. Wiggins, R. Valera, K. Bosnoyan, C. Agbo, O. Awosika, P. M. Zhao, J. de Vellis, and S. Woerly, "Strategies for endogenous spinal cord repair: HPMA hydrogel to recruit migrating endogenous stem cells," in Regenerative Biology of the Spine and Spinal Cord: Springer, 2012, pp. 25-52.
[30] B. Shrestha, K. Coykendall, Y. Li, A. Moon, P. Priyadarshani, and L. Yao, "Repair of injured spinal cord using biomaterial scaffolds and stem cells," Stem Cell Research & Therapy, vol. 5, no. 4, pp. 1-11, 2014.
[31] S. Sakiyama-Elbert, P. Johnson, S. Hodgetts, G. Plant, and A. Harvey, "Scaffolds to promote spinal cord regeneration," in Handbook of clinical neurology, vol. 109: Elsevier, 2012, pp. 575-594.
[32] E. López-Dolado, A. González-Mayorga, M. T. Portolés, M. J. Feito, M. L. Ferrer, F. Del Monte, M. C. Gutiérrez, and M. C. Serrano, "Subacute tissue response to 3D graphene oxide scaffolds implanted in the injured rat spinal cord," Advanced healthcare materials, vol. 4, no. 12, pp. 1861-1868, 2015.
[33] A. Domínguez-Bajo, A. González-Mayorga, E. López-Dolado, and M. C. Serrano, "Graphene-derived materials interfacing the spinal cord: outstanding in vitro and in vivo findings," Frontiers in Systems Neuroscience, vol. 11, p. 71, 2017.
[34] H. Liu, Y. Wang, Y. Yang, A. Wang, C. Huang, Z. Zhao, P. Li, M. Liu, and Y. Fan, "Aligned graphene/silk fibroin conductive fibrous scaffolds for guiding neurite outgrowth in rat spinal cord neurons," Journal of Biomedical Materials Research Part A, 2020.
[35] R. G. Bai, K. Muthoosamy, S. Manickam, and A. Hilal-Alnaqbi, "Graphene-based 3D scaffolds in tissue engineering: fabrication, applications, and future scope in liver tissue engineering," International journal of nanomedicine, vol. 14, p. 5753, 2019.
[36] F. J. O'Brien, "Biomaterials & scaffolds for tissue engineering," Materials Today, vol. 14, no. 3, pp. 88-95, 2011.
[37] E. Carletti, A. Motta, and C. Migliaresi, "Scaffolds for tissue engineering and 3D cell culture," 3D Cell Culture: Methods and Protocols, pp. 17-39, 2011.
[38] A. J. Mothe, R. Y. Tam, T. Zahir, C. H. Tator, and M. S. Shoichet, "Repair of the injured spinal cord by transplantation of neural stem cells in a hyaluronan-based hydrogel," Biomaterials, vol. 34, no. 15, pp. 3775-3783, 2013.
[39] B. G. Kim, Y. M. Kang, J. H. Phi, Y.-H. Kim, D. H. Hwang, J. Y. Choi, S. Ryu, A.-E. Elastal, S. H. Paek, and K.-C. Wang, "Implantation of polymer scaffolds seeded with neural stem cells in a canine spinal cord injury model," Cytotherapy, vol. 12, no. 6, pp. 841-845, 2010.
[40] E. D. Gomes, S. S. Mendes, H. Leite-Almeida, J. M. Gimble, R. Y. Tam, M. S. Shoichet, N. Sousa, N. A. Silva, and A. J. Salgado, "Combination of a peptide-modified gellan gum hydrogel

with cell therapy in a lumbar spinal cord injury animal model," Biomaterials, vol. 105, pp. 38-51, 2016.
[41] C. Li, X. Chen, S. Qiao, X. Liu, C. Liu, D. Zhu, J. Su, and Z. Wang, "Effects of Wharton's jelly cells of the human umbilical cord on acute spinal cord injury in rats, and expression of interleukin-1β and nerve growth factor in spinal cord tissues," Artificial cells, nanomedicine, and biotechnology, vol. 44, no. 5, pp. 1254-1258, 2016.
[42] L. Zhang, H.-T. Zhang, S.-Q. Hong, X. Ma, X.-D. Jiang, and R.-X. Xu, "Cografted Wharton's jelly cells-derived neurospheres and BDNF promote functional recovery after rat spinal cord transection," Neurochemical research, vol. 34, no. 11, pp. 2030-2039, 2009.
[43] J. Wang, R. Chu, N. Ni, and G. Nan, "The effect of Matrigel as scaffold material for neural stem cell transplantation for treating spinal cord injury," Scientific Reports, vol. 10, no. 1, pp. 1-11, 2020.
[44] J. Koffler, W. Zhu, X. Qu, O. Platoshyn, J. N. Dulin, J. Brock, L. Graham, P. Lu, J. Sakamoto, and M. Marsala, "Biomimetic 3D-printed scaffolds for spinal cord injury repair," Nature medicine, vol. 25, no. 2, pp. 263-269, 2019.
[45] E. S. Rosenzweig, J. H. Brock, P. Lu, H. Kumamaru, E. A. Salegio, K. Kadoya, J. L. Weber, J. J. Liang, R. Moseanko, and S. Hawbecker, "Restorative effects of human neural stem cell grafts on the primate spinal cord," Nature medicine, vol. 24, no. 4, p. 484, 2018.
[46] Y.-C. Kim, Y.-H. Kim, J.-W. Kim, and K.-Y. Ha, "Transplantation of mesenchymal stem cells for acute spinal cord injury in rats: comparative study between intralesional injection and scaffold based transplantation," Journal of Korean medical science, vol. 31, no. 9, pp. 1373-1382, 2016.
[47] S. Han, B. Wang, X. Li, Z. Xiao, J. Han, Y. Zhao, Y. Fang, Y. Yin, B. Chen, and J. Dai, "Bone marrow-derived mesenchymal stem cells in three-dimensional culture promote neuronal regeneration by neurotrophic protection and immunomodulation," Journal of Biomedical Materials Research Part A, vol. 104, no. 7, pp. 1759-1769, 2016.
[48] Y. H. Wang, J. Chen, J. Zhou, F. Nong, J. H. Lv, and J. Liu, "Reduced inflammatory cell recruitment and tissue damage in spinal cord injury by acellular spinal cord scaffold seeded with mesenchymal stem cells," Experimental and therapeutic medicine, vol. 13, no. 1, pp. 203-207, 2017.
[49] J. R. Mauney, T. Nguyen, K. Gillen, C. Kirker-Head, J. M. Gimble, and D. L. Kaplan, "Engineering adipose-like tissue in vitro and in vivo utilizing human bone marrow and adipose-derived mesenchymal stem cells with silk fibroin 3D scaffolds," Biomaterials, vol. 28, no. 35, pp. 5280-5290, 2007.
[50] S. Gerecht, J. A. Burdick, L. S. Ferreira, S. A. Townsend, R. Langer, and G. Vunjak-Novakovic, "Hyaluronic acid hydrogel for controlled self-renewal and differentiation of human embryonic stem cells," Proceedings of the National Academy of Sciences, vol. 104, no. 27, pp. 11298-11303, 2007.
[51] Z. Li, M. Leung, R. Hopper, R. Ellenbogen, and M. Zhang, "Feeder-free self-renewal of human embryonic stem cells in 3D porous natural polymer scaffolds," biomaterials, vol. 31, no. 3, pp. 404-412, 2010.
[52] E. Knight and S. Przyborski, "Advances in 3D cell culture technologies enabling tissue-like structures to be created in vitro," Journal of anatomy, vol. 227, no. 6, pp. 746-756, 2015.
[53] B. Chan and K. Leong, "Scaffolding in tissue engineering: general approaches and tissue-specific considerations," European Spine Journal, vol. 17, no. 4, pp. 467-479, 2008.
[54] C. M. Murphy and F. J. O'Brien, "Understanding the effect of mean pore size on cell activity in collagen-glycosaminoglycan scaffolds," Cell adhesion & migration, vol. 4, no. 3, pp. 377-381, 2010.
[55] C. M. Murphy, M. G. Haugh, and F. J. O'Brien, "The effect of mean pore size on cell attachment, proliferation and migration in collagen–glycosaminoglycan scaffolds for bone tissue engineering," Biomaterials, vol. 31, no. 3, pp. 461-466, 2010/01/01/ 2010.
[56] I. Bružauskaitė, D. Bironaitė, E. Bagdonas, and E. Bernotienė, "Scaffolds and cells for tissue regeneration: different scaffold pore sizes—different cell effects," Cytotechnology, vol. 68, no. 3, pp. 355-369, 2016.

[57] G. Altay, S. Tosi, M. García-Díaz, and E. Martínez, "Imaging the Cell Morphological Response to 3D Topography and Curvature in Engineered Intestinal Tissues," Frontiers in Bioengineering and Biotechnology, vol. 8, p. 294, 2020.
[58] B. J. Papenburg, E. D. Rodrigues, M. Wessling, and D. Stamatialis, "Insights into the role of material surface topography and wettability on cell-material interactions," Soft Matter, vol. 6, no. 18, pp. 4377-4388, 2010.
[59] A. A. Zadpoor, "Bone tissue regeneration: the role of scaffold geometry," Biomaterials science, vol. 3, no. 2, pp. 231-245, 2015.
[60] F. G. Lyons, A. A. Al-Munajjed, S. M. Kieran, M. E. Toner, C. M. Murphy, G. P. Duffy, and F. J. O'Brien, "The healing of bony defects by cell-free collagen-based scaffolds compared to stem cell-seeded tissue engineered constructs," Biomaterials, vol. 31, no. 35, pp. 9232-9243, 2010.
[61] B. N. Brown, J. E. Valentin, A. M. Stewart-Akers, G. P. McCabe, and S. F. Badylak, "Macrophage phenotype and remodeling outcomes in response to biologic scaffolds with and without a cellular component," Biomaterials, vol. 30, no. 8, pp. 1482-1491, 2009.
[62] T. Ozawa, D. A. Mickle, R. D. Weisel, N. Koyama, H. Wong, S. Ozawa, and R.-K. Li, "Histologic changes of nonbiodegradable and biodegradable biomaterials used to repair right ventricular heart defects in rats," The Journal of thoracic and cardiovascular surgery, vol. 124, no. 6, pp. 1157-1164, 2002.
[63] S. Blacher, V. Maquet, F. Schils, D. Martin, J. Schoenen, G. Moonen, R. Jérôme, and J.-P. Pirard, "Image analysis of the axonal ingrowth into poly (D, L-lactide) porous scaffolds in relation to the 3-D porous structure," Biomaterials, vol. 24, no. 6, pp. 1033-1040, 2003.
[64] D. W. Hutmacher, "Scaffolds in tissue engineering bone and cartilage," in The biomaterials: Silver jubilee compendium: Elsevier, 2000, pp. 175-189.
[65] T. C. Lee and P. Niederer, "Chapter IV: Biomaterials and Tissue Engineering," in Basic engineering for medics and biologists: an ESEM primer, vol. 152: IOS Press, 2010.
[66] S. J. Hollister, "Scaffold engineering: a bridge to where?," Biofabrication, vol. 1, no. 1, p. 012001, 2009.
[67] N. Zhu and X. Chen, "Biofabrication of tissue scaffolds," Advances in biomaterials science and biomedical applications, pp. 315-328, 2013.
[68] S. Kumar, D. Azam, S. Raj, E. Kolanthai, K. Vasu, A. Sood, and K. Chatterjee, "3D scaffold alters cellular response to graphene in a polymer composite for orthopedic applications," Journal of Biomedical Materials Research Part B: Applied Biomaterials, vol. 104, no. 4, pp. 732-749, 2016.
[69] B. Subia, J. Kundu, and S. Kundu, "Biomaterial scaffold fabrication techniques for potential tissue engineering applications," Tissue engineering, vol. 141, 2010.
[70] A. Mikos, L. Lu, J. Temenoff, and J. Tessmar, "Synthetic bioresorbable polymer scaffolds," An introduction to material in medicine, p. 743, 2004.
[71] C. Cha, S. R. Shin, X. Gao, N. Annabi, M. R. Dokmeci, X. Tang, and A. Khademhosseini, "Controlling mechanical properties of cell-laden hydrogels by covalent incorporation of graphene oxide," Small, vol. 10, no. 3, pp. 514-523, 2014.
[72] H. Liu and T. J. Webster, "Bioinspired nanocomposites for orthopedic applications," in Nanotechnology for the regeneration of hard and soft tissues, 2007, pp. 1-51.
[73] S. Zhang, "Fabrication of novel biomaterials through molecular self-assembly," Nature biotechnology, vol. 21, no. 10, p. 1171, 2003.
[74] D. Li, W. Nie, L. Chen, D. McCoul, D. Liu, X. Zhang, Y. Ji, B. Yu, and C. He, "Self-assembled hydroxyapatite-graphene scaffold for photothermal cancer therapy and bone regeneration," Journal of biomedical nanotechnology, vol. 14, no. 12, pp. 2003-2017, 2018.
[75] W. Nie, C. Peng, X. Zhou, L. Chen, W. Wang, Y. Zhang, P. X. Ma, and C. He, "Three-dimensional porous scaffold by self-assembly of reduced graphene oxide and nano-hydroxyapatite composites for bone tissue engineering," Carbon, vol. 116, pp. 325-337, 2017.
[76] A. F. Girão, G. Gonçalves, K. S. Bhangra, J. B. Phillips, J. Knowles, G. Irurueta, M. K. Singh, I. Bdkin, A. Completo, and P. A. Marques, "Electrostatic self-assembled graphene oxide-collagen scaffolds towards a three-dimensional microenvironment for biomimetic applications," RSC Advances, vol. 6, no. 54, pp. 49039-49051, 2016.

[77] H. Schoof, J. Apel, I. Heschel, and G. Rau, "Control of pore structure and size in freeze-dried collagen sponges," Journal of Biomedical Materials Research Part A, vol. 58, no. 4, pp. 352-357, 2001.
[78] B. B. Mandal and S. C. Kundu, "Cell proliferation and migration in silk fibroin 3D scaffolds," Biomaterials, vol. 30, no. 15, pp. 2956-2965, 2009.
[79] B. B. Mandal and S. C. Kundu, "Osteogenic and adipogenic differentiation of rat bone marrow cells on non-mulberry and mulberry silk gland fibroin 3D scaffolds," Biomaterials, vol. 30, no. 28, pp. 5019-5030, 2009.
[80] E. Boland, P. Espy, and G. Bowlin, "Tissue engineering scaffolds: In Encyclopaedia of Biomaterials and biomedical engineering," Wenk GE, Bowlin, GL (Edi) Richmong, Verginia, USA, pp. 1633-1635, 2004.
[81] S. Duan, X. Yang, F. Mei, Y. Tang, X. Li, Y. Shi, J. Mao, H. Zhang, and Q. Cai, "Enhanced osteogenic differentiation of mesenchymal stem cells on poly (L-lactide) nanofibrous scaffolds containing carbon nanomaterials," Journal of Biomedical Materials Research Part A, vol. 103, no. 4, pp. 1424-1435, 2015.
[82] M. Nair, D. Nancy, A. G. Krishnan, G. Anjusree, S. Vadukumpully, and S. V. Nair, "Graphene oxide nanoflakes incorporated gelatin–hydroxyapatite scaffolds enhance osteogenic differentiation of human mesenchymal stem cells," Nanotechnology, vol. 26, no. 16, p. 161001, 2015.
[83] C. Valencia, C. Valencia, F. Zuluaga, M. Valencia, J. Mina, and C. Grande-Tovar, "Synthesis and application of scaffolds of chitosan-graphene oxide by the freeze-drying method for tissue regeneration," Molecules, vol. 23, no. 10, p. 2651, 2018.
[84] C. Liang, Y. Luo, G. Yang, D. Xia, L. Liu, X. Zhang, and H. Wang, "Graphene Oxide Hybridized nHAC/PLGA Scaffolds Facilitate the Proliferation of MC3T3-E1 Cells," Nanoscale Research Letters, vol. 13, no. 1, pp. 15-15, 2018.
[85] S. Chakraborty, T. Ponrasu, S. Chandel, M. Dixit, and V. Muthuvijayan, "Reduced graphene oxide-loaded nanocomposite scaffolds for enhancing angiogenesis in tissue engineering applications," Royal Society open science, vol. 5, no. 5, p. 172017, 2018.
[86] F. Mohandes and M. Salavati-Niasari, "Freeze-drying synthesis, characterization and in vitro bioactivity of chitosan/graphene oxide/hydroxyapatite nanocomposite," Rsc Advances, vol. 4, no. 49, pp. 25993-26001, 2014.
[87] Y. He, N. Zhang, Q. Gong, H. Qiu, W. Wang, Y. Liu, and J. Gao, "Alginate/graphene oxide fibers with enhanced mechanical strength prepared by wet spinning," Carbohydrate polymers, vol. 88, no. 3, pp. 1100-1108, 2012.
[88] A. Mirabedini, J. Foroughi, B. Thompson, and G. G. Wallace, "Fabrication of Coaxial Wet-Spun Graphene–Chitosan Biofibers," Advanced Engineering Materials, vol. 18, no. 2, pp. 284-293, 2016.
[89] Y. Yang, X. Ding, T. Zou, G. Peng, H. Liu, and Y. Fan, "Preparation and characterization of electrospun graphene/silk fibroin conductive fibrous scaffolds," RSC Advances, vol. 7, no. 13, pp. 7954-7963, 2017.
[90] T. Zhou, G. Li, S. Lin, T. Tian, Q. Ma, Q. Zhang, S. Shi, C. Xue, W. Ma, and X. Cai, "Electrospun poly (3-hydroxybutyrate-co-4-hydroxybutyrate)/graphene oxide scaffold: enhanced properties and promoted in vivo bone repair in rats," ACS applied materials & interfaces, vol. 9, no. 49, pp. 42589-42600, 2017.
[91] A. Eltom, G. Zhong, and A. Muhammad, "Scaffold techniques and designs in tissue engineering functions and purposes: a review," Advances in Materials Science and Engineering, vol. 2019, 2019.
[92] G. M. Vlăsceanu, H. Iovu, and M. Ioniţă, "Graphene inks for the 3D printing of cell culture scaffolds and related molecular arrays," Composites Part B: Engineering, 2019.
[93] G. F. Caetano, W. Wang, W.-H. Chiang, G. Cooper, C. Diver, J. J. Blaker, M. A. Frade, and P. Bártolo, "3D-printed poly (ε-caprolactone)/graphene scaffolds activated with P1-latex protein for bone regeneration," 3D Printing and Additive Manufacturing, vol. 5, no. 2, pp. 127-137, 2018.

[94] W. Wang, G. Caetano, W. Ambler, J. Blaker, M. Frade, P. Mandal, C. Diver, and P. Bártolo, "Enhancing the hydrophilicity and cell attachment of 3D printed PCL/graphene scaffolds for bone tissue engineering," Materials, vol. 9, no. 12, p. 992, 2016.
[95] S. N. Jayasinghe, "Thoughts on scaffolds," Advanced Biosystems, vol. 1, no. 7, p. 1700067, 2017.
[96] F. Khan and M. Tanaka, "Designing smart biomaterials for tissue engineering," International journal of molecular sciences, vol. 19, no. 1, p. 17, 2017.
[97] L. Wang, J. A. Johnson, Q. Zhang, and E. K. Beahm, "Combining decellularized human adipose tissue extracellular matrix and adipose-derived stem cells for adipose tissue engineering," Acta biomaterialia, vol. 9, no. 11, pp. 8921-8931, 2013.
[98] M. Tallawi, E. Rosellini, N. Barbani, M. G. Cascone, R. Rai, G. Saint-Pierre, and A. R. Boccaccini, "Strategies for the chemical and biological functionalization of scaffolds for cardiac tissue engineering: a review," Journal of the Royal Society Interface, vol. 12, no. 108, p. 20150254, 2015.
[99] M. Abbasian, B. Massoumi, R. Mohammad-Rezaei, H. Samadian, and M. Jaymand, "Scaffolding polymeric biomaterials: Are naturally occurring biological macromolecules more appropriate for tissue engineering?," International journal of biological macromolecules, 2019.
[100] M. Farokhi, F. Jonidi Shariatzadeh, A. Solouk, and H. Mirzadeh, "Alginate Based Scaffolds for Cartilage Tissue Engineering: A Review," International Journal of Polymeric Materials and Polymeric Biomaterials, pp. 1-18, 2019.
[101] C.-C. Wang, K.-C. Yang, K.-H. Lin, H.-C. Liu, and F.-H. Lin, "A highly organized three-dimensional alginate scaffold for cartilage tissue engineering prepared by microfluidic technology," Biomaterials, vol. 32, no. 29, pp. 7118-7126, 2011.
[102] A. E. Pelling and R. J. Hickey, "Cellulose biomaterials for tissue engineering," Frontiers in Bioengineering and Biotechnology, vol. 7, p. 45, 2019.
[103] R. M. Domingues, M. E. Gomes, and R. L. Reis, "The potential of cellulose nanocrystals in tissue engineering strategies," Biomacromolecules, vol. 15, no. 7, pp. 2327-2346, 2014.
[104] J. C. Courtenay, R. I. Sharma, and J. L. Scott, "Recent advances in modified cellulose for tissue culture applications," Molecules, vol. 23, no. 3, p. 654, 2018.
[105] J. C. Courtenay, C. Deneke, E. M. Lanzoni, C. A. Costa, Y. Bae, J. L. Scott, and R. I. Sharma, "Modulating cell response on cellulose surfaces; tunable attachment and scaffold mechanics," Cellulose, vol. 25, no. 2, pp. 925-940, 2018.
[106] A. Laromaine, T. Tronser, I. Pini, S. Parets, P. A. Levkin, and A. Roig, "Free-standing three-dimensional hollow bacterial cellulose structures with controlled geometry via patterned superhydrophobic–hydrophilic surfaces," Soft matter, vol. 14, no. 19, pp. 3955-3962, 2018.
[107] J. Sundberg, C. Götherström, and P. Gatenholm, "Biosynthesis and in vitro evaluation of macroporous mineralized bacterial nanocellulose scaffolds for bone tissue engineering," Biomedical materials and engineering, vol. 25, no. 1, pp. 39-52, 2015.
[108] M. Rodríguez-Vázquez, B. Vega-Ruiz, R. Ramos-Zúñiga, D. A. Saldaña-Koppel, and L. F. Quiñones-Olvera, "Chitosan and its potential use as a scaffold for tissue engineering in regenerative medicine," BioMed research international, vol. 2015, 2015.
[109] N. Tanaka, I. Matsumoto, M. Suzuki, M. Kaneko, K. Nitta, R. Seguchi, A. Ooi, and H. Takemura, "Chitosan tubes can restore the function of resected phrenic nerves," Interactive cardiovascular and thoracic surgery, vol. 21, no. 1, pp. 8-13, 2015.
[110] M. C Echave, L. S Burgo, J. L Pedraz, and G. Orive, "Gelatin as biomaterial for tissue engineering," Current pharmaceutical design, vol. 23, no. 24, pp. 3567-3584, 2017.
[111] C. A. Martin, S. Radhakrishnan, S. Nagarajan, S. Muthukoori, J. M. Dueñas, J. L. G. Ribelles, B. S. Lakshmi, E. Nivethaa, J. A. Gómez-Tejedor, and M. S. Reddy, "An innovative bioresorbable gelatin based 3D scaffold that maintains the stemness of adipose tissue derived stem cells and the plasticity of differentiated neurons," RSC Advances, vol. 9, no. 25, pp. 14452-14464, 2019.
[112] S. H. Rao, B. Harini, R. P. K. Shadamarshan, K. Balagangadharan, and N. Selvamurugan, "Natural and synthetic polymers/bioceramics/bioactive compounds-mediated cell signalling in bone tissue engineering," International journal of biological macromolecules, vol. 110, pp. 88-96, 2018.

[113] E. S. Place, J. H. George, C. K. Williams, and M. M. Stevens, "Synthetic polymer scaffolds for tissue engineering," Chemical society reviews, vol. 38, no. 4, pp. 1139-1151, 2009.
[114] C. M. Patist, M. B. Mulder, S. E. Gautier, V. Maquet, R. Jérôme, and M. Oudega, "Freeze-dried poly (D, L-lactic acid) macroporous guidance scaffolds impregnated with brain-derived neurotrophic factor in the transected adult rat thoracic spinal cord," Biomaterials, vol. 25, no. 9, pp. 1569-1582, 2004.
[115] M. J. Mahoney and K. S. Anseth, "Three-dimensional growth and function of neural tissue in degradable polyethylene glycol hydrogels," Biomaterials, vol. 27, no. 10, pp. 2265-2274, 2006.
[116] A. Dolcimascolo, G. Calabrese, S. Conoci, and R. Parenti, "Innovative Biomaterials for Tissue Engineering," in Biomaterial-supported Tissue Reconstruction or Regeneration: IntechOpen, 2019.
[117] H.-S. Lee, S.-H. Byun, S.-W. Cho, and B.-E. Yang, "Past, present, and future of regeneration therapy in oral and periodontal tissue: a review," Applied Sciences, vol. 9, no. 6, p. 1046, 2019.
[118] N. Salehi-Nik, M. R. Rad, P. Nazeman, and A. Khojasteh, "Polymers for oral and dental tissue engineering," in Biomaterials for Oral and Dental Tissue Engineering: Elsevier, 2017, pp. 25-46.
[119] T. Garg, A. Bilandi, B. Kapoor, S. Kumar, and R. Joshi, "Scaffold: Tissue engineering and regenerative medicine," Int Res J Pharm, vol. 2, no. 12, pp. 37-42, 2011.
[120] A. Gloria, R. De Santis, and L. Ambrosio, "Polymer-based composite scaffolds for tissue engineering," Journal of Applied Biomaterials and Biomechanics, vol. 8, no. 2, pp. 57-67, 2010.
[121] Y. B. Kim and G. H. Kim, "PCL/alginate composite scaffolds for hard tissue engineering: fabrication, characterization, and cellular activities," ACS combinatorial science, vol. 17, no. 2, pp. 87-99, 2015.
[122] M.-D. Wang, P. Zhai, D. J. Schreyer, R.-S. Zheng, X.-D. Sun, F.-Z. Cui, and X.-B. Chen, "Novel crosslinked alginate/hyaluronic acid hydrogels for nerve tissue engineering," Frontiers of Materials Science, vol. 7, no. 3, pp. 269-284, 2013.
[123] Y. Wang, X. Wang, J. Shi, R. Zhu, J. Zhang, Z. Zhang, D. Ma, Y. Hou, F. Lin, and J. Yang, "A biomimetic silk fibroin/sodium alginate composite scaffold for soft tissue engineering," Scientific Reports, vol. 6, p. 39477, 2016.
[124] G. Wang, X. Wang, and L. Huang, "Feasibility of chitosan-alginate (Chi-Alg) hydrogel used as scaffold for neural tissue engineering: a pilot study in vitro," Biotechnology & Biotechnological Equipment, vol. 31, no. 4, pp. 766-773, 2017.
[125] Z.-a. Yao, F.-j. Chen, H.-l. Cui, T. Lin, N. Guo, and H.-g. Wu, "Efficacy of chitosan and sodium alginate scaffolds for repair of spinal cord injury in rats," Neural regeneration research, vol. 13, no. 3, p. 502, 2018.
[126] R. Eivazzadeh-Keihan, A. Maleki, M. de la Guardia, M. S. Bani, K. K. Chenab, P. Pashazadeh-Panahi, B. Baradaran, A. Mokhtarzadeh, and M. R. Hamblin, "Carbon based nanomaterials for tissue engineering of bone: Building new bone on small black scaffolds: A review," Journal of advanced research, 2019.
[127] B. Sitharaman, X. Shi, X. F. Walboomers, H. Liao, V. Cuijpers, L. J. Wilson, A. G. Mikos, and J. A. Jansen, "In vivo biocompatibility of ultra-short single-walled carbon nanotube/biodegradable polymer nanocomposites for bone tissue engineering," Bone, vol. 43, no. 2, pp. 362-370, 2008.
[128] Z. Zhou, X. Liu, W. Wu, S. Park, A. L. Miller II, A. Terzic, and L. Lu, "Effective nerve cell modulation by electrical stimulation of carbon nanotube embedded conductive polymeric scaffolds," Biomaterials science, vol. 6, no. 9, pp. 2375-2385, 2018.
[129] J. V. Veetil and K. Ye, "Tailored carbon nanotubes for tissue engineering applications," Biotechnology progress, vol. 25, no. 3, pp. 709-721, 2009.
[130] Y. Zhang, T. R. Nayak, H. Hong, and W. Cai, "Graphene: a versatile nanoplatform for biomedical applications," Nanoscale, vol. 4, no. 13, pp. 3833-3842, 2012.
[131] X. Ding, H. Liu, and Y. Fan, "Graphene-based materials in regenerative medicine," Advanced healthcare materials, vol. 4, no. 10, pp. 1451-1468, 2015.
[132] S. K. Lee, H. Kim, and B. S. Shim, "Graphene: an emerging material for biological tissue engineering," Carbon letters, vol. 14, no. 2, pp. 63-75, 2013.

[133] R. G. Bai, N. Ninan, K. Muthoosamy, and S. Manickam, "Graphene: A versatile platform for nanotheranostics and tissue engineering," Progress in Materials Science, vol. 91, pp. 24-69, 2018.
[134] S. H. Ku, M. Lee, and C. B. Park, "Carbon-based nanomaterials for tissue engineering," Advanced healthcare materials, vol. 2, no. 2, pp. 244-260, 2013.
[135] S. R. Shin, Y.-C. Li, H. L. Jang, P. Khoshakhlagh, M. Akbari, A. Nasajpour, Y. S. Zhang, A. Tamayol, and A. Khademhosseini, "Graphene-based materials for tissue engineering," Advanced Drug Delivery Reviews, vol. 105, pp. 255-274, 2016.
[136] I. Kanayama, H. Miyaji, H. Takita, E. Nishida, M. Tsuji, B. Fugetsu, L. Sun, K. Inoue, A. Ibara, and T. Akasaka, "Comparative study of bioactivity of collagen scaffolds coated with graphene oxide and reduced graphene oxide," International journal of nanomedicine, vol. 9, p. 3363, 2014.
[137] S. R. Shin, B. Aghaei-Ghareh-Bolagh, T. T. Dang, S. N. Topkaya, X. Gao, S. Y. Yang, S. M. Jung, J. H. Oh, M. R. Dokmeci, and X. Tang, "Cell-laden microengineered and mechanically tunable hybrid hydrogels of gelatin and graphene oxide," Advanced materials, vol. 25, no. 44, pp. 6385-6391, 2013.
[138] J. Li, X. Liu, J. M. Crook, and G. G. Wallace, "Development of a porous 3D graphene-PDMS scaffold for improved osseointegration," Colloids and Surfaces B: Biointerfaces, vol. 159, pp. 386-393, 2017.
[139] G. Zhao, H. Qing, G. Huang, G. M. Genin, T. J. Lu, Z. Luo, F. Xu, and X. Zhang, "Reduced graphene oxide functionalized nanofibrous silk fibroin matrices for engineering excitable tissues," NPG Asia Materials, vol. 10, no. 10, p. 982, 2018.
[140] T. P. D. Shareena, D. McShan, A. K. Dasmahapatra, and P. B. Tchounwou, "A Review on Graphene-Based Nanomaterials in Biomedical Applications and Risks in Environment and Health," Nano-Micro Letters, vol. 10, no. 3, p. 53, 2018.
[141] L. Jiang, D. Chen, Z. Wang, Z. Zhang, Y. Xia, H. Xue, and Y. Liu, "Preparation of an electrically conductive graphene oxide/chitosan scaffold for cardiac tissue engineering," Applied biochemistry and biotechnology, vol. 188, no. 4, pp. 952-964, 2019.
[142] N. Li, Q. Zhang, S. Gao, Q. Song, R. Huang, L. Wang, L. Liu, J. Dai, M. Tang, and G. Cheng, "Three-dimensional graphene foam as a biocompatible and conductive scaffold for neural stem cells," Scientific reports, vol. 3, p. 1604, 2013.
[143] S. Hong, J. Lee, S. Kang, E. Hwang, Y.-S. Hwang, M. Lee, D.-W. Han, and J.-C. Park, "Enhanced Neural Cell Adhesion and Neurite Outgrowth on Graphene-Based Biomimetic Substrates," BioMed Research International, vol. 2014, pp. 1-8, 2014.
[144] G. Lalwani, M. D'agati, A. Gopalan, M. Rao, J. Schneller, and B. Sitharaman, "Three-dimensional macroporous graphene scaffolds for tissue engineering," Journal of Biomedical Materials Research Part A, vol. 105, no. 1, pp. 73-83, 2017.
[145] J. Shen, B. Yan, T. Li, Y. Long, N. Li, and M. Ye, "Mechanical, thermal and swelling properties of poly (acrylic acid)–graphene oxide composite hydrogels," Soft Matter, vol. 8, no. 6, pp. 1831-1836, 2012.
[146] D. Yang, T. Li, M. Xu, F. Gao, J. Yang, Z. Yang, and W. Le, "Graphene oxide promotes the differentiation of mouse embryonic stem cells to dopamine neurons," Nanomedicine, vol. 9, no. 16, pp. 2445-2455, 2014.
[147] M. Lutolf and J. Hubbell, "Synthetic biomaterials as instructive extracellular microenvironments for morphogenesis in tissue engineering," Nature biotechnology, vol. 23, no. 1, pp. 47-55, 2005.
[148] S. Park, J. Park, S. Sim, M. Sung, K. S. Kim, B. Hong, and S. Hong, "Enhanced Differentiation of Human Neural Stem Cells into Neurons on Graphene," Advanced Materials, vol. 23, no. 36, 2011.
[149] T. Aydin, C. Gurcan, H. Taheri, and A. Yilmazer, "Graphene Based Materials in Neural Tissue Regeneration," in Cell Biology and Translational Medicine, Volume 3: Springer, 2018, pp. 129-142.
[150] C. L. Weaver and X. Cui, "Directed Neural Stem Cell Differentiation with a Functionalized Graphene Oxide Nanocomposite," Advanced Healthcare Materials, vol. 4, no. 9, pp. 1408-1416, 2015.

[151] A. Solanki, S. T. Chueng, P. T. Yin, R. Kappera, M. Chhowalla, and K. B. Lee, "Axonal Alignment and Enhanced Neuronal Differentiation of Neural Stem Cells on Graphene-Nanoparticle Hybrid Structures," Advanced Materials, vol. 25, no. 38, pp. 5477-5482, 2013.
[152] W. Lee, C. Y. X. Lim, H. Shi, L. A. L. Tang, Y. Wang, C. Lim, and K. Loh, "Origin of enhanced stem cell growth and differentiation on graphene and graphene oxide," ACS nano, vol. 5, no. 9, pp. 7334-7341, 2011.
[153] P. T. Yin, S. Shah, M. Chhowalla, and K.-B. Lee, "Design, synthesis, and characterization of graphene–nanoparticle hybrid materials for bioapplications," Chemical reviews, vol. 115, no. 7, pp. 2483-2531, 2015.
[154] F. Kim, L. J. Cote, and J. Huang, "Graphene oxide: surface activity and two-dimensional assembly," Advanced Materials, vol. 22, no. 17, pp. 1954-1958, 2010.
[155] M. R. Abidian, J. M. Corey, D. R. Kipke, and D. C. Martin, "Conducting-polymer nanotubes improve electrical properties, mechanical adhesion, neural attachment, and neurite outgrowth of neural electrodes," small, vol. 6, no. 3, pp. 421-429, 2010.
[156] S. Jain, A. Sharma, and B. Basu, "Vertical electric field stimulated neural cell functionality on porous amorphous carbon electrodes," Biomaterials, vol. 34, no. 37, pp. 9252-9263, 2013.
[157] A. T. Nguyen, S. Mattiassi, M. Loeblein, E. Chin, D. Ma, P. Coquet, V. Viasnoff, E. H. T. Teo, E. L. Goh, and E. K. Yim, "Human Rett-derived neuronal progenitor cells in 3D graphene scaffold as an in vitro platform to study the effect of electrical stimulation on neuronal differentiation," Biomedical Materials, vol. 13, no. 3, p. 034111, 2018.
[158] O. Akhavan, E. Ghaderi, S. A. Shirazian, and R. Rahighi, "Rolled graphene oxide foams as three-dimensional scaffolds for growth of neural fibers using electrical stimulation of stem cells," Carbon, vol. 97, pp. 71-77, 2016.
[159] C. Li and G. Shi, "Three-dimensional graphene architectures," Nanoscale, vol. 4, no. 18, pp. 5549-5563, 2012.
[160] N. Bhardwaj, D. Chouhan, and B. B. Mandal, "3D functional scaffolds for skin tissue engineering," in Functional 3D tissue engineering scaffolds: Elsevier, 2018, pp. 345-365.
[161] S. K. Ameri, P. Singh, R. D'Angelo, W. Stoppel, L. Black, and S. R. Sonkusale, "Three dimensional graphene scaffold for cardiac tissue engineering and in-situ electrical recording," in 38th Annual Int. Conference of the IEEE Engineering in Medicine and Biology Society (EMBC), 2016, pp. 4201-4203.
[162] Y. Liu, N. Fang, B. Liu, L. Song, B. Wen, and D. Yang, "Aligned porous chitosan/graphene oxide scaffold for bone tissue engineering," Materials Letters, vol. 233, pp. 78-81, 2018.
[163] X. Xie, K. Hu, D. Fang, L. Shang, S. D. Tran, and M. Cerruti, "Graphene and hydroxyapatite self-assemble into homogeneous, free standing nanocomposite hydrogels for bone tissue engineering," Nanoscale, vol. 7, no. 17, pp. 7992-8002, 2015.
[164] Z. Q. Feng, T. Wang, B. Zhao, J. Li, and L. Jin, "Soft graphene nanofibers designed for the acceleration of nerve growth and development," Advanced materials, vol. 27, no. 41, pp. 6462-6468, 2015.
[165] Y. Qi, Z. Tai, D. Sun, J. Chen, H. Ma, X. Yan, B. Liu, and Q. Xue, "Fabrication and characterization of poly (vinyl alcohol)/graphene oxide nanofibrous biocomposite scaffolds," Journal of applied polymer science, vol. 127, no. 3, pp. 1885-1894, 2013.
[166] Y. Qian, X. Zhao, Q. Han, W. Chen, H. Li, and W. Yuan, "An integrated multi-layer 3D-fabrication of PDA/RGD coated graphene loaded PCL nanoscaffold for peripheral nerve restoration," Nature communications, vol. 9, no. 1, pp. 1-16, 2018.
[167] J. Liao, Y. Qu, B. Chu, X. Zhang, and Z. Qian, "Biodegradable CSMA/PECA/graphene porous hybrid scaffold for cartilage tissue engineering," Scientific reports, vol. 5, p. 9879, 2015.
[168] Y. Luo, H. Shen, Y. Fang, Y. Cao, J. Huang, M. Zhang, J. Dai, X. Shi, and Z. Zhang, "Enhanced proliferation and osteogenic differentiation of mesenchymal stem cells on graphene oxide-incorporated electrospun poly (lactic-co-glycolic acid) nanofibrous mats," ACS applied materials & interfaces, vol. 7, no. 11, pp. 6331-6339, 2015.
[169] W. Wang, J. R. P. Junior, P. R. L. Nalesso, D. Musson, J. Cornish, F. Mendonça, G. F. Caetano, and P. Bártolo, "Engineered 3D printed poly (ε-caprolactone)/graphene scaffolds for bone tissue engineering," Materials Science and Engineering: C, vol. 100, pp. 759-770, 2019.

[170] J. B. Park, D. Sung, S. Park, K.-A. Min, K. W. Kim, Y. Choi, H. Y. Kim, E. Lee, H. S. Kim, and M. S. Jin, "3D graphene-cellulose nanofiber hybrid scaffolds for cortical reconstruction in brain injuries," 2D Materials, vol. 6, no. 4, p. 045043, 2019.
[171] Y. Qian, J. Song, X. Zhao, W. Chen, Y. Ouyang, W. Yuan, and C. Fan, "Tissue Engineering: 3D Fabrication with Integration Molding of a Graphene Oxide/Polycaprolactone Nanoscaffold for Neurite Regeneration and Angiogenesis (Adv. Sci. 4/2018)," Advanced Science, vol. 5, no. 4, p. 1870020, 2018.
[172] D. Wu, A. Samanta, R. K. Srivastava, and M. Hakkarainen, "Starch-derived nanographene oxide paves the way for electrospinnable and bioactive starch scaffolds for bone tissue engineering," Biomacromolecules, vol. 18, no. 5, pp. 1582-1591, 2017.
[173] O. Akhavan, E. Ghaderi, and S. A. Shirazian, "Near infrared laser stimulation of human neural stem cells into neurons on graphene nanomesh semiconductors," Colloids and Surfaces B: Biointerfaces, vol. 126, pp. 313-321, 2015.
[174] S. P. M. Cátia S.D.Cabral, Duartede Melo-Diogo, Ricardo O.Louro, Ilídio J.Correia, "Green reduced graphene oxide functionalized 3D printed scaffolds for bone tissue regeneration," Carbon, vol. 146, pp. 513-523, 2019.
[175] W. C. Lee, K. P. Loh, and C. T. Lim, "When stem cells meet graphene: Opportunities and challenges in regenerative medicine," Biomaterials, vol. 155, pp. 236-250, 2018.
[176] S. Sayyar, E. Murray, B. C. Thompson, S. Gambhir, D. L. Officer, and G. G. Wallace, "Covalently linked biocompatible graphene/polycaprolactone composites for tissue engineering," Carbon, vol. 52, pp. 296-304, 2013.
[177] P. De Marco, S. Zara, M. De Colli, M. Radunovic, V. Lazović, V. Ettorre, A. Di Crescenzo, A. Piattelli, A. Cataldi, and A. Fontana, "Graphene oxide improves the biocompatibility of collagen membranes in an in vitro model of human primary gingival fibroblasts," Biomedical Materials, vol. 12, no. 5, p. 055005, 2017.
[178] E. López-Dolado, A. González-Mayorga, M. C. Gutiérrez, and M. C. Serrano, "Immunomodulatory and angiogenic responses induced by graphene oxide scaffolds in chronic spinal hemisected rats," Biomaterials, vol. 99, pp. 72-81, 2016.
[179] Ç. Defteralı, R. Verdejo, L. Peponi, E. D. Martín, R. Martínez-Murillo, M. Á. López-Manchado, and C. Vicario-Abejón, "Thermally reduced graphene is a permissive material for neurons and astrocytes and de novo neurogenesis in the adult olfactory bulb in vivo," Biomaterials, vol. 82, pp. 84-93, 2016.
[180] P. Zorlutuna, N. E. Vrana, and A. Khademhosseini, "The expanding world of tissue engineering: the building blocks and new applications of tissue engineered constructs," IEEE Reviews in Biomedical Engineering, vol. 6, pp. 47-62, 2013.
[181] P. K. Gillian Dumsile Mahumane, Lisa Claire du Toit, Yahya Essop Choonara and Viness Pillay, "3D scaffolds for brain tissue regeneration: architectural challenges," Biomaterials Science, vol. 6, pp. 2812-2837, 2018.
[182] N. Sultana, M. I. Hassan, and M. M. Lim, Composite Synthetic Scaffolds for Tissue Engineering and Regenerative Medicine, 1 ed. (Springer Letters in Materials). Springer International Publishing, 2014.
[183] J. Valente, T. A. M. Valente, P. Alves, P. Ferreira, A. Silva, and I. Correia, "Alginate based scaffolds for bone tissue engineering," Materials Science and Engineering: C, vol. 32, no. 8, pp. 2596-2603, 2012.
[184] B. H. Rehm and M. F. Moradali, Alginates and Their Biomedical Applications (Springer Series in Biomaterials Science and Engineering). Springer, 2018.
[185] Y. Wan, X. Chen, G. Xiong, R. Guo, and H. Luo, "Synthesis and characterization of three-dimensional porous graphene oxide/sodium alginate scaffolds with enhanced mechanical properties," Materials express, vol. 4, no. 5, pp. 429-434, 2014.
[186] A. Sinha, Y. Choi, M. H. Nguyen, T. L. Nguyen, S. W. Choi, and J. Kim, "A 3D Macroporous Alginate Graphene Scaffold with an Extremely Slow Release of a Loaded Cargo for In Situ Long-Term Activation of Dendritic Cells," Advanced healthcare materials, vol. 8, no. 5, p. 1800571, 2019.

[187] D. de Melo-Diogo, R. Lima-Sousa, C. G. Alves, E. C. Costa, R. O. Louro, and I. J. Correia, "Functionalization of graphene family nanomaterials for application in cancer therapy," Colloids and Surfaces B: Biointerfaces, 2018.
[188] D. C. Marcano, D. V. Kosynkin, J. M. Berlin, A. Sinitskii, Z. Sun, A. Slesarev, L. B. Alemany, W. Lu, and J. M. Tour, "Improved Synthesis of Graphene Oxide," ACS Nano, vol. 4, no. 8, pp. 4806-4814, 2010/08/24 2010.
[189] Y. Li, H. Zhang, M. Fan, P. Zheng, J. Zhuang, and L. Chen, "A robust salt-tolerant superoleophobic alginate/graphene oxide aerogel for efficient oil/water separation in marine environments," Scientific Reports, Article vol. 7, p. 46379, 04/11/online 2017.
[190] A. Thomas, E. Johnson, A. K. Agrawal, and J. Bera, "Preparation and characterization of glass–ceramic reinforced alginate scaffolds for bone tissue engineering," Journal of Materials Research, vol. 34, no. 22, pp. 3798-3809, 2019.
[191] X. Yuan, Y. Wei, S. Chen, P. Wang, and L. Liu, "Bio-based graphene/sodium alginate aerogels for strain sensors," RSC Advances, 10.1039/C6RA12469K vol. 6, no. 68, pp. 64056-64064, 2016.
[192] S. Saravanan, A. Chawla, M. Vairamani, T. Sastry, K. Subramanian, and N. Selvamurugan, "Scaffolds containing chitosan, gelatin and graphene oxide for bone tissue regeneration in vitro and in vivo," International journal of biological macromolecules, vol. 104, pp. 1975-1985, 2017.
[193] L. Shahriary and A. A. Athawale, "Graphene Oxide Synthesized by using Modified Hummers Approach," International Journal of Renewable Energy and Environmental Engineering, vol. 2, pp. 58-63, 2014.
[194] D. N. Tran, S. Kabiri, L. Wang, and D. Losic, "Engineered graphene–nanoparticle aerogel composites for efficient removal of phosphate from water," Journal of Materials Chemistry A, vol. 3, no. 13, pp. 6844-6852, 2015.
[195] M. Sohail, M. Saleem, S. Ullah, N. Saeed, A. Afridi, M. Khan, and M. Arif, "Modified and improved Hummer's synthesis of graphene oxide for capacitors applications," Modern Electronic Materials, vol. 3, no. 3, pp. 110-116, 2017/09/01/ 2017.
[196] A. Gholampour, M. Valizadeh Kiamahalleh, D. N. Tran, T. Ozbakkaloglu, and D. Losic, "From Graphene Oxide to Reduced Graphene Oxide: Impact on the Physiochemical and Mechanical Properties of Graphene–Cement Composites," ACS applied materials & interfaces, vol. 9, no. 49, pp. 43275-43286, 2017.
[197] P. Smrdel, M. Bogataj, F. Podlogar, O. Planinšek, N. Zajc, M. Mazaj, V. Kaučič, and A. Mrhar, "Characterization of Calcium Alginate Beads Containing Structurally Similar Drugs," Drug Development and Industrial Pharmacy, vol. 32, no. 5, pp. 623-633, 2006/01/01 2006.
[198] Z. Wu, X. Su, Y. Xu, B. Kong, W. Sun, and S. Mi, "Bioprinting three-dimensional cell-laden tissue constructs with controllable degradation," Scientific Reports, Article vol. 6, p. 24474, 04/19/online 2016.
[199] C. Jiao, J. Xiong, J. Tao, S. Xu, D. Zhang, H. Lin, and Y. Chen, "Sodium alginate/graphene oxide aerogel with enhanced strength–toughness and its heavy metal adsorption study," International Journal of Biological Macromolecules, vol. 83, pp. 133-141, 2016/02/01/ 2016.
[200] A. Kovtun, M. J. Goeckelmann, A. A. Niclas, E. B. Montufar, M.-P. Ginebra, J. A. Planell, M. Santin, and A. Ignatius, "In vivo performance of novel soybean/gelatin-based bioactive and injectable hydroxyapatite foams," Acta biomaterialia, vol. 12, pp. 242-249, 2015.
[201] X. Yang, T. Zhou, B. Ren, A. Hursthouse, and Y. Zhang, "Removal of Mn (II) by sodium alginate/graphene oxide composite double-network hydrogel beads from aqueous solutions," Scientific reports, vol. 8, no. 1, p. 10717, 2018.
[202] W. Guo, J. Qiu, J. Liu, and H. Liu, "Graphene microfiber as a scaffold for regulation of neural stem cells differentiation," Scientific Reports, vol. 7, no. 1, p. 5678, 2017/07/18 2017.
[203] C. Wu, Z. Chen, F. Wang, Y. Hu, E. Wang, Z. Rao, and X. Zhang, "In situ reduction of graphene oxide to improve the thermal and wettability properties of urea-melamine-modified phenol formaldehyde resin composites," Materials Research Express, vol. 6, no. 2, p. 025302, 2018.
[204] H. Zheng, J. Yang, and S. Han, "The synthesis and characteristics of sodium alginate/graphene oxide composite films crosslinked with multivalent cations," Journal of Applied Polymer Science, vol. 133, no. 27, 2016.

[205] M. M. Eldin, A. Hashem, T. Tamer, A. Omer, M. Yossuf, and M. Sabet, "Development of cross linked chitosan/alginate polyelectrolyte proton exchanger membranes for fuel cell applications," Int. J. Electrochem. Sci, vol. 12, pp. 3840-3858, 2017.
[206] H. Nalvuran, A. E. Elçin, and Y. M. Elçin, "Nanofibrous silk fibroin/reduced graphene oxide scaffolds for tissue engineering and cell culture applications," International journal of biological macromolecules, vol. 114, pp. 77-84, 2018.
[207] H. Li, S. Liu, and L. Lin, "Rheological study on 3D printability of alginate hydrogel and effect of graphene oxide," International Journal of Bioprinting, printability; rheology; 3D printing; alginate hydrogel; graphene oxide vol. 2, no. 2, p. 54, 2016-06-27 2016.
[208] S. R. Shin, C. Zihlmann, M. Akbari, P. Assawes, L. Cheung, K. Zhang, V. Manoharan, Y. S. Zhang, M. Yüksekkaya, and K. t. Wan, "Reduced graphene oxide-gelMA hybrid hydrogels as scaffolds for cardiac tissue engineering," Small, vol. 12, no. 27, pp. 3677-3689, 2016.
[209] P. N. Khanam, D. Ponnamma, and M. Al-Madeed, "Electrical properties of graphene polymer nanocomposites," in Graphene-based polymer nanocomposites in electronics: Springer, 2015, pp. 25-47.
[210] X. Chang, Z. Wang, S. Quan, Y. Xu, Z. Jiang, and L. Shao, "Exploring the synergetic effects of graphene oxide (GO) and polyvinylpyrrodione (PVP) on poly (vinylylidenefluoride)(PVDF) ultrafiltration membrane performance," Applied Surface Science, vol. 316, pp. 537-548, 2014.
[211] X. Liu, W. Chen, C. T. Gustafson, A. L. Miller II, B. E. Waletzki, M. J. Yaszemski, and L. Lu, "Tunable tissue scaffolds fabricated by in situ crosslink in phase separation system," RSC advances, vol. 5, no. 122, pp. 100824-100833, 2015.
[212] Y. Zhang, Y. Liu, X. Wang, Z. Sun, J. Ma, T. Wu, F. Xing, and J. Gao, "Porous graphene oxide/carboxymethyl cellulose monoliths, with high metal ion adsorption," Carbohydrate polymers, vol. 101, pp. 392-400, 2014.
[213] N. Abzan, M. Kharaziha, and S. Labbaf, "Development of three-dimensional piezoelectric polyvinylidene fluoride-graphene oxide scaffold by non-solvent induced phase separation method for nerve tissue engineering," Materials & Design, vol. 167, p. 107636, 2019.
[214] K. S. Straley, C. W. P. Foo, and S. C. Heilshorn, "Biomaterial design strategies for the treatment of spinal cord injuries," Journal of neurotrauma, vol. 27, no. 1, pp. 1-19, 2010.
[215] N. L. Francis, P. M. Hunger, A. E. Donius, B. W. Riblett, A. Zavaliangos, U. G. Wegst, and M. A. Wheatley, "An ice-templated, linearly aligned chitosan-alginate scaffold for neural tissue engineering," Journal of Biomedical Materials Research Part A, vol. 101, no. 12, pp. 3493-3503, 2013.
[216] S. Wang, C. Sun, S. Guan, W. Li, J. Xu, D. Ge, M. Zhuang, T. Liu, and X. Ma, "Chitosan/gelatin porous scaffolds assembled with conductive poly (3, 4-ethylenedioxythiophene) nanoparticles for neural tissue engineering," Journal of Materials Chemistry B, vol. 5, no. 24, pp. 4774-4788, 2017.
[217] L. Ji, F. Chen, H. Huang, X. Sun, Y. Yan, and X. Tang, "Preparation of nickel–graphene composites by jet electrodeposition and the influence of graphene oxide concentration on the morphologies and properties," Surface and Coatings Technology, vol. 351, pp. 212-219, 2018.
[218] G. M. Vladimirovich and V. P. Melnikov, "Graphene Oxide/Reduced Graphene Oxide Aerogels," in Graphene Oxide-Applications and Opportunities: IntechOpen, 2018.
[219] S. Guan, X.-L. Zhang, X.-M. Lin, T.-Q. Liu, X.-H. Ma, and Z.-F. Cui, "Chitosan/gelatin porous scaffolds containing hyaluronic acid and heparan sulfate for neural tissue engineering," Journal of Biomaterials Science, Polymer Edition, vol. 24, no. 8, pp. 999-1014, 2013.
[220] K. Pietrucha, "Physicochemical properties of 3D collagen-CS scaffolds for potential use in neural tissue engineering," International journal of biological macromolecules, vol. 80, pp. 732-739, 2015.
[221] Z. Zhang, M. Rouabhia, Z. Wang, C. Roberge, G. Shi, P. Roche, J. Li, and L. H. Dao, "Electrically conductive biodegradable polymer composite for nerve regeneration: electricity-stimulated neurite outgrowth and axon regeneration," Artificial organs, vol. 31, no. 1, pp. 13-22, 2007.
[222] B. Xu, T. Bai, A. Sinclair, W. Wang, Q. Wu, F. Gao, H. Jia, S. Jiang, and W. Liu, "Directed neural stem cell differentiation on polyaniline-coated high strength hydrogels," Materials Today Chemistry, vol. 1, pp. 15-22, 2016.

[223] M. Pang, T. Shu, R.-Q. Chen, C. Liu, L. He, Y. Yang, A. S. A. Bardeesi, C.-K. Lin, L.-M. Zhang, and X. Wang, "Neural precursor cells generated from Induced pluripotent stem cells with gelatin sponge-electrospun PLGA/PEG nanofibers for spinal cord injury repair," International Journal of Clinical & Experimental Medicine, vol. 9, no. 9, 2016.
[224] V. Guarino, M. A. Alvarez-Perez, A. Borriello, T. Napolitano, and L. Ambrosio, "Conductive PANi/PEGDA macroporous hydrogels for nerve regeneration," Advanced healthcare materials, vol. 2, no. 1, pp. 218-227, 2013.
[225] H. Xu, J. M. Holzwarth, Y. Yan, P. Xu, H. Zheng, Y. Yin, S. Li, and P. X. Ma, "Conductive PPY/PDLLA conduit for peripheral nerve regeneration," Biomaterials, vol. 35, no. 1, pp. 225-235, 2014.
[226] F. Zamani, M. Amani-Tehran, A. Zaminy, and M.-A. Shokrgozar, "Conductive 3D structure nanofibrous scaffolds for spinal cord regeneration," Fibers and Polymers, vol. 18, no. 10, pp. 1874-1881, 2017.
[227] A. Subramanian, U. M. Krishnan, and S. Sethuraman, "Development of biomaterial scaffold for nerve tissue engineering: Biomaterial mediated neural regeneration," Journal of Biomedical Science, vol. 16, no. 1, p. 108, 2009.
[228] S. I. Cordoba De Torresi and A. C. da Silva, "Advances in Conducting, Biodegradable and Biocompatible Copolymers for Biomedical Applications," Frontiers in Materials, vol. 6, p. 98, 2019.
[229] C. J. Bullock and C. Bussy, "Biocompatibility considerations in the design of graphene biomedical materials," Advanced Materials Interfaces, vol. 6, no. 11, p. 1900229, 2019.
[230] A. Bianco, "Graphene: safe or toxic? The two faces of the medal," Angewandte Chemie International Edition, vol. 52, no. 19, pp. 4986-4997, 2013.
[231] H. F. Krug, "Nanosafety research—are we on the right track?," Angewandte Chemie International Edition, vol. 53, no. 46, pp. 12304-12319, 2014.
[232] F.-M. Chen and X. Liu, "Advancing biomaterials of human origin for tissue engineering," Progress in polymer science, vol. 53, pp. 86-168, 2016.
[233] L. Zhang, X. Liu, G. Li, P. Wang, and Y. Yang, "Tailoring degradation rates of silk fibroin scaffolds for tissue engineering," Journal of Biomedical Materials Research Part A, vol. 107, no. 1, pp. 104-113, 2019.
[234] K. N. Bitar and E. Zakhem, "Design strategies of biodegradable scaffolds for tissue regeneration," Biomedical engineering and computational biology, vol. 6, p. BECB. S10961, 2014.
[235] H. Zhang, L. Zhou, and W. Zhang, "Control of scaffold degradation in tissue engineering: a review," Tissue Engineering Part B: Reviews, vol. 20, no. 5, pp. 492-502, 2014.
[236] D. A. Jasim, N. Lozano, C. Bussy, I. Barbolina, A. F. Rodrigues, K. S. Novoselov, and K. Kostarelos, "Graphene-based papers as substrates for cell growth: Characterisation and impact on mammalian cells," FlatChem, vol. 12, pp. 17-25, 2018.
[237] A. J. Ryan, C. J. Kearney, N. Shen, U. Khan, A. G. Kelly, C. Probst, E. Brauchle, S. Biccai, C. D. Garciarena, and V. Vega-Mayoral, "Electroconductive biohybrid collagen/pristine graphene composite biomaterials with enhanced biological activity," Advanced Materials, vol. 30, no. 15, p. 1706442, 2018.
[238] Y. Yang, A. M. Asiri, Z. Tang, D. Du, and Y. Lin, "Graphene based materials for biomedical applications," Materials Today, vol. 16, no. 10, pp. 365-373, 2013.
[239] A. M. Pinto, I. C. Goncalves, and F. D. Magalhães, "Graphene-based materials biocompatibility: a review," Colloids and Surfaces B: Biointerfaces, vol. 111, pp. 188-202, 2013.
[240] M. Fiorillo, A. F. Verre, M. Iliut, M. Peiris-Pagés, B. Ozsvari, R. Gandara, A. R. Cappello, F. Sotgia, A. Vijayaraghavan, and M. P. Lisanti, "Graphene oxide selectively targets cancer stem cells, across multiple tumor types: Implications for non-toxic cancer treatment, via "differentiation-based nano-therapy"," Oncotarget, vol. 6, no. 6, p. 3553, 2015.
[241] F. Rodríguez-Lozano, D. García-Bernal, S. Aznar-Cervantes, M. Ros-Roca, M. Algueró, N. Atucha, A. Lozano-García, J. Moraleda, and J. Cenis, "Effects of composite films of silk fibroin and graphene oxide on the proliferation, cell viability and mesenchymal phenotype of

periodontal ligament stem cells," Journal of Materials Science: Materials in Medicine, vol. 25, no. 12, pp. 2731-2741, 2014.
[242] Y. Chong, Y. Ma, H. Shen, X. Tu, X. Zhou, J. Xu, J. Dai, S. Fan, and Z. Zhang, "The in vitro and in vivo toxicity of graphene quantum dots," Biomaterials, vol. 35, no. 19, pp. 5041-5048, 2014.
[243] H. Mao, W. Chen, S. Laurent, C. Thirifays, C. Burtea, F. Rezaee, and M. Mahmoudi, "Hard corona composition and cellular toxicities of the graphene sheets," Colloids and Surfaces B: Biointerfaces, vol. 109, pp. 212-218, 2013.
[244] N. Chatterjee, H.-J. Eom, and J. Choi, "A systems toxicology approach to the surface functionality control of graphene–cell interactions," Biomaterials, vol. 35, no. 4, pp. 1109-1127, 2014.
[245] J. Yuan, H. Gao, and C. B. Ching, "Comparative protein profile of human hepatoma HepG2 cells treated with graphene and single-walled carbon nanotubes: an iTRAQ-coupled 2D LC–MS/MS proteome analysis," Toxicology letters, vol. 207, no. 3, pp. 213-221, 2011.
[246] S. G. Han, J. K. Kim, J. H. Shin, J. H. Hwang, J. S. Lee, T.-G. Kim, J. H. Lee, G. H. Lee, K. S. Kim, and H. S. Lee, "Pulmonary responses of sprague-dawley rats in single inhalation exposure to graphene oxide nanomaterials," BioMed research international, vol. 2015, 2015.
[247] B. Wan, Z.-X. Wang, Q.-Y. Lv, P.-X. Dong, L.-X. Zhao, Y. Yang, and L.-H. Guo, "Single-walled carbon nanotubes and graphene oxides induce autophagosome accumulation and lysosome impairment in primarily cultured murine peritoneal macrophages," Toxicology letters, vol. 221, no. 2, pp. 118-127, 2013.
[248] D. R. Dreyer, A. D. Todd, and C. W. Bielawski, "Harnessing the chemistry of graphene oxide," Chemical Society Reviews, vol. 43, no. 15, pp. 5288-5301, 2014.
[249] A. F. Rodrigues, L. Newman, N. Lozano, S. P. Mukherjee, B. Fadeel, C. Bussy, and K. Kostarelos, "A blueprint for the synthesis and characterisation of thin graphene oxide with controlled lateral dimensions for biomedicine," 2D Materials, vol. 5, no. 3, p. 035020, 2018.
[250] A. B. Seabra, A. J. Paula, R. de Lima, O. L. Alves, and N. Duran, "Nanotoxicity of graphene and graphene oxide," Chemical research in toxicology, vol. 27, no. 2, pp. 159-168, 2014.
[251] F. M. Tonelli, V. A. Goulart, K. N. Gomes, M. S. Ladeira, A. K. Santos, E. Lorençon, L. O. Ladeira, and R. R. Resende, "Graphene-based nanomaterials: biological and medical applications and toxicity," Nanomedicine, vol. 10, no. 15, pp. 2423-2450, 2015.
[252] B. Zhang, Y. Wang, and G. Zhai, "Biomedical applications of the graphene-based materials," Materials Science and Engineering: C, vol. 61, pp. 953-964, 2016.
[253] Y. Zhang, D. Petibone, Y. Xu, M. Mahmood, A. Karmakar, D. Casciano, S. Ali, and A. S. Biris, "Toxicity and efficacy of carbon nanotubes and graphene: the utility of carbon-based nanoparticles in nanomedicine," Drug metabolism reviews, vol. 46, no. 2, pp. 232-246, 2014.
[254] D. Docter, D. Westmeier, M. Markiewicz, S. Stolte, S. Knauer, and R. Stauber, "The nanoparticle biomolecule corona: lessons learned–challenge accepted?," Chemical Society Reviews, vol. 44, no. 17, pp. 6094-6121, 2015.
[255] J. Yuan, H. Gao, J. Sui, H. Duan, W. N. Chen, and C. B. Ching, "Cytotoxicity evaluation of oxidized single-walled carbon nanotubes and graphene oxide on human hepatoma HepG2 cells: an iTRAQ-coupled 2D LC-MS/MS proteome analysis," Toxicological Sciences, vol. 126, no. 1, pp. 149-161, 2012.
[256] W. Guo, S. Wang, X. Yu, J. Qiu, J. Li, W. Tang, Z. Li, X. Mou, H. Liu, and Z. Wang, "Construction of a 3D rGO–collagen hybrid scaffold for enhancement of the neural differentiation of mesenchymal stem cells," Nanoscale, vol. 8, no. 4, pp. 1897-1904, 2016.
[257] Y. Zhang, S. F. Ali, E. Dervishi, Y. Xu, Z. Li, D. Casciano, and A. S. Biris, "Cytotoxicity effects of graphene and single-wall carbon nanotubes in neural phaeochromocytoma-derived PC12 cells," ACS nano, vol. 4, no. 6, pp. 3181-3186, 2010.
[258] N. Vallabani, S. Mittal, R. K. Shukla, A. K. Pandey, S. R. Dhakate, R. Pasricha, and A. Dhawan, "Toxicity of graphene in normal human lung cells (BEAS-2B)," Journal of biomedical nanotechnology, vol. 7, no. 1, pp. 106-107, 2011.
[259] D. A. Mbeh, O. Akhavan, T. Javanbakht, and M. Mahmoudi, "Cytotoxicity of protein corona-graphene oxide nanoribbons on human epithelial cells," Applied Surface Science, vol. 320, pp. 596-601, 2014.

[260] O. Akhavan, E. Ghaderi, H. Emamy, and F. Akhavan, "Genotoxicity of graphene nanoribbons in human mesenchymal stem cells," Carbon, vol. 54, pp. 419-431, 2013.
[261] Y. Talukdar, J. T. Rashkow, G. Lalwani, S. Kanakia, and B. Sitharaman, "The effects of graphene nanostructures on mesenchymal stem cells," Biomaterials, vol. 35, no. 18, pp. 4863-4877, 2014.
[262] M. Lv, Y. Zhang, L. Liang, M. Wei, W. Hu, X. Li, and Q. Huang, "Effect of graphene oxide on undifferentiated and retinoic acid-differentiated SH-SY5Y cells line," Nanoscale, vol. 4, no. 13, pp. 3861-3866, 2012.
[263] C. Wei, Z. Liu, F. Jiang, B. Zeng, M. Huang, and D. Yu, "Cellular behaviours of bone marrow-derived mesenchymal stem cells towards pristine graphene oxide nanosheets," Cell proliferation, vol. 50, no. 5, p. e12367, 2017.
[264] J. Kim, K. Yang, J. S. Lee, Y. H. Hwang, H. J. Park, K. I. Park, D. Y. Lee, and S. W. Cho, "Enhanced Self-Renewal and Accelerated Differentiation of Human Fetal Neural Stem Cells Using Graphene Oxide Nanoparticles," Macromolecular Bioscience, 2017.
[265] O. Akhavan, E. Ghaderi, and A. Akhavan, "Size-dependent genotoxicity of graphene nanoplatelets in human stem cells," Biomaterials, vol. 33, no. 32, pp. 8017-8025, 2012.
[266] L. Du, S. Wu, Y. Li, X. Zhao, X. Ju, and Y. Wang, "Cytotoxicity of PEGylated graphene oxide on lymphoma cells," Bio-medical materials and engineering, vol. 24, no. 6, pp. 2135-2141, 2014.
[267] Y. Chang, S.-T. Yang, J.-H. Liu, E. Dong, Y. Wang, A. Cao, Y. Liu, and H. Wang, "In vitro toxicity evaluation of graphene oxide on A549 cells," Toxicology letters, vol. 200, no. 3, pp. 201-210, 2011.
[268] J. M. Unagolla and A. C. Jayasuriya, "Enhanced cell functions on graphene oxide incorporated 3D printed polycaprolactone scaffolds," Materials Science and Engineering: C, vol. 102, pp. 1-11, 2019.
[269] G. Choe, S. Oh, J. M. Seok, S. A. Park, and J. Y. Lee, "Graphene oxide/alginate composites as novel bioinks for three-dimensional mesenchymal stem cell printing and bone regeneration applications," Nanoscale, vol. 11, no. 48, pp. 23275-23285, 2019.
[270] Q. Ma, L. Yang, Z. Jiang, Q. Song, M. Xiao, D. Zhang, X. Ma, T. Wen, and G. Cheng, "Three-Dimensional Stiff Graphene Scaffold on Neural Stem Cells Behavior," ACS Applied Materials & Interfaces, vol. 8, no. 50, pp. 34227-34233, 2016.
[271] M. Wojtoniszak, X. Chen, R. J. Kalenczuk, A. Wajda, J. Łapczuk, M. Kurzewski, M. Drozdzik, P. K. Chu, and E. Borowiak-Palen, "Synthesis, dispersion, and cytocompatibility of graphene oxide and reduced graphene oxide," Colloids and Surfaces B: Biointerfaces, vol. 89, pp. 79-85, 2012.
[272] S. Mullick Chowdhury, S. Dasgupta, A. E. McElroy, and B. Sitharaman, "Structural disruption increases toxicity of graphene nanoribbons," Journal of Applied Toxicology, vol. 34, no. 11, pp. 1235-1246, 2014.
[273] H. Yue, W. Wei, Z. Yue, B. Wang, N. Luo, Y. Gao, D. Ma, G. Ma, and Z. Su, "The role of the lateral dimension of graphene oxide in the regulation of cellular responses," Biomaterials, vol. 33, no. 16, pp. 4013-4021, 2012.
[274] S. M. Hussain and J. M. Frazier, "Cellular toxicity of hydrazine in primary rat hepatocytes," Toxicological Sciences, vol. 69, no. 2, pp. 424-432, 2002.
[275] F. Roe, G. Grant, and D. Millican, "Carcinogenicity of hydrazine and 1, 1-dimethylhydrazine for mouse lung," Nature, vol. 216, no. 5113, pp. 375-376, 1967.
[276] D. McManus, S. Vranic, F. Withers, V. Sanchez-Romaguera, M. Macucci, H. Yang, R. Sorrentino, K. Parvez, S.-K. Son, and G. Iannaccone, "Water-based and biocompatible 2D crystal inks for all-inkjet-printed heterostructures," Nature nanotechnology, vol. 12, no. 4, p. 343, 2017.
[277] S. M. Chowdhury, G. Lalwani, K. Zhang, J. Y. Yang, K. Neville, and B. Sitharaman, "Cell specific cytotoxicity and uptake of graphene nanoribbons," Biomaterials, vol. 34, no. 1, pp. 283-293, 2013.
[278] M. Ginouves, B. Carme, P. Couppie, and G. Prevot, "Comparison of tetrazolium salt assays for evaluation of drug activity against Leishmania spp," Journal of clinical microbiology, vol. 52, no. 6, pp. 2131-2138, 2014.

[279] F. Joris, B. B. Manshian, K. Peynshaert, S. C. De Smedt, K. Braeckmans, and S. J. Soenen, "Assessing nanoparticle toxicity in cell-based assays: influence of cell culture parameters and optimized models for bridging the in vitro–in vivo gap," Chemical Society Reviews, vol. 42, no. 21, pp. 8339-8359, 2013.
[280] V. Gies and S. Zou, "Systematic toxicity investigation of graphene oxide: evaluation of assay selection, cell type, exposure period and flake size," Toxicology research, vol. 7, no. 1, pp. 93-101, 2018.
[281] G. Ciofani, S. Danti, D. D'Alessandro, S. Moscato, and A. Menciassi, "Assessing cytotoxicity of boron nitride nanotubes: interference with the MTT assay," Biochemical and biophysical research communications, vol. 394, no. 2, pp. 405-411, 2010.
[282] L. Belyanskaya, P. Manser, P. Spohn, A. Bruinink, and P. Wick, "The reliability and limits of the MTT reduction assay for carbon nanotubes–cell interaction," Carbon, vol. 45, no. 13, pp. 2643-2648, 2007.
[283] K.-H. Liao, Y.-S. Lin, C. W. Macosko, and C. L. Haynes, "Cytotoxicity of graphene oxide and graphene in human erythrocytes and skin fibroblasts," ACS applied materials & interfaces, vol. 3, no. 7, pp. 2607-2615, 2011.
[284] X. Zhou, Y. Pan, R. Liu, X. Luo, X. Zeng, D. Zhi, J. Li, Q. Cheng, Z. Huang, and H. Zhang, "Biocompatibility and biodegradation properties of polycaprolactone/polydioxanone composite scaffolds prepared by blend or co-electrospinning," Journal of Bioactive and Compatible Polymers, vol. 34, no. 2, pp. 115-130, 2019.
[285] F. Rostami, E. Tamjid, and M. Behmanesh, "Drug-eluting PCL/graphene oxide nanocomposite scaffolds for enhanced osteogenic differentiation of mesenchymal stem cells," Materials Science and Engineering: C, p. 111102, 2020.
[286] N. Mansouri, S. F. Al-Sarawi, J. Mazumdar, and D. Losic, "Advancing fabrication and properties of three-dimensional graphene–alginate scaffolds for application in neural tissue engineering," RSC Advances, vol. 9, no. 63, pp. 36838-36848, 2019.
[287] H. Samadian, S. Farzamfar, A. Vaez, A. Ehterami, A. Bit, M. Alam, A. Goodarzi, G. Darya, and M. Salehi, "A tailored polylactic acid/polycaprolactone biodegradable and bioactive 3D porous scaffold containing gelatin nanofibers and Taurine for bone regeneration," Scientific reports, vol. 10, no. 1, pp. 1-12, 2020.
[288] S. D. Purohit, R. Bhaskar, H. Singh, I. Yadav, M. K. Gupta, and N. C. Mishra, "Development of a nanocomposite scaffold of gelatin–alginate–graphene oxide for bone tissue engineering," International journal of biological macromolecules, vol. 133, pp. 592-602, 2019.
[289] M. Ghibaudo, L. Trichet, J. Le Digabel, A. Richert, P. Hersen, and B. Ladoux, "Substrate topography induces a crossover from 2D to 3D behavior in fibroblast migration," Biophysical journal, vol. 97, no. 1, pp. 357-368, 2009.
[290] B. M. Baker and C. S. Chen, "Deconstructing the third dimension–how 3D culture microenvironments alter cellular cues," Journal of cell science, vol. 125, no. 13, pp. 3015-3024, 2012.
[291] C. Jensen and Y. Teng, "Is It Time to Start Transitioning From 2D to 3D Cell Culture?," Frontiers in Molecular Biosciences, vol. 7, p. 33, 2020.
[292] A. Pisciotta, L. Bertoni, M. Riccio, J. Mapelli, A. Bigiani, M. La Noce, M. Orciani, A. de Pol, and G. Carnevale, "Use of a 3D floating sphere culture system to maintain the neural crest-related properties of human dental pulp stem cells," Frontiers in physiology, vol. 9, p. 547, 2018.
[293] M. S. Liberio, M. C. Sadowski, C. Soekmadji, R. A. Davis, and C. C. Nelson, "Differential effects of tissue culture coating substrates on prostate cancer cell adherence, morphology and behavior," PLoS One, vol. 9, no. 11, p. e112122, 2014.
[294] Y. Qian, J. Song, X. Zhao, W. Chen, Y. Ouyang, W. Yuan, and C. Fan, "3D fabrication with integration molding of a graphene oxide/polycaprolactone nanoscaffold for neurite regeneration and angiogenesis," Advanced Science, vol. 5, no. 4, p. 1700499, 2018.
[295] V. Karageorgiou and D. Kaplan, "Porosity of 3D biomaterial scaffolds and osteogenesis," Biomaterials, vol. 26, no. 27, pp. 5474-5491, 2005/09/01/ 2005.
[296] F. J. O'Brien, B. A. Harley, I. V. Yannas, and L. J. Gibson, "The effect of pore size on cell adhesion in collagen-GAG scaffolds," Biomaterials, vol. 26, no. 4, pp. 433-441, 2005.

[297] F. J. O'Brien, B. A. Harley, M. A. Waller, I. V. Yannas, L. J. Gibson, and P. J. Prendergast, "The effect of pore size on permeability and cell attachment in collagen scaffolds for tissue engineering," Technology and Health Care, vol. 15, no. 1, pp. 3-17, 2007.
[298] C. M. Conde, F. F. Demarco, L. Casagrande, J. C. Alcazar, J. E. Nör, and S. B. C. Tarquinio, "Influence of poly-L-lactic acid scaffold's pore size on the proliferation and differentiation of dental pulp stem cells," Brazilian dental journal, vol. 26, no. 2, pp. 93-98, 2015.
[299] R. A. Morsy, H. Beherei, M. Ellithy, H. E. Tarek, and M. Mabrouk, "The odontogenic performance of human dental pulp stem cell in 3-dimensional chitosan and nano-bioactive glass-based scaffold material with different pores size," Journal of The Arab Society for Medical Research, vol. 14, no. 2, p. 82, 2019.
[300] M. Domingos, F. Intranuovo, T. Russo, R. De Santis, A. Gloria, L. Ambrosio, J. Ciurana, and P. Bartolo, "The first systematic analysis of 3D rapid prototyped poly (ε-caprolactone) scaffolds manufactured through BioCell printing: the effect of pore size and geometry on compressive mechanical behaviour and in vitro hMSC viability," Biofabrication, vol. 5, no. 4, p. 045004, 2013.
[301] Y. Luo, A. Lode, A. R. Akkineni, and M. Gelinsky, "Concentrated gelatin/alginate composites for fabrication of predesigned scaffolds with a favorable cell response by 3D plotting," RSC Advances, vol. 5, no. 54, pp. 43480-43488, 2015.
[302] S. Dinescu, M. Ionita, S.-R. Ignat, M. Costache, and A. Hermenean, "Graphene Oxide Enhances Chitosan-Based 3D Scaffold Properties for Bone Tissue Engineering," International journal of molecular sciences, vol. 20, no. 20, p. 5077, 2019.
[303] M. Kalbacova, A. Broz, J. Kong, and M. Kalbac, "Graphene substrates promote adherence of human osteoblasts and mesenchymal stromal cells," Carbon, vol. 48, no. 15, pp. 4323-4329, 2010.
[304] C. F. Jones and D. W. Grainger, "In vitro assessments of nanomaterial toxicity," Advanced drug delivery reviews, vol. 61, no. 6, pp. 438-456, 2009.
[305] J. Van der Valk, D. Mellor, R. Brands, R. Fischer, F. Gruber, G. Gstraunthaler, L. Hellebrekers, J. Hyllner, F. Jonker, and P. Prieto, "The humane collection of fetal bovine serum and possibilities for serum-free cell and tissue culture," Toxicology in vitro, vol. 18, no. 1, pp. 1-12, 2004.
[306] V. Bonnamain, R. Thinard, S. Sergent-Tanguy, P. Huet, G. Bienvenu, P. Naveilhan, J.-C. Farges, and B. Alliot-Licht, "Human dental pulp stem cells cultured in serum-free supplemented medium," Frontiers in physiology, vol. 4, p. 357, 2013.
[307] L. Xiao and T. Tsutsui, "Characterization of human dental pulp cells-derived spheroids in serum-free medium: Stem cells in the core," Journal of cellular biochemistry, vol. 114, no. 11, pp. 2624-2636, 2013.
[308] J. Jung, J.-W. Kim, H.-J. Moon, J. Y. Hong, and J. K. Hyun, "Characterization of neurogenic potential of dental pulp stem cells cultured in xeno/serum-free condition: in vitro and in vivo assessment," Stem cells international, vol. 2016, 2016.
[309] W. Hu, C. Peng, M. Lv, X. Li, Y. Zhang, N. Chen, C. Fan, and Q. Huang, "Protein corona-mediated mitigation of cytotoxicity of graphene oxide," ACS nano, vol. 5, no. 5, pp. 3693-3700, 2011.
[310] X.-Q. Wei, L.-Y. Hao, X.-R. Shao, Q. Zhang, X.-Q. Jia, Z.-R. Zhang, Y.-F. Lin, and Q. Peng, "Insight into the interaction of graphene oxide with serum proteins and the impact of the degree of reduction and concentration," ACS applied materials & interfaces, vol. 7, no. 24, pp. 13367-13374, 2015.
[311] A. Lesniak, A. Campbell, M. P. Monopoli, I. Lynch, A. Salvati, and K. A. Dawson, "Serum heat inactivation affects protein corona composition and nanoparticle uptake," Biomaterials, vol. 31, no. 36, pp. 9511-9518, 2010.
[312] A. Lesniak, F. Fenaroli, M. P. Monopoli, C. Åberg, K. A. Dawson, and A. Salvati, "Effects of the presence or absence of a protein corona on silica nanoparticle uptake and impact on cells," ACS nano, vol. 6, no. 7, pp. 5845-5857, 2012.
[313] O. Karaman and Z. B. Yaralı, "Determination of minimum serum concentration to develop scaffold free micro-tissue," The European Research Journal, vol. 4, no. 3, pp. 145-151, 2018.

[314] K. Zhang, Y. Fan, N. Dunne, and X. Li, "Effect of microporosity on scaffolds for bone tissue engineering," Regenerative biomaterials, vol. 5, no. 2, pp. 115-124, 2018.
[315] M. Sopotnik, A. Leonardi, I. Križaj, P. Dušak, D. Makovec, T. Mesarič, N. P. Ulrih, I. Junkar, K. Sepčić, and D. Drobne, "Comparative study of serum protein binding to three different carbon-based nanomaterials," Carbon, vol. 95, pp. 560-572, 2015.
[316] D. Liu, N. Pavathuparambil Abdul Manaph, M. Al-Hawwas, L. Bobrovskaya, L.-L. Xiong, and X.-F. Zhou, "Coating Materials for Neural Stem/Progenitor Cell Culture and Differentiation," Stem Cells and Development, vol. 29, no. 8, pp. 463-474, 2020.
[317] S. P. H. Miyagi, I. Kerkis, C. M. da Costa Maranduba, C. M. Gomes, M. D. Martins, and M. M. Marques, "Expression of extracellular matrix proteins in human dental pulp stem cells depends on the donor tooth conditions," Journal of endodontics, vol. 36, no. 5, pp. 826-831, 2010.
[318] S. Liu, T. Schackel, N. Weidner, and R. Puttagunta, "Biomaterial-supported cell transplantation treatments for spinal cord injury: challenges and perspectives," Frontiers in cellular neuroscience, vol. 11, p. 430, 2018.
[319] Q. Zhang, B. Shi, J. Ding, L. Yan, J. P. Thawani, C. Fu, and X. Chen, "Polymer scaffolds facilitate spinal cord injury repair," Acta biomaterialia, vol. 88, pp. 57-77, 2019.
[320] Z. Zhang, L. H. Klausen, M. Chen, and M. Dong, "Electroactive Scaffolds for Neurogenesis and Myogenesis: Graphene-Based Nanomaterials," Small, vol. 14, no. 48, p. 1801983, 2018.
[321] C. Chen, X. Bai, Y. Ding, and I.-S. Lee, "Electrical stimulation as a novel tool for regulating cell behavior in tissue engineering," Biomaterials Research, vol. 23, no. 1, p. 25, 2019.
[322] H. P. Bei, Y. Yang, Q. Zhang, Y. Tian, X. Luo, M. Yang, and X. Zhao, "Graphene-based nanocomposites for neural tissue engineering," Molecules, vol. 24, no. 4, p. 658, 2019.
[323] S. M. Willerth and S. E. Sakiyama-Elbert, "Approaches to neural tissue engineering using scaffolds for drug delivery," Advanced drug delivery reviews, vol. 59, no. 4-5, pp. 325-338, 2007.

# Biography

Negar Mansouri was born in 1992, Tehran, Iran. She received her B.Eng. in Electronics Engineering at Multimedia University (MMU), Malaysia in 2014 and M.Eng. in Biomedical Engineering at University of Malaya (UM), Malaysia in 2016. Her experience in carrying out research began with being employed as a research assistant at Nanotechnology & Catalysis Research Centre (NANOCAT), The University of Malaya (UM). The group of researchers she worked with investigated the application and functionalization of carbon nanomaterials, particularly graphene derivatives, in biosensing applications. This opportunity has significantly helped her to acquire new skills to study structure and morphology of carbon-based materials, conduct extensive data analysis and investigate the potential of graphene-based materials for biomedical applications. In 2017, she was awarded an International Scholarship Adelaide (ASI) from The University of Adelaide to conduct her doctoral studies where she joined the School of Electrical and Electronic Engineering under supervision of Dr Said Al-Sarawi, Prof. Dusan Losic and Prof. Jagan Mazumdar. During her PhD project, she joined ARC Graphene Research Hub Team to develop graphene-based scaffolds based to promote a tissue microenvironment conducive to tissue sparing and neural regeneration. She also conducts extensive researches on bridging the gap between regenerative medicine and spinal cord injury at Neil Sachse Centre for Spinal Cord Research, the South Australian Health and Medical Research Institute (SAHMRI). Her current research interests span several areas of biomedical engineering with a focus on tissue engineering, biomaterials, and regenerative medicine. Moreover, she has been actively conducting research in development and application of graphene-based aerogels.